TU WIEN Informatics

Simulating Vision Impairments in Virtual and Augmented Reality

DISSERTATION

zur Erlangung des akademischen Grades

Doktorin der Technischen Wissenschaften

eingereicht von

Dipl.-Ing. Katharina Krösl, BSc.
Matrikelnummer 0325089

an der Fakultät für Informatik

der Technischen Universität Wien

Betreuung: Associate Prof. Dipl.-Ing. Dipl.-Ing. Dr.techn. Michael Wimmer
Zweitbetreuung: Ao.Univ.Prof. Dipl.-Arch. Dr.phil. Georg Suter

Diese Dissertation haben begutachtet:

Mark Billinghurst	Tobias Langlotz

Wien, 6. November 2020

Katharina Krösl

TU WIEN Informatics

Simulating Vision Impairments in Virtual and Augmented Reality

DISSERTATION

submitted in partial fulfillment of the requirements for the degree of

Doktorin der Technischen Wissenschaften

by

Dipl.-Ing. Katharina Krösl, BSc.
Registration Number 0325089

to the Faculty of Informatics

at the TU Wien

Advisor: Associate Prof. Dipl.-Ing. Dipl.-Ing. Dr.techn. Michael Wimmer
Second advisor: Ao.Univ.Prof. Dipl.-Arch. Dr.phil. Georg Suter

The dissertation has been reviewed by:

Mark Billinghurst	Tobias Langlotz

Vienna, 6th November, 2020

Katharina Krösl

Technische Universität Wien
A-1040 Wien ▪ Karlsplatz 13 ▪ Tel. +43-1-58801-0 ▪ www.tuwien.at

Erklärung zur Verfassung der Arbeit

Dipl.-Ing. Katharina Krösl, BSc.

Hiermit erkläre ich, dass ich diese Arbeit selbständig verfasst habe, dass ich die verwendeten Quellen und Hilfsmittel vollständig angegeben habe und dass ich die Stellen der Arbeit – einschließlich Tabellen, Karten und Abbildungen –, die anderen Werken oder dem Internet im Wortlaut oder dem Sinn nach entnommen sind, auf jeden Fall unter Angabe der Quelle als Entlehnung kenntlich gemacht habe.

Wien, 6. November 2020

Katharina Krösl

Acknowledgements

First of all, I would like to thank my supervisor Michael Wimmer for giving me the chance to follow my research where ever it led me and supporting me on my journey to becoming an independent researcher. Thank you to my second supervisor Georg Suter for making time for me whenever I needed, and providing his expertise in Architecture.

I owe my deepest gratitude to Steven Feiner for welcoming me to his lab at Columbia University during a three-month research stay that kick-started a long-lasting collaboration, which already resulted in a number of publications. Steve never stopped encouraging me to improve my work further, which I believe made me a better researcher.

I very much appreciate that Henry Fuchs took the time to discuss my research with me every time he visited Vienna. His enthusiasm for research is inspiring and I just hope I will always stay as excited as he is when he talks about VR or AR.

Since my time at Columbia, I have been working closely together with Carmine Elvezio, who became a mentor, a colleague, and a friend. I am very grateful for the numerous video calls we had, discussing different approaches, finding solutions to problems, outlining studies, and planning the next paper targets.

My research is very interdisciplinary and this would not have been possible without the help of Sonja Karst, who never got tired of sharing her medical expertise with me.

I would also like to thank to all my co-authors and students who worked with me, especially Matthias Hürbe, who went above and beyond while helping me to finish our simulations under intense time pressure. Thank you to Johanna Schmidt, Reinhold Preiner and Gabriel Mistelbauer for showing me how to navigate the jungle that is academia, and to my colleague Markus Schütz, who became my partner in crime during long hours and weekend sessions at the lab before paper deadlines. Thanks also to our secretary Max Höfferer and our technicians, especially Andreas Weiner who helped me to set up our VR lab. Special thanks also to all my colleagues from the *Institute of Visual Computing & Human-Centered Technology* and from *VRVis*. A heartfelt thank you to Didi Drobna for her masterplan for getting my research a great deal of public attention.

I owe a huge thank you to Thomas Rausch for countless reviews, corrections, suggestions, for always believing in me, constantly pushing me to leave my comfort zone, and throwing chocolate at me from a safe distance when necessary.

Thank you to my parents for their never ending support, their encouraging words, and providing food for me to prevent me from starving before paper deadlines.

Finally, I would also like to express my gratitude to Mark Billinghurst and und Tobias Langlotz for giving me invaluable feedback during my first doctoral consortium at ISMAR 2018 and for doing me the honor of reviewing this thesis.

This research was enabled by the Doctoral College Computational Design (DCCD) of the Center for Geometry and Computational Design (GCD) at TU Wien and by the Competence Centre VRVis. VRVis is funded by BMK, BMDW, Styria, SFG and Vienna Business Agency in the scope of COMET - Competence Centers for Excellent Technologies (854174) which is managed by FFG.

Kurzfassung

Laut aktuellen Schätzungen der WHO gibt es weltweit mindestens 2,2 Milliarden Menschen mit Sehbehinderungen oder Augenkrankheiten wie Grauer Star, diabetische Retinopathie, Glaukom oder Makuladegeneration. Die meisten dieser Augenkrankheiten sind altersbedingt. Aufgrund einer zunehmend älter werdenden Bevölkerung wird mit einem weiteren Anstieg an Personen mit Augenkrankheiten gerechnet.

Medizinischen Publikationen, AugenärztInnen oder betroffene PatientInnen können Einblick in Sehbehinderungen und deren AUswirkung auf die visuelle Wahrnehmung geben. Dennoch ist es für Menschen mit normaler Sicht oft schwer nachvollziehbar wie sehr eine Augenkrankheit das tägliche Leben beeinträchtigen kann. Studien mit PatientInnen können wichtige Informationen liefern und zu einem besseren Verständis für Sehbehinderungen beitragen. Jedoch sind solche Studien oft schwer durchführbar, da eine statistische Auswertung der Daten nur dann möglich ist, wenn eine gewisse Anzahl an TeilnehmerInnen mit exakt gleicher Sehbehinderung for die Studie rekrutiert werden kann. Da Augenkrankheiten aber von Betroffenen mitunter sehr unterschiedlich wahrgenommen werden, und auch mit Sehtests nicht alle Symptome objektiv genau erfasst werden können, ist es in manchen Fällen gar nicht möglich eine passende Stichprobe zu finden.

In dieser Dissertation stellen wir ein System und eine Methodologie vor, die es erstmals ermöglichen Studien mit Personen mit normaler Sicht und simulierten Sehbehinderungen in Virtual Reality (VR) und Augmented Reality (AR) durchzuführen. Wir beschreiben wie einzelne Effekte für NutzerInnen kalibriert werden können um deren Sehstärke, sowie Hardware Limitierungen (z.B. die Auflösung des VR-Dsiplays) zu berücksichtigen um so das gleiche Level an Sehbehinderung für alle NutzerInnen zu simulieren.

Im Rahmen dieser Arbeit haben wir drei Studien in VR bzw AR durchgeführt. Unsere Messungen von Erkennungsdistanzen von Fluchtwegsschildern unter virtuell reduzierter Sehstärke haben ergeben dass atuell gültige Normen und internationale Standards Personen mit Sehbehinderungen nicht ausreichend berücksichtigen. Durch unsere Simulation von Grauem Star in VR konnten wir zeigen, dass verschiedene Arten von Beleuchtungssystemen positive oder negative Auswirkungen auf die Wahrnehmung von Personen mit Grauem Star haben können. In einer Studie mit PatientInnen, die auf einem Auge Grauen Star hatten konnten wir unsere verbesserte AR Simulation von Grauem Star testen und die Flexibilität unseres Systems demonstrieren. In Zukunft planen wir neben unseren Simulationen von Grauem Star, Kurzsichtigkeit, Weitsichtigkeit, Hornhauterkrankung

und Makuladegeneration noch weitere Augenkrankheiten zu simulieren und unseren Code öffentlich zugänglich zu machen. Wir hoffen, dass unsere Software Architekten und Lichtplanern dabei helfen kann ihrer Designs auf Barrierefreiheit zu testen, dass unser Tool in der Schulung von medizinischem Personal helfen und generell dazu beitragen kann mehr Verständnis für Menschen mit Sehbehinderungen zu schaffen.

Abstract

There are at least 2.2 billion people affected by vision impairments worldwide, and the number of people suffering from common eye diseases like cataracts, diabetic retinopathy, glaucoma or macular degeneration, which show a higher prevalence with age, is expected to rise in the years to come, due to factors like aging of the population.

Medical publications, ophthalmologists and patients can give some insight into the effects of vision impairments, but for people with normal eyesight (even medical personnel) it is often hard to grasp how certain eye diseases can affect perception. We need to understand and quantify the effects of vision impairments on perception, to design cities, buildings, or lighting systems that are accessible for people with vision impairments. Conducting studies on vision impairments in the real world is challenging, because it requires a large number of participants with exactly the same type of impairment. Such a sample group is often hard or even impossible to find, since not every symptom can be assessed precisely and the same eye disease can be experienced very differently between affected people.

In this thesis, we address these issues by presenting a system and a methodology to simulate vision impairments, such as refractive errors, cataracts, cornea disease, and age-related macular degeneration in virtual reality (VR) and augmented reality (AR), which allows us to conduct user studies in VR or AR with people with healthy eyesight and graphically simulated vision impairments. We present a calibration technique that allows us to calibrate individual simulated symptoms to the same level of severity for every user, taking hardware constraints as well as vision capabilities of users into account.

We measured the influence of simulated reduced visual acuity on maximum recognition distances of signage in a VR study and showed that current international standards and norms do not sufficiently consider people with vision impairments. In a second study, featuring our medically based cataract simulations in VR, we found that different lighting systems can positively or negatively affect the perception of people with cataracts. We improved and extended our cataract simulation to video–see-through AR and evaluated and adjusted each simulated symptom together with cataract patients in a pilot study, showing the flexibility and potential of our approach. In future work we plan to include further vision impairments and open source our software, so it can be used for architects and lighting designers to test their designs for accessibility, for training of medical

personnel, and to increase empathy for people with vision impairments. This way, we hope to contribute to making this world more inclusive for everyone.

Contents

CHAPTER 1

Introduction

"Seeing, contrary to popular wisdom, isn't believing. It's where belief stops, because it isn't needed any more."

— Terry Pratchett, *Pyramids*

1.1 Motivation

The *World Health Organization* (WHO) reported in 2019, that globally, at least 2.2 billion people were affected by vision impairments or blindness [WHO19]. The total number of people affected by vision impairments is expected to continuously increase due to different factors like population aging, urbanization, or behavioral and lifestyle changes. Population aging has a particularly grave impact, as many conditions, like presbyopia, cataract, glaucoma and age-related macular degeneration (AMD), show a higher prevalence in age groups of 40 years and older. The *National Eye Institute* (NEI) [NEIb] predicts that the number of people with vision impairments will rise until it will have approximately doubled from 2010 to 2050. Even though a significant portion of the population is affected by vision impairments, these people are hardly ever taken into account in city planning, or architectural and lighting design, because architects and designers lack the tools and the methodology to evaluate design concepts with regard to their accessibility for people with vision impairments.

With an increasing number of people being affected by vision impairments, inclusive architecture and lighting design is more pressing than ever. However, the biggest challenges here are to remove or mitigate barriers to empathy and create a common understanding of the effects of vision impairments for affected people and their environment. Standardized tests for different symptoms of eye diseases have been established to characterize the severity of a symptom, and books, medical papers, medical professionals, and verbal descriptions from patients can give some insight into the extent of vision impairment. However, verbal descriptions from patients can be inaccurate, since some vision impairments can progress slowly over time and affected people sometimes do not notice

symptoms, especially if both eyes are affected and they lack a healthy eye for reference. Textual descriptions, 2D images, or even current state-of-the-art 3D simulations, are often insufficient to grasp the effect a specific vision impairment has on the whole visual perception of a patient. While there are some existing simulations of vision impairments such as cataracts, which work with live camera imagery, they are inadequate to produce a realistic depiction of vision with this impairment by overly simplifying the effects that are experienced. This can make it difficult for a healthy person to relate to how a person with cataracts sees the world, experiences light, or accomplishes crucial tasks such as reading escape-route signs. People, whether relatives of people with eye diseases or medical personnel, could benefit from realistic, immersive simulations of visual impairments to increase their understanding and empathy.

Accurate vision impairment simulations are also critical for facilitating inclusive design of everyday objects, architectural planning, or the development of standards to increase accessibility of public spaces. In architectural design and lighting design, concepts for escape-route signposting and lighting are developed during the planning phase of a building by experts in the respective fields. In addition to the information given by international standards and norms, designers have to rely on their own expertise to take visually impaired people into account when planning emergency lighting and signage. There is a lack of data to show precisely how to consider people with vision impairments in the design process, as well as a lack of tools to evaluate a design for accessibility. User studies with affected people could help to gain insights, essentially reducing the barriers to empathy. However, conducting user studies to gain data for the revision of standards and norms, or to evaluate the accessibility of architectural or lighting designs, can be extremely difficult, since such studies currently require participation by many people with the same form of vision impairment to allow for statistical analysis of sufficient power.

1.2 Problem Statement

To be able to develop truly accessible designs for the majority of the population, architects and lighting designers need clear guidelines and tools to help them evaluate the suitability of their design for people with vision impairments. Inclusive design is only possible if we reduce the barriers to empathy, gaining a better understanding for people with vision impairments, and give standardization committees, architects and designers the necessary tools to gather quantitative data on the effects of vision impairments on perception and evaluate designs for accessibility under vision impairments. These are important factors for the revision of current norms and standards and the development and improvement of guidelines for architects and designers.

It can be hard for standardization committees to estimate the effects of a reduced visual acuity (VA), caused by vision impairments, on the readability or recognition distances of signs. Conducting a user study to obtain and analyze empirical data would be helpful to gain insights. However, a high reliability of the statistical analysis of such a study requires a high number of participants with the same form of vision impairment, and

getting larger samples can be difficult. Moreover, for eye diseases such as cataracts, diabetic retinopathy, glaucoma or AMD, it is difficult to determine exactly how a person experiences the visually degrading effects caused by the disease, other than by asking them for a verbal description. Some participants might have an eye disease with similar extent (e.g., a similarly clouded lens) as estimated by eye exams, but since the experience of the individual symptoms is highly subjective, it is unlikely that two people experience the exact same form of vision impairment and it is difficult to even find out if this is the case. This makes it infeasible for real-world user studies to determine the exact effects of eye diseases such as cataracts on perception. An alternative is to use participants with normal sight and simulate the vision impairment. Wood et al. [WCCC10], for example, conducted a user study on the effects of cataracts and refractive blur on night-time driving, using modified goggles. The problem with such experiments is that the different vision capabilities of the study participants can influence the results.

Conducting real-world studies with affected patients is difficult, costly, and may even be dangerous for participants. A safe and inexpensive alternative is to conduct user studies in virtual reality (VR) or augmented reality (AR) with healthy participants and graphically simulate the vision impairments, but we have to investigate how to do this correctly. To that end, we aim to answer the following research questions:

- *Q1: How can we efficiently quantify the effects of a reduced VA on the recognizability of signage?*
- *Q2: How can architects and lighting designers test their designs for accessibility for people with different vision impairments?*
- *Q3: How can we create realistic simulations of vision impairments, based on the first-hand experience of affected people?*

We hypothesize that VR and AR technologies can be leveraged to answer these question, by conducting studies with participants with healthy eyes and simulating vision impairments, based on medical expert knowledge, as well as on medical eyesight tests, adapted for the use in VR or AR. Furthermore, we presume that an interactively adjustable vision impairment simulation system facilitates user studies with people with vision impairments, allowing us to tweak simulations live during experiments with affected people, based on their feedback, to match their experienced vision impairment and as a result obtain realistic depictions of these impairments.

1.3 Approach

In this thesis, we present a methodology and system for conducting quantitative and qualitative user studies of visual impairments in VR and AR. Our **methodology** describes how to calibrate individual symptoms, combine them to simulate eye disease patterns and adjust them with patients, using our symptom-matching approach. This methodology

is complemented by a **system** that builds on state-of-the art VR, AR and eye-tracking technology, integrates an effects pipeline to combine simulated symptoms as well as different viewing modes for VR, AR and 360° images. To **evaluate** our methodology and test our system, we conducted two user studies in VR with people with healthy eyes and one study, in AR and our 360° image mode, with cataract patients.

1.3.1 Proposed Methodology

We present a methodology that comprises a novel *symptom calibration* approach, a method for simulating individual symptoms and combining them in an effects pipeline to *simulate eye disease patterns*, and a *symptom matching* technique to create realistic simulations together with people who experience the respective vision impairment on one eye.

Symptom Calibration

For user studies in VR or AR with simulated vision impairments, it is important to recruit participants with normal sight to avoid applying the simulation on top of a pre-existing vision impairment and thus degrading a user's vision more than intended by the simulated impairments alone. However, even people with normal sight have varying vision capabilities [Col02] that need to be accounted for. Furthermore, the resolution of VR headsets is lower than that of the human eye. Therefore, users already experience a mild form of vision impairment (as defined by the WHO [WHO19]) when wearing a VR headset. Consequently, individual vision capabilities as well as deficiencies of the head-worn display (HWD) have to be taken into account. To that end, we calibrate simulated symptoms of vision impairments (see Chapter 6), such as reduced VA and reduced contrast, to the same level for each user, so they all experience the same amount of degraded vision. We use this calibration methodology in a user study to calibrate the vision of each user to a pre-defined level of reduced VA and measure the effects of reduced VA on maximum recognition distances (MRDs) of escape-route signs in buildings.

Simulation of Eye Disease Patterns

In our second and third study, we used simulations of complex eye disease patterns, such as different types of cataracts. In order to create these disease patterns, we developed an effects pipeline (see Chapter 5), consisting of multiple vision-degrading symptoms. This approach allows us to simulate and calibrate each symptom at a time and then combine them. We used this methodology to create simulations of different types of cataract vision, refractive errors, cornea disease and AMD. All of our simulations have been developed in close collaboration with ophthalmologists and are therefore based on medical expert knowledge.

Symptom Matching

In order to validate and improve the realism of our medically based simulation, we present a novel approach to evaluate and adjust the simulated symptoms with patients affected by the respective symptoms. For this purpose, we developed an AR application that allows us to show a user our simulation applied to a video–see-through AR stream to one eye and the unmodified video stream to the other eye (see Chapter 9).

Our research is targeted at simulating different types of vision impairments, but for our system prototype and our user studies, we focused on cataracts in particular. In general, cataracts are easy to treat with surgery. Most cataract surgeons do not perform bilateral same-day surgery [Ame15] (i.e., operating both eyes of a patient on the same day). Although same-day surgery is preferable in certain situations, there is a remaining risk of bilateral complications and sometimes the first eye's outcome is used as a reference to better plan the second eye surgery [Don16]. Therefore, we have a short time window between surgeries, when we can conduct experiments with cataract patients, while one of their eyes is already corrected and lets them see clearly, but not the other. These patients can look at our cataract simulation with their already corrected eye and compare it to their vision with their still remaining cataract-affected eye when looking at the unmodified video–see-through AR stream. During such an experiment, we can adjust our simulation at run-time to match the cataract vision of a participant and consequently obtain parameter values for simulated symptoms that can be used for realistic simulations of cataract vision. This symptom-matching methodology can be used to adjust the simulation of any vision impairment, where the patient has a clear vision on one eye when the experiment is conducted. Vision impairments such as cataracts, glaucoma, cornea disease, AMD, diabetic rethinopathy or others could be adjusted with this methodology, if only one eye of a participant is affected and if the available simulations provide the functionality to adjust all the included effects at run-time.

1.3.2 System

To apply our methodology in different application scenarios, we developed a system to simulate a wide range of visual impairments, employing efficient post-processing effects that run in real-time. Since some symptoms of certain eye diseases affect only parts of the visual field (like a dark shadow in the center), we use eye tracking to implement gaze-dependent effects.

Because eye-disease symptoms can vary greatly from one person to another, it was crucial to make the simulations as adjustable as possible to support a wide range of characteristics of the involved symptoms. Furthermore, to enable our symptom-calibration methodology, we needed a system that provides possibilities to adjust simulation parameters at run-time. This also allows, for the first time, to conduct user studies with patients, by employing our symptom-matching methodology to achieve simulations that represent vision impairments of these patients. We can now create simulations of eye disease patterns and match them to very subjective symptoms that are otherwise hard to assess. So far, we implemented

simulations of cataract vision, refractive errors, cornea disease and AMD, demonstrating that our system is flexible and easy to extend in order to add simulations of other vision impairments.

With our recent prototype, *XREye*, users wearing a HWD can experience the simulated visual impairments in VR, video–see-through AR, or when viewing 360° images, and seamlessly switch between viewing modes, allowing for a wide range of applications or study settings.

1.3.3 Evaluation and Results

We demonstrate our approach and its feasibility in three key studies.

Study 1: Reduced Visual Acuity

We conducted our first quantitative study entirely in VR to investigate the MRD of escape-route signs in buildings, under reduced VA, with people with normal or corrected sight (wearing glasses or lenses) and graphically simulated impaired vision. To calibrate the vision of each user in the HWD to specific levels of reduced VA, we applied our symptom-calibration methodology and validated it with eyesight tests in VR. We measured the MRDs for different size escape-route signs, different viewing angles and different levels of vision impairment and compared our measurements to the values prescribed by current norms and standards for the installation of signage. Our results show that current norms and standards do not sufficiently consider people with vision impairments.

Study 2: Cataracts in VR

In a second study, we measured MRDs under simulated cataract vision (with people with healthy eyes) as well as the influence of different illumination scenarios on perception under these conditions. We calibrated the VA as well as the contrast vision of participants and simulated eye disease patterns for three types of cataracts by combining the reduced VA and reduced contrast with other symptoms, using our effects pipeline. The quantitative study confirmed our initial assumption that cataracts affect vision significantly and degrade a person's ability to read signage. We also found that indirect lighting can be beneficial for people with cataracts, since it can reduce discomfort from blinding effects. Furthermore, participants reported that participating in this study helped them to better understand the difficulties people with cataracts face every day.

Study 3: Cataracts in AR

For our third study, we recruited cataract patients between surgeries of their left and right eye, to help us evaluate and adjust our simulation and test our symptom-matching methodology. In this primarily qualitative study, participants looked at our cataract simulation blended over a video–see-trough AR stream with their already operated, healthy eye, and compared it to their own cataract vision when looking at the unmodified AR stream

with the other eye, that still had cataracts. We also conducted remote experiments by showing some participants our simulation on their desktop screen via video call and asked them to compare it to simulations done in related work. We tested the symptom-matching methodology and flexibility of our system by interactively adjusting the simulation at run-time together with participants to match their own cataract vision. This pilot study and our remote experiments showed that AR solutions can help to create vision impairment simulations with symptom matching and represents a first step towards more realistic simulations.

Our results show the limitations of current standards and norms in their inclusivity of people with vision impairments. We confirmed our assumption that different lighting conditions can positively or negatively influence perception for people with eye diseases, such as direct light sources, which create uncomfortable blinding effects especially for people with cataracts due to their clouded eye lens, which scatters light more than a clear lens. These facts both highlight the need for proper simulation and evaluation tools in this area. With this thesis, we show that modern extended reality (XR)[1] technologies can be leveraged for this purpose.

1.4 Contributions

The main contributions of this thesis can be summarized as follows:

- We introduce a novel **methodological framework** for simulating vision impairments and conducting user studies to investigate the influence of different eye conditions on visual perception.
  - Our *symptom calibration* methodology enables us to calibrate vision impairments to the same level of severity for each user, taking into account a user's vision capabilities, as well as hardware constraints of the VR HWD and is based on medical eyesight tests.
  - We present a *simulation of eye disease patterns* by creating effects to simulate individual symptoms and then combining them to form complex disease patterns.
  - Using our *symptom matching* technique, we can adjust our medically based simulations of eye diseases and create realistic simulations with the help of patients affected by the respective eye disease.
- We present a flexible **system** to simulate various vision impairments and eye diseases in eye-tracked XR. Our tool provides medically based simulations of three different types of cataracts (nuclear, cortical and posterior subcapsular) and refractive errors (myopia, hyperopia, and presbyopia), two types of AMD (wet and

[1] refers to any combination of real and virtual environments and objects, including virtual reality (VR), augmented reality (AR) and mixed reality (MR)

dry), as well as cornea disease, and can easily be extended to support further eye conditions. Different modes allow to switch between VR, video–see-through AR and 360° images while a vision impairment simulation is active, and adjust each symptom at run-time.

- To **evaluate** our methodology and system for different applications, we conducted three user studies, each one building upon the results from the previous study:
  - In our first study, we *evaluated current norms* and standards for signage and present our results compared to values prescribed by these norms.
  - We then tested our approach for *accessibility considerations* in a VR user study and investigated the influence of cataracts on visual perception under different lighting scenarios, showing that indirect lighting creates less disturbing blinding effects for people with cataracts.
  - Finally, we conducted a study to *evaluate and adjust our cataract simulation with cataract patients* between surgeries. This study allowed us to demonstrate the feasibility of our methodology and the presented system to create realistic depictions of eye diseases together with patients.

Our system and methodology facilitate the creation of various vision impairment simulations that can help to increase understanding for vision impairments. Our approach can also be used to help standardization committees to revise standards and norms. Based on our research, we can provide tools for architects and designers to create more accessible designs. Furthermore, our work can be used to train medical personnel or serve as basis to develop novel diagnostic methods for vision impairments in the future.

CHAPTER 2

Overview

The content of this thesis is based on three full papers, one research demo and one book chapter. To give a concise report of this research, we have combined the respective parts of each publication in thematic chapters, which we will outline in the following sections.

2.1 Outline

To understand vision impairment simulations and their implementation, it is useful to first understand the basics of human vision. We therefore discuss the concept of visual acuity (VA), how it is measured, as well as different VA scales and tests, in Chapter 3. We also describe what factors might influence the vision of a person wearing a VR headset and provide background on cataracts, different types of this eye disease, and how they affect a person's vision.

In Chapter 4, we give a brief overview of different approaches to simulate vision impairments, including different display modalities.

We consolidated the methodology of our publications on the topic of vision impairment simulations in two chapters: In Chapter 5 we describe how to simulate complex eye disease patterns by using our effects pipeline. We focus on cataracts and use this eye disease as an exemplary vision impairment for building such an effects pipeline, but also present adaptations for other eye diseases. Because some symptoms that can degrade a person's vision are gaze dependent, we also discuss eye tracking for simulations of gaze-dependent effects in Section 5.5. To complete our methodology, Chapter 6 outlines how different symptoms of eye diseases, such as reduced VA or reduced contrast, can be calibrated to take vision capabilities of users and hardware constraints into account.

In Chapters 7, 8 and 9 we present the three studies we conducted during this research project to validate our approach, as well as results and insights gained from these experiments.

Finally, we summarize and conclude our research in Chapter 10, answering our initial research questions, and give an outlook on future work.

2.2 Publications

In the following we give a short summary of each of the publications this thesis is based on:

Paper 1: Katharina Krösl, Dominik Bauer, Michael Schwärzler, Henry Fuchs, Georg Suter and Michael Wimmer. "A VR-based User Study on the Effects of Vision Impairments on Recognition Distances of Escape-Route Signs in Buildings" in *The Visual Computer* 34(6-8), 911-923, 2018

Paper 2: Katharina Krösl, Carmine Elvezio, Matthias Hürbe, Sonja Karst, Michael Wimmer and Steven Feiner. "ICthroughVR: Illuminating Cataracts through Virtual Reality" in *2019 IEEE Conference on Virtual Reality and 3D User Interfaces (VR)* (pp. 655-663). IEEE, 2019

Paper 3: Katharina Krösl, Carmine Elvezio, Laura R. Luidolt, Matthias Hürbe, Sonja Karst, Steven Feiner and Michael Wimmer. "CatARact: Simulating Cataracts in Augmented Reality" in *2020 IEEE International Symposium on Mixed and Augmented Reality (ISMAR)*. IEEE, 2020.

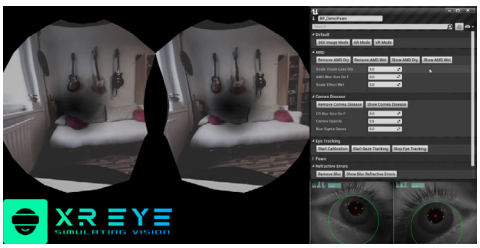

Research Demo: Katharina Krösl, Carmine Elvezio, Matthias Hürbe, Sonja Karst, Steven Feiner and Michael Wimmer. "XREye: Simulating Visual Impairments in Eye-Tracked XR" in *2020 IEEE Conference on Virtual Reality and 3D User Interfaces Abstracts and Workshops (VRW)*. IEEE, 2020. **Best Research Demo Award**

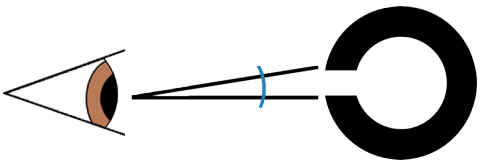

Book Chapter: Katharina Krösl. "Simulating Cataracts in Virtual Reality" *accepted for publication in Springer Book: Digital Anatomy, 2020*

2.2.1 Paper 1: A VR-based User Study on the Effects of Vision Impairments on Recognition Distances of Escape-Route Signs in Buildings [KBS+18]

In workplaces or publicly accessible buildings, escape routes are signposted according to official norms or international standards that specify distances, angles and areas of interest for the positioning of escape-route signs. In homes for the elderly, in which the residents commonly have degraded mobility and suffer from vision impairments caused by age or eye diseases, the specifications of current norms and standards may be insufficient. We present our methodology to simulate and calibrate reduced VA in Section 5.1.1 and Section 6.3 of our methodology chapters (Chapter 5 and 6). In Chapter 7 we present our user study to quantify the effects of reduced VA on the maximum recognition distances (MRDs) of escape-route signs. By conducting a user study in virtual reality (VR) we are able to use participants with normal or corrected sight (wearing glasses or lenses) and simulate vision impairments graphically. The use of standardized medical eyesight tests in VR allows us to calibrate the VA of all our participants to the same level, taking their respective VA into account. Since we primarily focus on homes for the elderly, we accounted for their often limited mobility by implementing a wheelchair simulation for our VR application. We compare the results of our user study to existing norms and standards for escape-route signage and show that there is a need to revise current regulations.

Contributions

With this work, we made the following contributions:

- A *realistic simulation of reduced VA (based on scientific medical findings) that can be calibrated to any level that is more severe than the reduction in VA induced by the low resolution of the VR headset.* Our simulation of loss of VA is calibrated relative to the actual VA of the user and takes into account display deficiencies, for the first time allowing to adjust the perceived VA of different users to the same level.

- *A user study based on this methodology to investigate recognition distances of escape-route signs.* To provide a highly immersive environment, we introduce an interactive, controlled test environment including a wheelchair-based type of locomotion, and use high-quality lighting simulation.

- *We provide an analysis of the data obtained from our user study in comparison to the values prescribed by international standards and European norms.*

2.2.2 Paper2: ICthroughVR: Illuminating Cataracts through Virtual Reality [KEH+19]

Vision impairments or eye diseases, such as cataracts, affect a significant portion of the population, worldwide. Yet, these impairments are hardly taken into account in architecture and lighting design today, because architects and designers lack the tools to evaluate their designs under impaired vision conditions. To address this, we present an effects pipeline in Chapter 5 and show how it can be used to develop a medically informed simulation of different types of cataracts in VR, using eye tracking for gaze-dependent effects. During this work, we developed a simulation of:

- reduced VA, using a depth-of-field effect (Section 5.1.1),
- reduced contrast, by interpolating with a gray image (Section 5.1.2),
- a color shift, by color interpolation (Section 5.1.3),
- dark shadows, using average image brightness to simulate adjustments of the pupil size (Section 5.1.4) and
- sensitivity to light, using a bloom effect (Section 5.1.5).

In Chapter 6, we extend our calibration methodology, previously used for reduced VA, to also calibrate reduced contrast (Section 6.4) to the same level for every user, taking vision capabilities of users, as well as hardware constraints of the VR head-worn display (HWD) into account. Using this methodology, we conducted a user study, investigating the effect of cataracts on the MRDs of users, as well as the influence of different lighting conditions on perception under cataract vision, which we describe in Chapter 8. The results of this study show that we are able to calibrate the vision of all our participants to a similar level of impairment and that maximum recognition distances for escape route signs with simulated cataracts are significantly smaller than without. After testing the effects of different illumination scenarios on visual perception under these conditions, we found that luminaires which are visible in the field of view of users are perceived as especially disturbing due to the glaring effects they create.

Contributions

The main contributions of this work can be summarized as follows:

- *A more extensive simulation than in previous work of different forms of cataracts in VR, using eye tracking for gaze-dependent effects.* Our simulation comprises multiple effects, representing different symptoms that are simulated separately and then combined to form certain disease patterns of cataracts. Hence, instead of simple approximations of cataract vision, our approach is the first to plausibly simulate different forms of cataracts, such as nuclear cataracts, cortical cataracts, and subcapsular cataracts.

- *A Simulation of the influence of light on the visual perception of people with cataracts.* We simulate intensified blinding effects when looking into bright lights, as well as brightness-dependent widening and contraction of the pupil that exposes more or less area of a clouded lens to light and therefore influences vision differently. This can aid in architectural design.

- *An improved methodology for conducting user studies in VR using participants with normal sight.* In addition to reduced VA, we also calibrate contrast loss to the same level for every user-study participant, taking into account the actual vision of the user and the hardware constraints of the VR headset. This is an important prerequisite to studying cataracts with normal-sighted participants.

2.2.3 Paper 3: CatARact: Simulating Cataracts in Augmented Reality [KEL+20]

For our society to be more inclusive and accessible, the more than 2.2 billion people worldwide with limited vision should be considered more frequently in design decisions, such as architectural planning. To help architects in evaluating their designs and also increase the understanding medical personnel have of how patients experience cataracts, we worked with ophthalmologists to develop the first medically informed, pilot-studied simulation of cataracts in eye-tracked augmented reality (AR). We extended our effects pipeline (Chapter 5) with a more accurate simulation of:

- reduced contrast, by compressing the luminance values of the image (Section 5.1.2),
- a color shift, based on a simulated color filter (Section 5.1.3),
- dark shadows, using a gaze-tracked brightness value to simulate adjustments of the pupil size (Section 5.1.4) and
- sensitivity to light, using a perceptual glare effect (Section 5.1.5).

To test our methodology and evaluate our simulation, we conducted a primarily qualitative pilot study with cataract patients between operations on their two cataract-affected eyes. Participants compared the vision of their corrected eye, viewing through simulated cataracts, to that of their still affected eye, viewing an unmodified AR view. In addition, we conducted remote experiments via video call, live adjusting our simulation and comparing it to related work, with participants who had cataract surgery a few months before. We describe the study and present our findings and insights from these experiments in Chapter 9.

Contributions

This work is a continuation of Paper 2 (*ICthroughVR* [KEH+19]) with the following new contributions:

- We present the first system to simulate symptoms of cataracts in AR using an HWD with eye-tracking technology and parameterized visualizations that are informed by ophthalmology professionals.

- We present a methodology to generate realistic simulations of eye diseases, such as cataracts, via interactive per-symptom adjustment at run-time and comparison of real cataract vision to simulated symptoms observed with healthy eyesight.

- We extend previous work in this area with more sophisticated and perceptually accurate simulations and compare them to our previous cataract simulation in VR [KEH+19].

- We test our methodology and evaluate the realism of our simulation through a pilot study with participants who are post-operative cataract surgery in one eye, and awaiting surgery for their second eye.

2.2.4 Research Demo: XREye: Simulating Visual Impairments in Eye-Tracked XR [KEH+20]

Many people suffer from visual impairments, which can be difficult for patients to describe and others to visualize. To aid in understanding what people with visual impairments experience, we demonstrate a set of medically informed simulations in eye-tracked XR of several common conditions that affect visual perception:

- While we have already shown how to reduce VA in previous work [KBS+18, KEH+19], we discuss how a Gaussian blur or a depth-of-field effect can be used to simulate different types of refractive errors (myopia, hyperopia, and presbyopia), in VR, AR or when viewing HDR 360° images, in Section 5.2.

- We explain how our effects pipeline can be adapted to simulate cornea disease in Section 5.3.

- In Section 5.4 we also show how to extend our effects pipeline to support a simulation of age-related macular degeneration (AMD) (wet and dry).

Our visual impairment simulations run in VR or video–see-through AR and can also be experienced when viewing 360° images, using an HTC Vive Pro HWD with a Pupil Labs 200Hz binocular eye tracker add-on. Users can experience our simulated vision impairments while exploring a VR scene, looking at their actual surroundings in video–see-through AR, or viewing HDR 360° images, can seamlessly switch between these viewing modes and compare different levels of severity of symptoms when parameters are modified at run-time.

Contributions

With this research demo we made the following contributions:

- We introduce the first medically informed AR/VR simulation of common eye diseases, such as cornea disease or AMD, using an eye-tracked AR/VR HWD.
- In addition, we modified our earlier framework [KBS+18, KEH+19] to make it easy to extend with further visual impairment simulations, already providing functionality to steer gaze-dependent effects with the eye tracker, seamlessly switch between VR, AR or 360° image viewing, and expose adjustable parameters to modify the simulation at run-time.

2.2.5 Book Chapter: Simulating Cataracts in Virtual Reality

This book chapter is based on Paper 2 *ICthroughVR* [KEH+19], illustrating how to simulate vision impairments in VR on the example of cataracts and explaining how the presented methodology can be used to calibrate simulated symptoms to the same level of severity for different users. We discuss what factors have to be considered when creating vision impairment simulations in general, and give a detailed explanation of our calibration methodology in Chapter 6, based on descriptions presented in the book chapter. We also consolidate some background information on human vision and how to understand and measure VA in this book chapter and Chapter 3 of this thesis.

2.2.6 Additional Publications

Besides the publications that constitute this thesis, the author has conducted further research in the context of VR/AR and lighting design, which led to the following additional publication:

- Luidolt, L. R., Wimmer, M. and **Krösl, K.**[1], "Gaze-Dependent Simulation of Light Perception in Virtual Reality" in *IEEE Transactions on Visualization and Computer Graphics*, doi: 10.1109/TVCG.2020.3023604.
- **Krösl, K.**, Steinlechner, H., Donabauer, J., Cornel, D. and Waser, J. "Master of Disaster: Virtual-Reality Response Training in Disaster Management" in *The 17th International Conference on Virtual-Reality Continuum and its Applications in Industry (VRCAI '19)*, November 14–16, 2019, Brisbane, QLD, Australia. ACM, New York, NY, USA 2 Pages.
- **Krösl, K.** "Simulating Vision Impairments in VR and AR" in *ACM SIGGRAPH THESIS FAST FORWARD 2019*. June 2019. **3rd place**

[1] supervised the work and coordinated the research project

- Schütz, M., **Krösl, K.**, and Wimmer, M. "Real-Time Continuous Level of Detail Rendering of Point Clouds" in *2019 IEEE Conference on Virtual Reality and 3D User Interfaces (VR)*. IEEE, 2019.
- **Krösl, K.**, "[DC] Computational Design of Smart Lighting Systems for Visually Impaired People, using VR and AR Simulations" in *Proceedings of the 2018 IEEE International Symposium on Mixed and Augmented Reality* (ISMAR Adjunct). IEEE, 2018.
- **Krösl, K.**, Felnhofer, A., Kafka, J. X., Schuster, L., Rinnerthaler, A., Wimmer, M., and Kothgassner, O. D. "The Virtual Schoolyard: Attention Training in Virtual Reality for Children with Attentional Disorders" in *ACM SIGGRAPH 2018 Posters* (p. 27). ACM, 2018.
- Walch, A., **Krösl, K.**, Luksch, C., Pipp, T., Pichler, D., and Schwärzler, M., "An Automated Verification Workflow for Planned Lighting Setups using BIM" in *Proceedings of the 23rd International Conference on Urban Planning and Regional Development in the Information Society*. GeoMultimedia, 2018.
- **Krösl, K.**, Luksch, C., Schwärzler, M., and Wimmer, M. "LiteMaker: Interactive Luminaire Development using Progressive Photon Tracing and Multi-Resolution Upsampling" in *Proceedings of Vision, Modeling and Visualization*, 2017.

CHAPTER 3

Background

This chapter is based on the following publication:

Katharina Krösl. "Simulating Cataracts in Virtual Reality" *accepted for publication in Springer Book: Digital Anatomy, 2020*

In this chapter we briefly discuss how human vision is measured and classified, and what factors can influence someone's visual perception in a VR headset. We also give some medical background information and explain how cataracts impact a person's vision.

3.1 Understanding Visual Acuity

Visual acuity (VA) describes in a quantifiable way a person's ability to recognize small details. It is measured by showing the subject different optotypes (standardized symbols used in medical eyesight tests, such as the Landolt C, shown in Figure 3.1) of different sizes at a predefined distance, and determining which size can be recognized and which cannot. VA is usually expressed relative to 6/6, the Snellen fraction for the test distance of $6m$, or 20/20 in feet, or the decimal value of these fractions.

A person has normal vision when they can recognize a detail that spans 1 arc minute (1/60 of a degree), which would be a size of $\sim 1.75mm$ at 6 meters distance (see Figure 3.2).

Figure 3.1: *Landolt C*, or *Landolt ring*, with a gap at one of eight possible positions: top, bottom, left, right, or 45° in between.

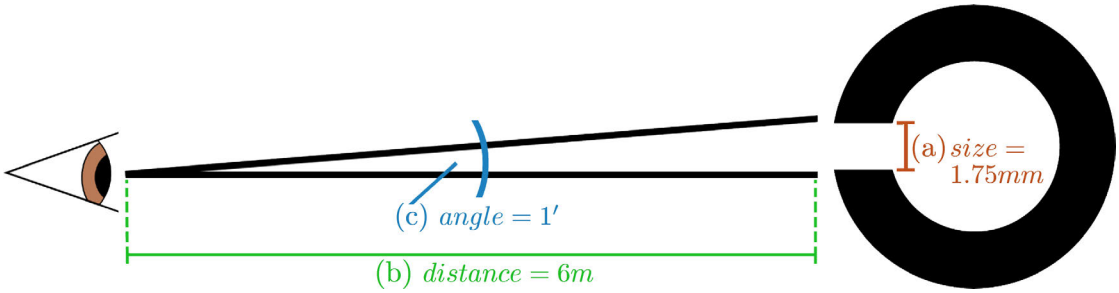

Figure 3.2: A person with normal sight can recognize a detail, such as (a) the gap in the Landolt C, of size $\sim 1.75mm$ at (b) 6 m distance. (c) The respective viewing angle corresponds to 1 arc minute (1/60 of a degree).

This can theoretically be tested at any viewing distance as long as the detail in question is appropriately scaled in relation to the distance. Shortsighted people can see very close objects well and only have a reduced VA at a certain distance. Therefore the test distance should not be too short (e.g. not under 1 meter). A common test distance is 6 meters or 20 feet.

In the context of classifying vision impairments, normal vision is defined as a range from 0.8 to 1.6 decimal acuity (dA), or better [Col02]. However, when we speak of normal sight as a reference value in the context of visual acuity (VA) calculations, we refer to 1.0 *decimal acuity* or 6/6 vision (in the metric system) or 20/20 vision (using foot as unit). In 6/6 or 20/20 vision, the numerator specifies the viewing distance (6 meters or 20 feet) at which a person who is tested can recognize the same size of optotypes as a person with normal sight (1.0 *decimal acuity*, 6/6, or 20/20 vision) can from the distance given by the denominator. The result of this fraction is the decimal acuity value of the tested person.

Other common notations besides decimal acuity are the Snellen fraction [Sne62], which is tested with a Snellen chart (see Figure 3.3). The Snellen fraction is given by the test distance as numerator and the distance at which a normal-sighted person could still correctly identify the same symbol as denominator. The decimal value of this fraction is equal to the decimal acuity value. ISO 8596 also defines LogMAR acuity as the *"logarithm (base 10) of the minimum angle of resolution in minutes of arc"* [Int09]. Consequently, the decimal acuity value dA can be computed from the LogMAR value lM as

$$dA = 10^{-lM}. \tag{3.1}$$

The angular extent of the gap in the Landolt ring used for testing a certain VA level can therefore be directly converted to these three common measures for VA and vice versa (see Table 3.1).

Example: A person's VA is examined using a vision test where optotypes are displayed at a distance of $6m$. The smallest details the person recognizes at $6m$ viewing distance

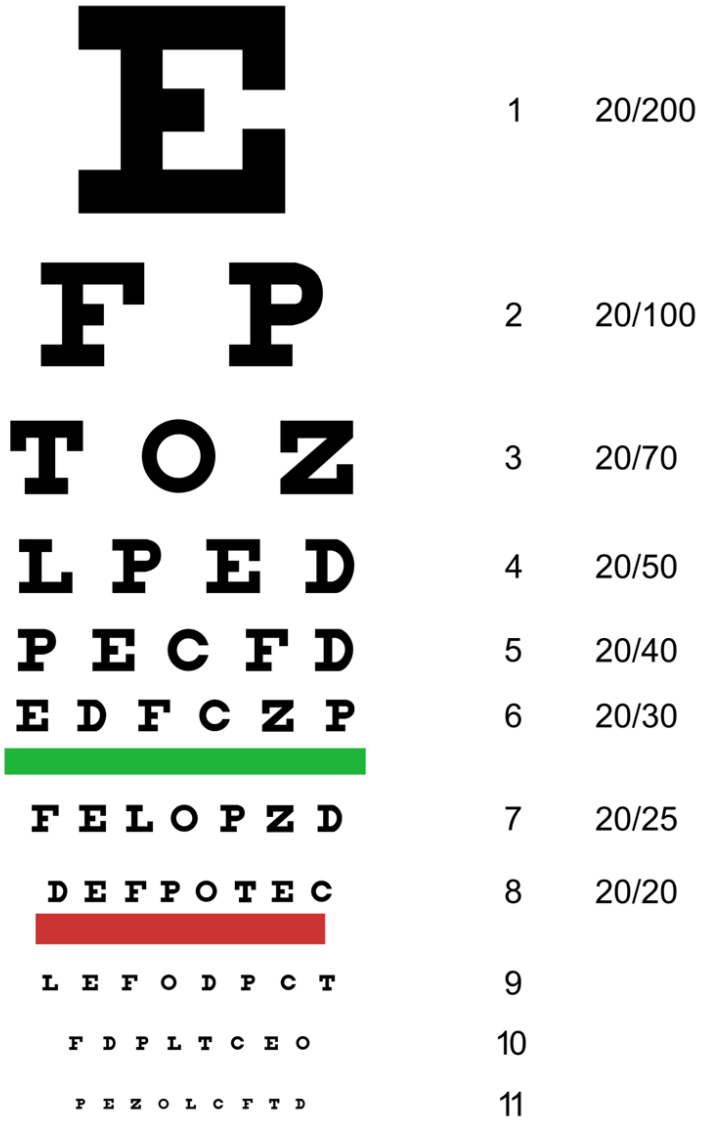

Figure 3.3: The Snellen chart is used in medical eyesight tests to determine VA. [Jef08]

decimal acuity	6 m	20 ft	arc minutes	LogMAR
2.00	6/3.01	20/9.87	0.50	-0.30
1.58	6/3.79	20/12.42	0.63	-0.20
1.26	6/4.77	20/15.64	0.79	-0.10
1.00	6/6.00	20/19.69	1.00	0.00
0.79	6/7.55	20/24.78	1.26	0.10
0.63	6/9.51	20/31.20	1.58	0.20
0.50	6/11.97	20/39.28	2.00	0.30
0.40	6/15.07	20/49.45	2.51	0.40
0.32	6/18.97	20/62.25	3.16	0.50
0.25	6/23.89	20/78.37	3.98	0.60
0.20	6/30.07	20/98.66	5.01	0.70
0.16	6/37.86	20/124.20	6.31	0.80
0.13	6/47.66	20/156.36	7.94	0.90
0.10	6/60.00	20/196.85	10.00	1.00
0.08	6/75.54	20/247.82	12.59	1.10
0.06	6/95.09	20/311.99	15.85	1.20
0.05	6/119.72	20/392.77	19.95	1.30
0.04	6/150.71	20/494.47	25.12	1.40
0.03	6/189.74	20/622.50	31.62	1.50
0.03	6/238.86	20/783.68	39.81	1.60
0.02	6/300.71	20/986.59	50.12	1.70

Table 3.1: Conversion between visual acuity scales: decimal acuity, Snellen fraction for the test distance of $6m$ and $20ft$, arcminutes and LogMAR (values rounded to the 2$^{\text{nd}}$ position after decimal point).

are of size $\sim 3.5mm$ (2 arc minutes), which is double the size (or double the angle) of what a person with normal sight would be able to recognize. In other words, the tested person recognizes details of a certain size that a person with normal sight would already be able to recognize at double the viewing distance. The tested person therefore has a VA of 6/12 or 20/40, which is equivalent to 0.5 decimal acuity.

Another unit used by lens makers and ophthalmologists is called *diopter*. A diopter is a measurement to describe the optical power of a lens to bend or focus light and is given by the reciprocal of the focal length measured in meters [Col01]. This means that a lens of X diopter is able to focus parallel light at $1/X$ meters from it. Colenbrander [Col01] presents a nomogram to demonstrate the relationship between letter size, viewing distance in diopters and visual acuity.

The World Health Organization (WHO) defines three stages of visual impairment and one for blindness, as shown in Table 3.2, using the reference value set of 20/20 expressed in feet, or 6/6 expressed in meters.

stage	Snellen fraction		decimal acuity
mild	<20/40 ft	<6/12 m	<0.5
moderate	<20/60 ft	<6/18 m	<0.3
severe	<20/200 ft	<6/60 m	<0.1
blind	<20/400 ft	<3/60 m	<0.05

Table 3.2: Stages of visual impairment, as defined by the WHO [WHO19], shown as Snellen fraction (in feet and meters) and decimal acuity. Smaller VA values correspond to more severe impairments.

Figure 3.4: Eyesight test. Image taken from the *National Eye Institute* [Nata]

3.2 Measuring Visual Acuity

VA is measured with an eyesight test, where optotypes are shown to the test subject (see Figure 3.4) who has to correctly recognize them. Different optotypes can be used, such as letters on a Snellen chart (see Figure 3.3), Landolt Cs (see Figure 3.1) or the Lea Symbols Chart [HNL80] designed specifically for children (see Figure 3.5).

The ISO standard ISO 8596 [Int09] defines test symbols and procedures to determine a subject's VA under daytime conditions. It also specifies how to use a Landolt C as optotype. To test for a VA of 20/20 or 1.0 decimal, the diameter of the ring should

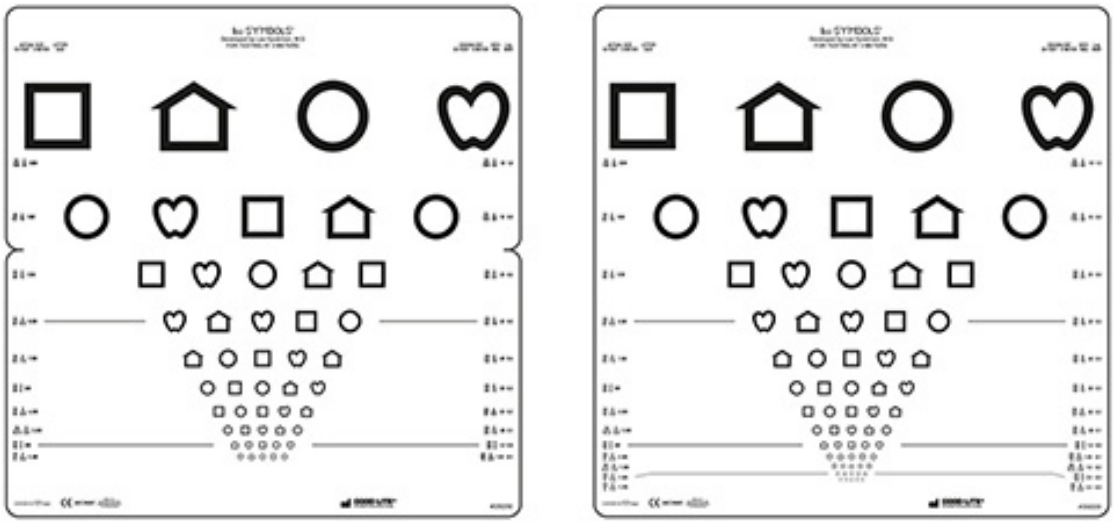

Figure 3.5: Lea Symbols Chart, used to test VA in children. Retrieved from [Hyv18].

be chosen such that the gap in the ring spans 1 angular minute when viewed from the selected test distance. This defines the gap size and the thickness of the ring and consequently the diameter of the ring. The position of the gap should be horizontally left or right, vertically up or down or diagonally in-between for a total of eight possible positions. The angular extent of the gap is the reciprocal of the decimal acuity value. Thus, to test for other VA levels, the rings can simply be scaled according to the decimal acuity value.

ISO 8596:2017 [Int17] suggest to use at least five rings per acuity level to be tested, with random positions of the gap. The set of five Landolt rings is displayed at a predefined distance. If the user recognizes the direction of the gap in the ring correctly for at least 60% (three out of five rings), the next set of smaller Landolt rings is used. A test subject has reached the limit of VA when less than 60% of rings can be correctly identified. The actual VA of the test subject corresponds to that of the previous correct row of test symbols in the Landolt chart.

There are also online vision tests, such as the Freiburg Vision Test ('FrACT') [B$^+$96], which treats VA as psychometric function by relating the percentage of correct answers to the size of the optotype. At very small sizes, this percentage corresponds to the guessing rate of $\frac{1}{8} = 12.5\%$. The algorithm zeros in on the threshold (which determines the final VA) by decreasing step sizes depending on the answers of the user. The likelihood of a threshold is calculated based on a set of correct and incorrect answers at certain sizes. After each trial a new threshold (the most probable) is calculated and the next optotype is presented at this threshold.

3.3 Perception in Virtual Reality

There are many more factors that can influence the perception and cognition of virtual or augmented content. Kruijff et al. [KSF10] present an extensive list of issues and problems, especially for augmented content, where the real physical environment and the capturing process play an important role.

The structure of the **environment**, the color scheme of the scene, variety of color, and the conditions of the environment when capturing can influence the perception of a user [KSF10].

When **capturing** (e.g. for video-see-through AR) the image resolution and filtering, the lens characteristics, exposure, color correctness and contrast of the camera, as well as the frame rate directly affect the image or video quality. These factors automatically result in images that are no longer perfect representations of the real world [KSF10].

Additionally, Kruijff et al. [KSF10] list a number of factors that affect perception, related to **augmentation**, such as registration errors, occlusion, layer interference and layout (resulting in foreground-background interpretation problems), or a rendering and resolution mismatch between virtual and real content.

The **display device** itself also has certain hardware limitations, such as display brightness, contrast, resolution, color fidelity, possible reflections, or latency, that can affect any virtual reality (VR) or augmented reality (AR) simulation. The field of view is also much smaller inside a head-worn display (HWD) as compared to the visual field of the human eyes [KSF10].

The particular **user** of an AR app also needs to be considered. How a user experiences depth cues (from motion parallax, perspective, the movement of the eyes, vergence, accommodation, pupil size, and inter-pupillary distance), depth disparity between virtual and real content, or a conflict between vergence and accommodation can affect visual perception as well [KSF10].

Koulieris et al. [KAS+19] discuss human vision, hardware limitations of near-eye displays and imperfect tracking technologies and rendering of light in context of VR and AR. The authors give a thorough introduction to the **human visual system** and its physiological and perceptual properties, such as optical properties, receptor processes, motor function, and cortical processing abilities. In addition to the factors listed by Kruijff et al. [KSF10], Koulieris et al. also state that when combining vision with other sensory channels, such as audio, vibration, or smell, they may affect each other. Furthermore, memory and attention can also affect processing of visual information and therefore cognition.

Our eyes are able to follow moving objects with smooth and steady eye movement. Pixels are visible for the whole duration of a frame, so moving objects are rendered by changing pixel values at discrete times (every frame) instead of continuously. This can create **noticeable blur**, called *hold-type blur*. This can be avoided by utilizing low-persistence modes that essentially turn pixels off after a very short time, showing a black screen

for the remaining duration of the frame. However, there are a few drawbacks to these techniques, including reduced brightness and potentially visible flicker [KAS+19].

Faithful representation and **rendering of light** are also limited by current algorithms and hardware capabilities and create a discrepancy between the real and the virtual world and affect how we perceive virtual content. In the real world, we are exposed to light intensities in a dynamic range of 14 orders of magnitude, while current VR HWDs usually only offer a dynamic range of two to three orders of magnitude [KAS+19]. Therefore, algorithms need to use effects to simulate light phenomena that cannot otherwise be displayed inside a HWD [LWK20].

As we can see, a multitude of factors affect our perception in VR, AR, and the real world. We selected some of the factors that are most relevant for our vision impairment simulations and calibrations in VR:

- Vision capabilities of participants (with normal or corrected sight).
- Resolution of the VR HWD.
- Fixed focal distance of the VR HWD, leading to a vergence-accommodation conflict.
- Possible misplacement of the VR HWD.
- Latency, refresh rate, and flicker of the display.
- Dynamic range and color correctness of the display.

When conducting user studies in VR with simulated vision impairments, it is important to recruit participants with normal sight to avoid degrading a user's vision more than intended by the simulated impairments. However, even people with normal sight have varying **vision capabilities** that need to be accounted for. Furthermore, the **resolution of VR headsets** is lower than that of the human eye. Therefore, users already experience a mild form of vision impairment when wearing a VR headset. A HWD also has a **fixed focal distance** relative to the eyes of the user. This can create a mismatch between vergence and accommodation [Kra15, KSF10] of a user's eyes, leading to visual fatigue after a certain time, and consequently to a further reduced VA. The lenses that are built into a VR headset focus the light in a specific area of the retina. Similar to a **misplacement** of glasses, an HWD that does not sit correctly on a user's head can cause images to be perceived as less sharp, resulting in an additional reduction of VA. A HWD might also have a noticeable latency, especially when used for video–see-through AR. Additionally, the **dynamic range** of most displays is significantly smaller than what a human eye can perceive [LWK20] and colors are mostly not represented as experienced in the real world and are dependent on the display calibration. The limited color bit-depth can even lead to banding or contouring artifacts [KAS+19]. Lastly, a low **refresh rate** could cause the brightness of a display to drop for a very short, but noticeable time, resulting in visual flicker.

We have to be aware of these factors if we want to achieve a consistent visual experience (of a simulated vision impairment) for all our users. Currently, we cannot account for all factors that affect human visual perception and are therefore not able to create a VR simulation that is indistinguishable from real life. However, we can target some of these factors to make the visual perception in VR as similar to real life as possible under current hardware and software limitations. We can also take caution in how we select the users we recruit for our studies; participants should have normal or corrected sight (wearing lenses), experiences in VR should be limited to short periods of time to avoid visual fatigue, and we have to make sure the headset is worn correctly. The low resolution of the display is a factor we can take into account in our simulation, as described in Section 6.2. Latency, dynamic range and color representations, as well as the refresh rate of a display, are hardware limitations that we can only mitigate by using modern HWDs (ideally including low-latency, high-dynamic-range (HDR), foveated displays with high refresh rates). However, making sure our software is fast enough to render at a maximum of 11ms per frame is crucial to avoid adding any additional latency. Furthermore, with the limited color range our HWD is able to display, it is important to perform calculations in the correct color space to avoid limiting color perception further. For a realistic simulation of vision impairments, such as cataracts, we also need to understand their impact on vision, which we will cover in the following section.

3.4 Eye Diseases

The WHO estimates that about 2.2 billion people worldwide are affected by vision impairments. These impairments include presbyopia (1.8 billion) and other refractive errors such as myopia or hypermetropia (123.7 million), cataracts (65.2 million), age-related macular degeneration (AMD) (10.4 million), glaucoma (6.9 million), corneal opacities (4.2 million), diabetic retinopathy (3 million), trachoma (2 million), and other eye diseases [WHO19].

Some impairments, such as refractive errors, are very common, and in most cases easy to correct with glasses or contact lenses. Other eye diseases, such as AMD, have a sustained impact on visual function and can lead to central vision loss [Nate]. While highly treatable, cataracts represent one of the leading causes of vision impairments (33%) after refractive errors (43%) and are, with 51%, the leading cause for blindness [PM12].

3.4.1 Refractive Errors

Refractive errors create a blurry vision (see Figure 3.6a) for affected persons and are the major cause (43%) of vision impairments worldwide [PM12]. The most common reason for this blurry vision is an increase or decrease in axial length of the eye. The condition is called *myopia* (also known as nearsightedness or shortsightedness) if the eye grows too long, or *hyperopia* (farsightedness or longsightedness) if the eye grows too short from front to back [Natf].

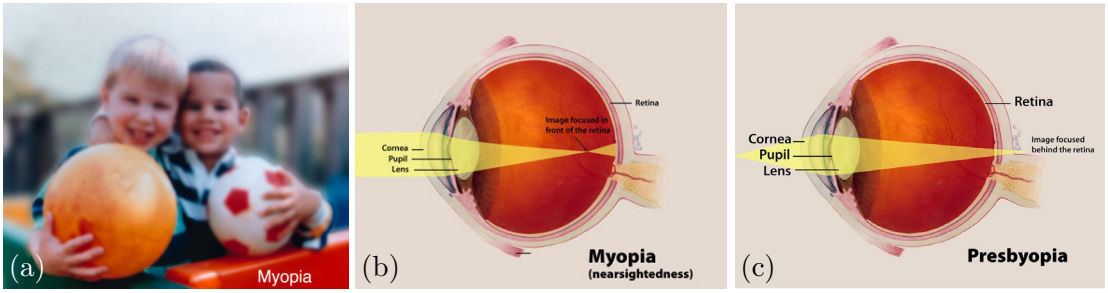

Figure 3.6: (a) blurry vision caused by myopia. Eyes affected by (b) myopia, (c) presbyopia or hyperopia focus images at a point in front or behind the retina. Images taken from the *National Eye Institute* [Nata].

Myopia causes blurry vision due to images being focused at a point in front of the retina (see Figure 3.6b), which creates a blurred image on the retina. People with myopia have good near vision, but vision gets blurred with distance [Natf].

Hyperopia, where eyes focus images on a point behind the retina (see Figure 3.6c), due to a too short eyeball or a deformation of the cornea, causes blurred vision of near objects, while far objects can appear clear [Natf].

Presbyopia (see Figure 3.6c) also causes blurred vision of near objects, due to aging and a reduction of accommodation abilities of the eyes [Natf].

3.4.2 Cornea Disease

The transparent front layer of the eye is known as the cornea. Different conditions can affect the cornea and therefore the vision of a person, such as injuries, allergies, inflammation (keratitis), dry eye or corneal dystrophies [Natd].

Pink eye, also called allergic conjunctivitis, can cause swelling and redness, itchy burning and watery eyes. Affected people can experience blurry vision and sensitivity to bright light [Cen].

Keratitis is an eye infection linked to wearing contact lenses. This condition can occur when contact lens wearers do not take care of their lenses as instructed, increasing the possibility of germs invading the cornea. Viruses, bacteria, fungi or parasites can then cause an inflammation of the cornea, leading to irritated, red eyes, pain, sensitivity to light, blurry vision and watery eyes [Natd].

Dry eye is a very common condition, where the eyes don't produce enough tears, which leads to red eyes and scratchy, stinging or burning feelings in the eyes and can also cause vision problems, such as blurry vision or sensitivity to light [Natd].

Corneal dystrophies, such as *keratoconus*, *Fuchs' dystrophy*, or *lattice dystrophy* and *map-dot dystrophy* can cause fogging or a swelling of the cornea, or material build-ups in the cornea. Besides itchy feelings and pain, symptoms can include blurry vision,

Figure 3.7: Depiction of (a) vision with Fuchs' dystrophy (left part of image) as compared to the original (right part of image) and (b) photo of an eye with advanced Fuchs' dystrophy. Images taken from [Par].

clouded vision and sensitivity to light [Natd]. Figure 3.7 shows how a person with Fuchs' dystrophy might see the world and a photo of an eye affected by advanced Fuchs' dystrophy.

3.4.3 Age-Related Macular Degeneration

The macula is the central area of the retina, containing the most photoreceptors, with the highest density at the fovea, which is responsible for the central vision. AMD is a leading cause of vision loss, affecting primarily people over 50 years of age [Nate]. AMD does not cause total blindness, but the reduction or loss of central vision can have a high impact on perception (see Figure 3.8a) and make tasks such as reading, cleaning, cooking or recognizing faces challenging [Nate]. There are two main types of AMD:

Dry AMD is characterized by deposits that build up beneath the retina and can further lead to a destruction of photo-receptive cells.

Wet AMD causes abnormal blood vessels to grow under the retina, which leak into the retina and finally create scar tissue.

All stages of AMD can affect the vision differently [Sho02]. Symptoms primarily affect the center of the field of view and include blurry vision, reduced brightness, loss of central vision and distorted vision, often described as "strait lines looking wavy".

3.4.4 Cataracts

Cataracts are opacities in the lens of the eye (see Figure 3.9), which occlude parts of the visual field and can also lead to vision loss when left untreated. Depending on their characteristics and the region of the lens that is affected, cataracts are categorized as *nuclear*, *cortical*, or *posterior subcapsular* cataracts [MB11].

Figure 3.8: Depictions of (a) vision with AMD, compared to (b) normal vision and (c) cataract vision. Images taken from the *National Eye Institute* [Nata].

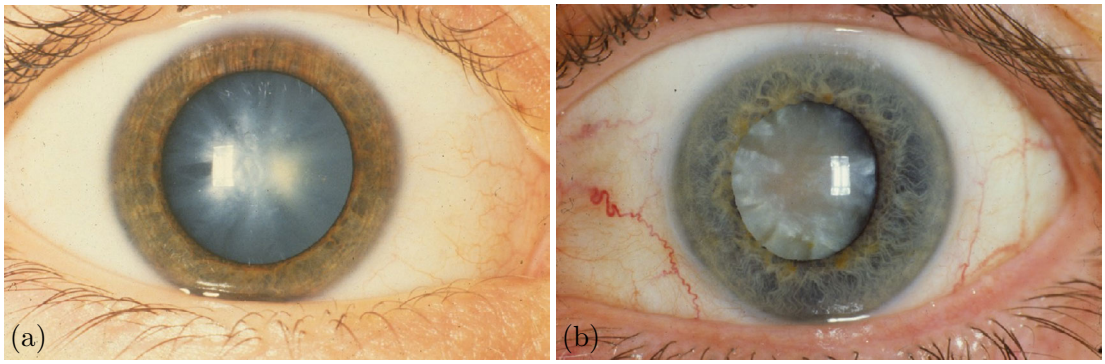

Figure 3.9: (a) White congenital cataract and (b) hyper-mature age-related cortico-nuclear cataract with brunescent (brown) nucleus. Images taken from the *National Eye Institute* [Nata].

Nuclear cataracts manifest as a ubiquitous yellow tinting (or clouding) in one's vision, with increased straylight. This is due to an accumulation of yellow-brown pigment or protein in the central area (nucleus) of the lens, which creates a homogeneous clouding of the lens, often with a yellowish/brownish tint, and results in increased light scattering [MB11].

Cortical cataracts appear as dot-like opacities, peripheral radial opacities (called "shades"), or spoked opacities near the periphery. These are caused by an opacity forming at the lens cortex, due to protein aggregation or damage to the fibers in this area. Cortical cataracts with spoked opacities near the periphery are the most common form of cataracts [MB11].

Posterior subcapsular cataracts are caused by defective fiber production in the lens and result in opacities forming at the posterior pole of the lens, perceived as dark shadows in the center of one's vision. It is the least common of the three cataract forms mentioned here. Because of its location near to the visual axis, its effect on vision is very severe, even for a low density of defective fibers [MB11].

These three forms of cataract can develop to different extents within the same eye, and their severity can be graded in a slit-lamp examination in *mydriasis* (dilation of the pupil) [CWS+93]. Figure 3.8c shows how cataract vision could look like.

According to the NEI [NEIa] and reports from ophthalmologist and patients, the following symptoms can be caused by cataracts:

- Cloudy or blurry vision (reduced VA)
- Faded colors (reduced contrast)
- Tinted vision (color shift)
- Troubles seeing at night (bloom/glare)
- Increased sensitivity to light (bloom/glare)
- Halos around lights
- Double vision

The effect of lens opacities on vision depends on their location and on the pupil size. In daylight, when the pupil diameter is small, only opacities within the pupillary zone are likely to affect vision. If ambient light is further reduced and the pupil diameter becomes larger, vision is further affected as an increasing amount of straylight (light that is scattered by parts of the eye, due to optical imperfections like particles in a clouded lens [VdB86]) falls on the retina. [MVRVDB+09]

CHAPTER 4

Related Work

4.1 Assistive Technology

There have been many efforts to develop technology that can assist people with vision impairments in their everyday lives.

Hwang and Peli [HP14] worked with Google Glass devices to develop vision enhancement tools in augmented reality. They developed an augmented reality (AR) application using Laplacian edge detection as edge enhancements technique targeted at improving the visual perception of people with central vision loss. The authors used diffuser film to simulate vision loss in their user study. Guo et al. [GCQ+16] developed a smartphone AR app that assists a users with vision impairments when using a real-world interface (such as buttons on a microwave). Pundlik et al. [PYL+16] also used a smartphones, but connected to Google Glass, to provide low-vision users with an augmented magnification display via a Google Glass screen sharing app. With this system, the user can move their head to control which area of the displayed smartphone screenshot should be magnified and is presented with the respective magnified image part inside the google glass goggles. To assist people with low vision in search tasks, Zhao et al. [ZSKA16] developed *CueSee*, a system for an AR head-worn displays (HWDs) that is able to recognize a product in a store automatically and provide visual cues in the field of view of the user to make this product easier to find. Following the idea to "*augment rater than replace*", Stearns et al. [SFF18] presented an AR head-worn magnification aid, using a Microsoft Hololens in combination with a handheld smartphone or finger-worn camera. Reichinger et al. [RCW+18] made tactile reliefs of paintings with interactive audio guides to also let blind or visually impaired people experience art. To combat vision impairments caused by color vision deficiency (CVD), Langlotz et al. [LSZ+18] developed computational glasses, called ChromaGlasses, a head-mounted display that is able to compensate for CVDs. In an effort to mitigate the vergence-accommodation conflict (which can cause visual fatigue and result in blurry vision) and end the need to use prescription lenses

for AR displays, Chakravarthula et al. [CDAF18] presented auto-focus AR glasses that are able to dynamically and automatically adjust their focus. Sutton et al. [SLI19] discuss the different types of computational glasses to compensate for vision impairments. Zhao et al. [ZCH+19, ZKC+19, ZKR+20, ZSA15] also worked on developing simulations to compensate for low vision. For further information on assistive technology is also provided by Hu et al. [HCZ+19], who compiled a whole list of wearable and portable assistive technology devices from assistive canes to assistive glasses featuring direction recognition, color contrast enhancement, obstacle detection, navigation, text reading or other vision enhancement techniques.

Please note that besides assistive technology, there was also software developed that was not just accessible, but specifically designed for the use of people with vision impairments [APLBB18, TM20, WBW+19, ZBB+18].

Sometimes similar methods are used for the development of assistive technology and for the simulation of vision impairments. In the following section we will have a closer look at research aimed at simulating vision impairments as this is more closely related to the work we present in this thesis.

4.2 Vision Impairment Simulations

There has been some research on simulating visual impairments across different display modalities and for different purposes like educational purposes, raising awareness, accessibility inspection, design aids or user studies. We will now give an overview of different approaches.

4.2.1 Goggles

Physical goggles with special lenses have been used to recreate the effects of eye diseases, run studies [AT07] and educate people about how these impairments affect perception.

Figure 4.1: Commercially available vision simulator goggles from Vision Rehabilitation Services LLC. Image taken from [Vis19].

Zimmerman [Zim13] created the first vision simulation product in 1979. The goal was to help people with normal sight better understand the impact of low vision. The *Zimmerman Low Vision Simulation Kit* is a set of non-virtual reality (VR) goggles with exchangeable lenses that each simulate different impairments.

Wood et al. [WCCC10] also used modified goggles in a study to investigate the potential effects of simulated visual impairments on night-time driving performance and pedestrian recognition under real road conditions. They simulated cataracts and refractive blur, and measured sign recognition, avoidance of low contrast road hazards, time to complete the course, and lane keeping. Their results showed that the simulated visual impairments had a significant impact on driving performance, with cataract being the impairment leading to the largest degradation.

Hwang et al. [HTBGP18] investigated the effect of cataracts on night-time driving, specifically how glare reduces the visibility of objects or pedestrians. The authors used a headlight glare simulator and simulated cataracts with Bangerter diffusion foil (a diffuse, translucent foil) on plano lenses. Their study showed a combination of headlight glare and simulated cataracts significantly reduces the ability of drivers to recognize pedestrians.

Similarily, Zagar and Baggarly [ZB10] used a set of physical goggles in order to help student pharmacists understand how patients with various ocular diseases and visual impairments might interact with medication. They developed individual sets of (non-VR) goggles to simulate glaucoma, cataracts, macular degeneration, diabetic retinopathy, and retinitis pigmentosa, and used them to rate the presence and severity of disease-specific characteristics.

Physical goggles (Figure 4.1) designed to simulate the decreased visual acuity (VA) and increased glare of generic cataracts are available commercially from *Vision Rehabilitation Services LLC.*[Vis19], but with the express disclaimer that they are not intended to replicate a specific user's visual impairment.

Although real goggles might be suitable for educational purposes, they limit the experiment environment of user studies to the real world, where environmental changes like fire or smoke are hard to simulate safely. Furthermore, each set of goggles only simulates one particular vision impairment. They are not adjustable to the vision capabilities of users or to simulate different levels of severity of a vision impairment and have limited field of view and immersion.

4.2.2 2D Images

A widely used approach to convey the effects of vision impairments is to modify 2D images. There is an extensive body of research on simulating CVDs dating back to at least 1988, when Meyer and Greenberg [MG88] implemented the Farnsworth-Munsell 100-hue test on a computer to test users for CVD on a color television monitor. Moreover, they synthesized pictures that showed the reduced color vision of dichromats by mapping a full-color image into the reduced color space perceivable by dichromats.

Figure 4.2: Simulation of (A) glaucoma and (B) age-related macular degeneration (AMD) by Banks and Crindle. Reprinted from [BM08].

Brettel et al. [BVM97] also simulated dichromacy for users with normal vision by modifying images. They represent colors as vectors in the LMS color space and use an algorithm that projects these color onto a reduced surface polygon.

Another work that leverages LMS color space is presented by Viénot et al. [VBM99], who constructed replacement colormaps to evaluate color schemes for protanopes and deuteranopes. In this work they represent a dichromat's colour space by two half-planes in the LMS color space and use their technique to modify videos for Cathode Ray Tube (CRT) monitors.

Later, Machao et al. [MOF09] presented a physiologically-based model for simulating CVD by interpreting CVD as changes in the spectral absorption of photoreceptors. This allowed them to also simulate anomalous trichromacy by shifting the spectral sensitivity function in the LMS color space. They implemented their algorithm in MATLAB and integrated it into a visualization system.

Similar to Machao et al., the goal of Flatla and Gutwin [FG12] was to simulate dichromacy and also anomalous trichromacy. Their approach was to measure color perception abilities of users during a calibration procedure and create a personalized simulation based on these measurements. The authors used a color vision test on a computer screen, displaying colored Landolt Cs on a gray background and recorded which colors could be recognized by the user and which could not. This information was then used to modify the colors of an image to fit into the shifted or reduced color space. Calculations were done in the perceptually-uniform *1976 CIE L*u*v** color space. This kind of color test and calibration could also be done in VR or AR and added to our own simulation framework.

Banks and Crindle [BM08], attempted to recreate the visual effects of several ocular diseases, such as glaucoma or AMD (see Figure 4.2) by combining different image-processing effects and creating overlays and filters for 2D images or rendered images from a 3D scene (viewed on a desktop display).

Hogervorst and Van Damme [HVD06] also modified 2D images to give unimpaired persons insight into the problems people with vision impairments face every day. They conducted a user study to evaluated the relationship between blurred imagery and VA. When measuring the VA with eye-sight tests using the *Landolt C*, the authors found a linear

correlation between VA and a just-recognizable threshold for blurring an image. We build upon these findings in our calibration procedure (see Section 6.3), using a blur filter to adapt a user's vision to a certain level of VA.

Web based simulators such as VisionSimulations.com [vis] modify 2D images to raise awareness or to evaluate the accessibility of websites. Leventhal [Aar13] for example created an extension for the Chrome web browser that allows the user to inspect websites with simulated vision impairments such as low VA, low contrast sensitivity, CVD, visual snow, glare, ghosting, cataracts, nystagmus, floaters, obstructed central or peripheral vision. Since there is no eye tracking integration, effects are not gaze dependent. The author also states that "*simulations are not medically/scientifically accurate*".

Goodman-Deane et al. [GDLC+07] developed a tool in Adobe Flash to simulate vision and hearing impairments. The tool can simulate cataracts, AMD, loss of accommodation, glaucoma and color blindness and levels of severity can be adjusted. The simulator was presented at ASSETS'07 as a software tool for aiding design tasks.

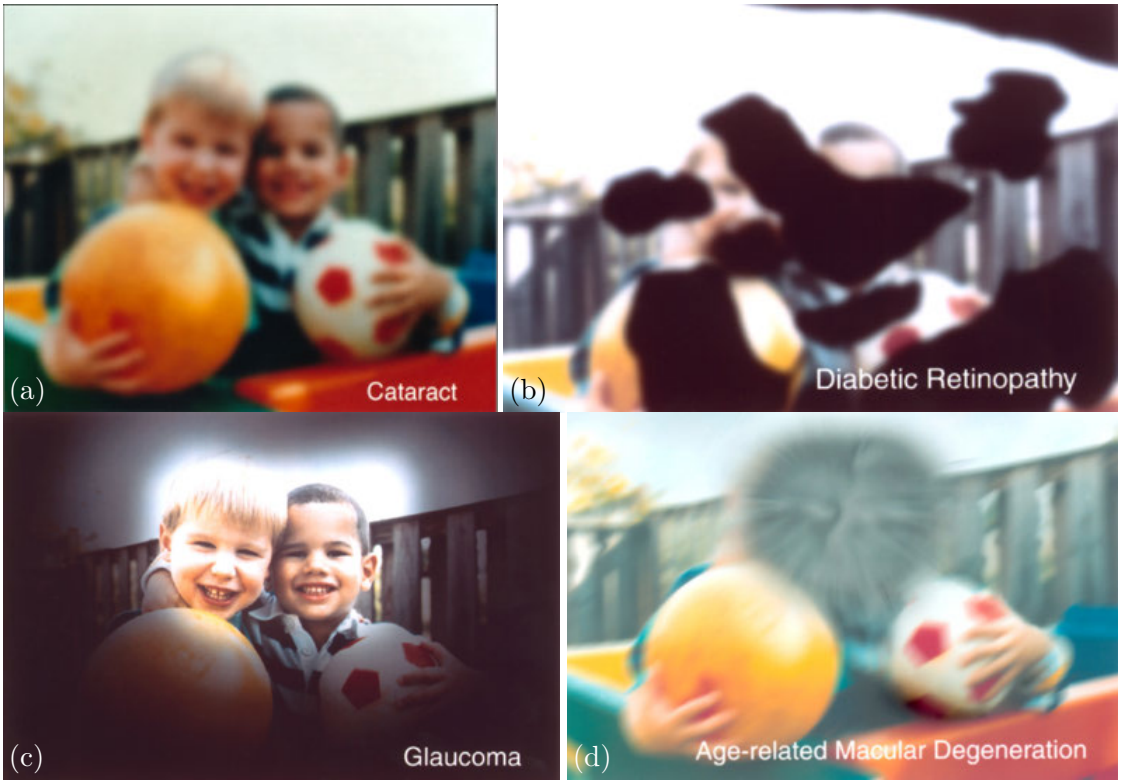

Figure 4.3: Depiction of vision with (a) cataracts, (b) diabetic rethinopathy, (c) glaucoma and (d) age-related macular degeneration. Images taken from the *National Eye Institute* [Natb].

Very well-known depictions of vision impairments are provided by the NEI [Natb]. These images (see Figure 4.3) inform a lot of research work in the area of vision impairment

simulations (e.g. [AFF15]). However, it should be noted that these images show simplified versions of the respective vision impairments and can lead to misconceptions about vision impairments [TM20]. This becomes especially apparent when looking at images of vision with glaucoma. The effects of glaucoma are not black or dark areas in the periphery of one's vision. The visual field of people with glaucoma becomes smaller when they lose more and more of their peripheral vision, a circumstance that is hard to visualize in a 2D image.

While 2D images are a cheap and easy way to visualize impaired vision, these static images do not allow calibrating for individual users, reacting to eye movements or providing an immersive experience.

4.2.3 3D Simulations

Simulations in 3D environments (like in 3D computer games) offer more possibilities than 2D images to investigate and understand vision impairments, as they provide a higher level of immersion.

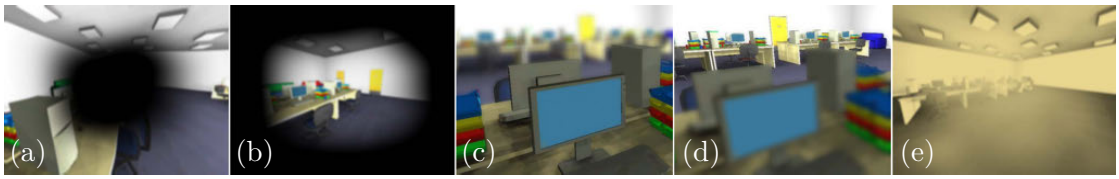

Figure 4.4: Simulation of (a) AMD, (b) glaucoma, (c) hyperopia, (d) myopia and (e) cataracts by Lewis et al. in a game-like 3D environment. Reprinted from [LSB12].

Lewis et al. [LBCM11] used the Unreal Engine 3 to apply post-processing effects to simulate common eye diseases in a 3D game or explorable environment on a desktop screen. The systems were evaluated by opticians, specialists and test users, and even though the simulated symptoms are not fully accurate, they were still deemed suitable to raise awareness and gain a good understanding of the effects of visual impairments. Yet the severity of symptoms is not controllable and the vision impairments are not adjusted to each individual user's vision capabilities. A later version of this system [LSB12], using the Microsoft XNA framework to simulate AMD, glaucoma, hyperopia, myopia and cataracts (see Figure 4.4), provides means to adjust the simulated vision impairments, but still does not take vision capabilities into account. We also chose a game engine (Unreal Engine 4 [Epic]) to implement our application. However, to achieve a more realistic situation than a typical computer game played on a standard monitor could provide, we deemed it vital to use VR for our study, especially in order to be able to measure distances and angles that can be compared to real-world measurements.

4.2.4 Virtual Reality Simulations

With the advent of modern VR and eye-tracking technology, it became possible to graphically simulate vision impairments in VR using HWDs, but research in this area

started even before modern HWDs were available.

In 2000, Ai et al. [AGR+00] already developed a VR simulation of glaucoma, diplopia (double vision) and AMD. Their goal was to teach medical professionals about the impact of vision impairments and increase awareness among relatives and friends of patients. The authors used image masks, based on clinical data (measuring visual fields of patient), to simulate visual field loss caused by glaucoma. To simulate diplopia, incorrect viewing directions were used and AMD was realized by warping the central area of the field of view. Ai et al. used the *ImmersaDesk* for their simulation, a CAVE-derived, projection-based VR display in combination with shutter glasses, which provides stereo vision with head tracking.

Using the same hardware, Jin et al. [JAR05] developed a system to educate and train ophthalmologists, physical therapists or students by letting them navigate through a model of a typical home with simulated vision impairments. The authors provided a complex eye anatomy model for simulating visual impairments in VR based on medical measurements. They used a scotoma texture, created from perimetry exam data from real patients, to define regions of degraded vision. This texture is the same for every user and does not account for a user's vision capabilities. Jin et al. [JAR05] also tried to recreate the effects of color deficiency *protanopia* (an absence of red cones) in a virtual environment (VE), using a database associating colors perceived with normal vision and and those with protanopia.

Coggins et al. [CARM15] developed SonicWalker, a game demo simulating blindness in VR. Using an Oculus Rift HWD and an Xbox 360 controller, users have to navigate through a virtual city model with no visual information displayed, relying on information from simulated city sounds alone. The simulation suggests that blindness implies the complete absence of light and visual information. While there are such cases where, it is not the medical norm. According to the WHO [WHO19] all people with VA worse than 0.05 decimal acuity (20/400 ft or 3/60 m) is classified as *blind*.

Väyrynen et al. [VCH16] targeted their research towards giving architectural designers an idea of the challenges with which visually impaired people are often confronted. They used the Oculus Rift and Unity3D to create a system for evaluating the effect of visual impairments in path-finding tasks in a 3D city model. Impairments like AMD, cataracts, myopia or glaucoma (see Figure 4.5) are simulated based on images from online simulators or hardware-based simulations and implemented using standard effects in Unity3D. This is similar to our first version of macular degeneration and cataract, which served to create some task variety in our first user study on the influence of reduced VA on maximum recognition distances (MRDs) (presented in Chapter 7), in Unreal Engine 4. However, by applying our calibration technique (see Section 6.3), we are able to adapt the reduced VA, one of the major symptoms of these diseases, to the actual vision capacities of each individual user, which provides a consistent experience for each user regarding reduced VA. The cataract simulation of Väyrynen et al. is described as consisting only of a flare-layer component in each virtual camera and a lens-flare component for each scene

Figure 4.5: VR simulation of (a) normal vision, (b) macular degeneration, (c) cataracts, (d) myopia, and (e) glaucoma by Väyrynen et al. Reprinted from [VCH16].

light source (Figure 4.5c). In this thesis we present a more complex simulation of cataract vision, informed by medical expertise (see Section 5.1).

Maruyama et al. [MKD16] used Unity and the Oculus Rift DK2 to develop a virtual accessibility evaluation system. The system creates a simulation in which a digital human model (DHM) moves autonomously through a VE that was created using structure from motion (SfM). With the HWD, a user can perceive the VE with the simulated vision impairments from the DHM's point of view. The goal was to identify locations with missing or unclear signage, look at proposed rearrangements and investigate the accessibility of signage with a virtual eyesight simulator (VES). To build this VES, Maruyama et al. obtained impairment filters for blurred vision (realized with a Gaussian blur) and color blindness (protanopia and deuteranopia) from the Unity asset store. The severity of each impairment filter can be adjusted via the game-pad controller, but unlike in our framework, simulations of complex eye disease patterns are not included.

Another VR application investigating the impact of vision impairments on locomotion in urban environments was presented by Wu et al. [WAAB18]. The authors assessed the street crossing behavior of pedestrians with simulated AMD in VR. The central loss of vision caused by AMD was simulated by using an opacity filter to overly a black circle in the center of the field of view, and blurring the surrounding circular area. To estimate which amount of blur represents which level of VA, 8 people were asked to read a Snellen chart, inside a VE. This is similar to the VA calibration (see Section 6.3) we developed for our first user study (see Section 7). However, while we calibrated reduced VA for every user, Wu et al. collected measurements of all users to relate their blur size to VA and fit it to an exponential curve. They used an NVis SX60 HWD with an Arrington eye tracker to move the simulated impairment with the gaze of the user. Other effects like distortion or desaturation were not included in their AMD simulation.

Choo et al. [CBW+17] introduced their system *Empath-D* to enable *Empathetic User Interface Design*. They envisioned the use of VR/AR displays to allow designers to test the usability and accessibility of their websites or applications. A Samsung Gear VR with a Galaxy Note 4 was used as AR device. Their application was aimed at designing for motor problems, using impairment profiles, representing the interactions of a person with a certain impairment, as well as visual impairments. The authors used Unity's Gaussian blur to simulate cataracts, describing the eye disease as "[...] *a vision impairment that is experienced as blurred vision*". Although blurred vision is one of the predominant symptoms caused by cataracts, simulating cataracts only with blurry vision

is not medically sound, as we discuss in Section 3.4.4. The simulation should therefore be more appropriately called a simulation of refractive errors.

The Empath-D system was later extended by Kim et al. [KCL+18] to work in a purely VE for accessibility-aware design of smartphone apps, using a commodity VR HWD. A physical smartphone and the hand holding it are tracked (including finger tracking) and the app that should be evaluated for accessibility is mapped onto the physical smartphone. The improved version of Empath-D features a glaucoma simulation with a blurred inner circle in the center of the field of view and black periphery around it. The previous cataract simulation was extended with an unspecified contrast reduction filter. Similar to our simulations, the intensity of each effect is adjustable at run-time. However, the included vision impairment simulations in the Empath-D system are still simplified versions of the respective eye diseases and the system lacks support for eye tracking, which is crucial for a realistic simulation of vision impairments that affect different areas of the visual field differently, such as glaucoma, cortical cataracts, or posterior subcapsular cataracts do.

In a recent study, Choo et al. [CBL19] evaluated their Empath-D system with its augmented virtuality impairment simulation for its effectiveness in enabling app designers to improve the accessibility of apps and tested it on a mockup of the *Instagram* app. They recruited four elderly participants with cataracts to investigate their usability challenges when using mobile apps, but did not do side-by-side comparisons with their cataract simulation. In our research, we go one step further and let people with cataracts on one eye compare their cataract vision to our simulation observed with their non-cataract affected eye.

With the same goal as Choo et al. [CBW+17, CBL19] and Kim et al. [KCL+18], Stock et al. [SES18] presented a research platform for testing apps and devices for accessibility for people with vision impairments such as cataract, glaucoma and AMD. They also used Unity and simulated vision impairments with adjustable post-processing effects based on previous work [AFF15, BM08, JAR05, LBCM11, VCH16] and information from the NEI. Their application also allows to integrate ophthalmologic perimetry data visualize visual field data of patients, but does not consider vision capabilities of users and was not evaluated in a user study. Our goal is also to provide a framework that can be used for accessibility evaluations and can be extended to include various vision impairments simulations. In future work, importing of ophthalmologic data similar to Stock et al. could easily be integrated into our framework as well.

Zavlanou and Lanitis [ZL19] developed a VR simulation of age-related visual deficiencies (using the Oculus Rift CV1 VR HWD) in order to detect design flaws in pharmaceutical package design. They simulated cataracts by blurring the image and reducing contrast and brightness. For their AMD simulation they used an overlay in the center of the field of view, similar to the effect we use to darken the central vision for our AMD simulation. In contrast to Zavlanou and Lanitis, we also include other effects such as distortion or desaturation in our AMD simulation, and use eye tracking to move effects according to

the gaze of the user. The realism of the vision impairment simulations of Zavlanou and Lanitis was not evaluated with patients or medical experts.

Alexander et al. [ANK+20] presented a research demo, simulating AMD in a virtual home environment, using Unity 3D and an HTC Vive. Implementation details are not provided, but images of their AMD simulation show only a dark shadow in the central field of view, suggesting that their simulation is a simplified version of AMD. Their application is designed for a physical diagnosis course at university, to help medical students develop empathy for geriatric patients. We also see the training of medical personnel as one mayor use case for our vision impairment simulations and would like to integrate similar training tasks in our framework in future work.

4.2.5 AR Simulations

McAlpine and Flatla [MF16] extended earlier work of Flatla and Gutwin [FG12] on personalized CVD simulations, to work in real time on mobile devices. The type and severity of a person's CVD was assessed during a calibration procedure to later simulate the reduced color vision of that person. To allow for real-time performance, a look-up table for all possible RGB values is generated to map the original RGB values of any image to the personalized CVD simulated values. This look-up table is then used at run-time to modify the live video feed from a mobile device's camera and show it on the display. The goal of their work was to allow people with normal vision to explore different severities of CVD. Similarly, the aim of our work is to create simulations that allow people with normal eyesight to experience different vision impairments, but also eye disease patterns, including multiple symptoms.

Using the Oculus Rift HWD and a PlayStation 4 camera as AR setup, Ates et al. [AFF15] conducted a user study with focus on accessibility inspection of user interfaces. Their simulation of vision impairments (see Figure 4.6) is based on photos of the NEI [NEIb] and implemented through a VR media player that can render stereoscopic video files. The level of intensity of the simulated impairments can be adjusted via keyboard. However,

Figure 4.6: AR simulation of (a) macular degeneration, (b) diabetic rethinopathy, (c) glaucoma, (d) cataracts, (e) protanopia (color blindness) and (f) diplopia (double vision) by Ates et al. For these visualizations the authors applied their developed filters onto 2D images, using a VR media player. We can expect a significantly blurrier image when viewed on the Oculus Rift, due to the resolution of this HWD, also mentioned as limitation by the Ates et al. Reprinted from [AFF15].

unlike in our approach, the existing VA of the user is not taken into account when calibrating the visual impairment. The accuracy of the simulation was not evaluated, but the authors compared their tool to a smartphone-based simulator in a qualitative study and found a significantly higher level of immersion and potential for detecting accessibility problems with their solution. The authors state that the low resolution of the HWD limits their tool, as it does not allow reading text on a mobile phone. Their implemented impairments are simplified approximations and do not attempt to recreate the impaired vision of specific persons. The cataract simulation is restricted to a Gaussian blur and does not include other symptoms. AMD and glaucoma are simulated with a Gaussian blur mixed with black pixels, and for diabetic retinopathy, they used a texture overlay with black areas. Eye tracking is not supported.

Werfel et al. [WWFG16] developed an AR and VR system for empathizing with people with audiovisual sense impairments, which also includes a cataract module. They modeled audiovisual sensory impairments using real-time audio and visual filters experienced in a video–see-through AR HWD (IDS UI-3240-LE-C-HQ industry camera mounted on an Oculus Rift DK2). Visual impairments, such as macular degeneration, diabetic retinopathy, and retinitis pigmentosa were modeled according to information and illustrations from the German Association for the Blind and Visually Handicapped (DBSV). Their cataract simulation was realized with a blur, decreased saturation, and modified contrast and brightness, but without eye tracking for gaze-dependent effects.

The work by Jones and Ometto [JO18] aims not only at creating a teaching or empathy aid, but also a tool for accessibility evaluations. Their VR/AR simulation of different visual impairment symptoms allows adjusting symptoms, integrates eye-tracking data, and achieves near real-time rendering. We take their approach one step further and simulate complex eye diseases, such as cataracts, AMD and cornea disease, comprising multiple symptoms, with eye tracking, in real time, making it possible to use these simulations in VR or AR HWDs while minimizing the risk of VR sickness.

In more recent work, Jones et al. [JSCWBC20] used their developed software *OpenVisSim* to simulate glaucoma with a gaze-dependent region of variable blur, defined by a scotoma texture, which was generated from perimetric data from a real patient. Using a VR scene with the FOVE HWD, and an AR mode, featuring an HTC Vive Pro Eye HWD with ZEDmini stereoscopic cameras mounted on top, they measured task completion time of two different search tasks. Their participants were people with healthy eyesight, experiencing two types of simulated glaucoma. Results showed that task completion times increased with simulated impairments. Jones et al. also conducted experiments under photopic and mesopic lighting conditions, which yielded significant difference. The glaucoma simulation used in their study does not take vision capabilities or hardware constraints into account, and currently only consist of the mentioned gaze-dependent region of variable blur, which is a simplification of this vision impairment. However, the used *OpenVisSim* software also offers simulations of some other effects that could be used to extend this simulation in future work.

In recent work by Aniruddha et al. [AZTZ19] the authors proposed a parameterized

model to simulate AMD. Their model includes modeling luminance degradation, the perceptual deficit region, rotational distortion and spatial distortion (as spatial shift defined by a vector field). Similar to Aniruddha et al., we chose to include effects for distortion and darkening of the central vision, but also added desaturation and reduced contrast, as advised by our medical experts. With their model, the Aniruddha et al. expect to be able to use patients affected by AMD on one eye in future studies to adjust their simulation parameters and create a parameterized model of their own vision impairment, similar to our study with cataract patients. The authors further propose to apply the inverse of the adjusted parametric model to compensate the vision impairment of affected people. They conducted a small preliminary study (Zaman et al. [ZTZ20]) with healthy participants, presenting them with already simulated AMD in one eye. Participants then had to adjust parameters of the model in order to replicate the existing simulated AMD for the second eye. Even though this approach is promising, it has not been tested with people who actually have AMD, which makes it hard to verify whether the simulation is able to replicate a user's vision with AMD sufficiently well for the inverse model to correctly compensate the vision impairment instead of distorting the user's vision even more. The authors plan to recruit 80 participants, including 50 people with AMD with well defined scotomas. For this approach to work, it is necessary to have participants with corrected vision in one eye, while the other eye is still affected. Unlike for cataracts, there is treatment to slow down the progression of AMD, but no cure for the disease and it usually affects both eyes (although late AMD can also just affect one eye) [Natc]. It might therefore be extremely difficult to find participants for such a study. Another limitation of this work compared to our simulation is the lack of eye tracking, an important feature for realistic vision impairment simulations, especially when the impairments affect different areas of the field of view differently.

There are also commercial smartphone applications available that simulate vision impairments. For example, the Novartis ViaOpta Simulator [Nov18] for Android and iOS processes the live smartphone camera feed to address a broad set of impairments, including vitreomacular traction syndrome, diabetic macular edema, glaucoma, and cataract. However, the provided cataract simulation affects only VA and color vision, can be adjusted only in severity and not per symptom, and supports just one generic cataract type. Another commercially available iOS smartphone app is VisionSim [Bra], developed by Braille Institute of America. It provides simulations for AMD, cataracts, chronic open-angle glaucoma, corneal edema, diabetic retinopathy, homonymous hemianopia, retinal detachment, and retinitis pigmentosa. While smartphones are ubiquitous and thus can reach a broad audience, they have a far smaller field of view than current VR head-worn displays when held at a comfortable distance, are monoscopic, and do not support eye tracking for simulating gaze-dependent effects.

4.3 Summary

Simulations of vision impairments have been done using modified goggles, 2D images, 3D, VR or AR simulations, but were limited in their realism, immersiveness, and/or

adjustability.

Most existing approaches of vision impairment simulations are targeted at educational or demonstrative purposes and do not take the user's actual vision capabilities or hardware limitations of the VR/AR headsets into account. Hence, they are not feasible for user studies and often only provide very simplified simulations of eye diseases. Hardly any previous work uses eye tracking for gaze-dependent effects, and only some simulations are informed by medical expert knowledge or evaluated with patients who could give feedback, based on their first-hand experience with the respective impairments.

So far, the actual influence of vision impairments on the MRD has not yet been thoroughly investigated or quantified. Hence, legal regulations and norms only provide informal recommendations based on assumptions derived from medical definitions of VA. As we see the population with vision impairments and eye diseases rising, intensive research in this area should be conducted, especially for environments for people with special needs, such as the elderly.

We try to contribute in this area with our research. In contrast to most prior work, we collaborate with ophthalmology experts to achieve a plausible simulation, and each of our simulated effects is highly adjustable and can be applied to one or both eyes. This allows us to introduce a new methodology for finding parameters for realistic vision impairment simulations by conducting experiments with patients.

CHAPTER 5

Simulating Eye Disease Patterns

This chapter is based on the following publications:

- Katharina Krösl, Dominik Bauer, Michael Schwärzler, Henry Fuchs, Georg Suter and Michael Wimmer. "A VR-based User Study on the Effects of Vision Impairments on Recognition Distances of Escape-Route Signs in Buildings" in *The Visual Computer*, 34(6-8), 911-923, 2018
- Katharina Krösl, Carmine Elvezio, Matthias Hürbe, Sonja Karst, Michael Wimmer and Steven Feiner. "ICthroughVR: Illuminating Cataracts through Virtual Reality" in *2019 IEEE Conference on Virtual Reality and 3D User Interfaces (VR)*, (pp. 655-663). IEEE, 2019
- Katharina Krösl, Carmine Elvezio, Laura R. Luidolt, Matthias Hürbe, Sonja Karst, Steven Feiner and Michael Wimmer. "CatARact: Simulating Cataracts in Augmented Reality" in *2020 IEEE International Symposium on Mixed and Augmented Reality (ISMAR)*, IEEE, 2020
- Katharina Krösl, Carmine Elvezio, Matthias Hürbe, Sonja Karst, Steven Feiner and Michael Wimmer. "XREye: Simulating Visual Impairments in Eye-Tracked XR" to appear in *2020 IEEE Conference on Virtual Reality and 3D User Interfaces (VR)*, IEEE, 2020

In this chapter we present methods to simulate eye diseases, such as cataracts, for people with normal sight. There have been different approaches and devices used for such simulations in the past. The newest generation of virtual reality (VR) and augmented reality (AR) devices now provide opportunities to create more immersive and more realistic simulations than ever before. However, the development of a vision impairment simulation remains a challenging task, because different factors influence the perception of users in VR. We have to consider the vision capabilities of users, the impacts of immersive

hardware on a user's vision as well as the impacts of the respective vision impairment or eye disease on different aspects of the human visual system and the purpose or designated application area for the simulation. In this chapter we will present our approach to simulate vision impairments in VR or AR and discuss the effects pipeline we developed for this purpose. We use this approach to simulate different eye diseases, but focus on cataracts.

5.1 Effects Pipeline for Simulating Cataracts

The leading causes of vision impairment worldwide, as identified by the WHO, are uncorrected refractive errors and cataracts. Cataracts are an age-related eye disease, which causes opacities to form in the lens of the eye. The effects of cataracts are at first often only noticed as blurred peripheral vision or intensified glare effects when driving at night. However, depending on the type of cataract (nuclear, cortical or posterior subcapsular) and severity of symptoms, even tasks like finding one's way out of a building

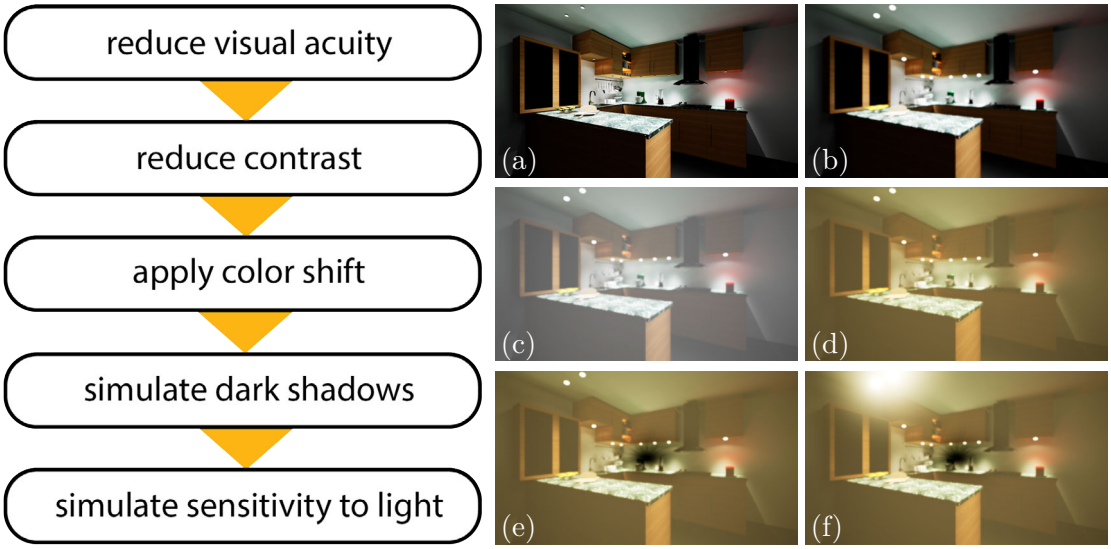

(1) Effects pipeline. (2) Results after each stage.

Figure 5.1: To combine all effects for a simulation of cataract vision, we take (a) the original image and first (b) reduce the visual acuity, and (c) the contrast of the image and then (d) apply a color shift. Next we use a texture to simulate (e) the dark shadows that people with cortical or posterior subcapsular cataracts (as shown in this figure) typically experience. We modify this effect according to the brightness of the virtual environment the user is currently viewing and add a (f) bloom or glare effect to simulate straylight and sensitivity to light. Each stage in this effects pipeline simulates one symptom. To create simulations of other eye diseases, stages can be added, removed or changed.

in case of an emergency can become difficult. Symptoms of cataracts, like described in Section 3.4.4, can be simulated separately and then combined for a simulation of the whole disease pattern. This approach can be applied to several eye diseases that cause different distinct symptoms. As example, we will now discuss our effects pipeline to combine the most common cataract symptoms: blurred vision, contrast loss, tinted vision, dark shadows, and increased sensitivity to light (see Section 3.4.4 for further information on symptoms). According to the ophthalmologists we worked with, symptoms such as halos around lights or double vision are less common for cataract vision and were therefore not included in our simulation. (However, such symptoms could easily be added to our framework in future work.)

For each frame, the image that is to be displayed on the VR headset is modified in several ways by applying different effects in sequence. Figure 5.1 show this effects pipeline and the resulting image of each stage.

We use Unreal Engine (UE) and an HTC Vive Pro headset with the Pupil Labs [Pup] binocular eye tracker add-on for our simulations and user studies. Our presented method can be used with any modern VR head-worn display (HWD). We chose the HTC Vive Pro, since it was an available and inexpensive option to test our simulation in VR as well as video–see-through AR (using the Vive's front cameras) with eye tracking via pupil labs eye tracker plugin. (Section 9.4.2 provides a more detailed discussion on the used hardware and its limitations.)

5.1.1 Reduce Visual Acuity

The most common symptom present in vision impairments is the reduction of visual acuity (VA). We used two different approaches to simulate reduced VA in our studies, a Gaussian blur, and a depth-of-field effect. Note that the limited resolution of the VR HWD already reduces the VA of a user. Other factors, such as the fixed focal distance of the VR HWD or a possible misplacement of the HWD can reduce the experienced VA further (see Section 3.3). These factors, as well as the vision capabilities of users have to be taken into account for simulating and calibrating reduced VA (see Section 6.1 for more details).

Gaussian Blur

Hogervorst et al. [HVD06] determined a relation between the σ parameter of a just recognizable Gaussian blur and the VA of a person. Following these findings, we simulate a reduced VA by applying a Gaussian blur to the image (see Figure 5.2(b)) that is related to the level of VA we want to simulate. We determine the sigma parameter and size of the Gauss kernel in a calibration phase (see Section 6.3 for details).

Depth of Field

A simple uniform Gaussian blur might be sufficient to simulate the reduced VA caused by cataracts. However, since cataracts are an age-related vision impairment, many people

Figure 5.2: (a) Original image. (b) Reduced VA.

with this eye disease often also have a refractive error (nearsightedness, farsightedness, astigmatism, or presbyopia). Therefore, an effect that is able to also simulate reduced VA dependent on viewing distance can help to create a more realistic simulation of the vision of people with cataracts. We can simulate this distance-dependent reduction of VA by using a depth-of-field effect and adjusting its effect size with the sigma parameter for the blur. Unreal Engine has a built-in depth-of-field effect that we can leverage for this purpose. The advantage of a depth-of-field effect is that it can also be used to create a more realistic simulation of myopia (nearsightedness) or hyperopia (farsightedness), where the VA of people is also dependent on the distance of objects. Nearsighted people can sharply see objects that are very close to their eyes, while everything in the distance appears blurred. This can easily be achieved with a depth-of-field effect and also inverted to simulate farsighted vision. However, as mentioned before, there are certain factors that can reduce the VA of a user when putting on the VR HWD. Consequently, when we try to simulate myopia or hyperopia, even the regions that would be seen sharply in

reality are experienced with a reduced VA in the VR HWD, due to limitations of the hardware and possibly reduced vision capabilities of the user. The relative difference in VA depending on the distance can still give a good impression of myopia or hyperopia. Also, using a built-in engine effect is very efficient, which is important for VR or AR simulations to maintain a high frame rate and avoid VR sickness. Furthermore, for studies assessing accessibility, or educational applications showing the effects of reduced VA and vision, the main focus lies on the large range of distances, that are affected by the simulated condition. The small range of short distances where people should see sharp are less important, so we calibrate our effects for a defined test distance (see Chapter 6) and just add a user-defined unaffected distance range with falloff to the large region of reduced VA for effect. The resulting image C_{rVA} with reduced VA is then reduced in contrast in the next step.

5.1.2 Reduce Contrast

A loss of contrast is often experienced as faded colors (see Figure 5.3), which may be implemented in a number of different ways in VR. Using an approach that shrinks the histogram of a frame by using min and max values of the image is not feasible, because intensity changes from one frame to the next could change the color and intensity distribution in the image. This could yield very sudden changes of the histogram and introduce flickering artifacts. Instead, we need a way to reduce contrast that is consistent over multiple frames. Furthermore, our simulation needs to run in real time, which means we need to avoid expensive calculations.

Interpolation with gray

A simple way to reduce the contrast is to interpolate between the current image C_{rVA} (with already reduced VA) and a uniformly gray image (represented by the linear RGB color value $(0.5, 0.5, 0.5)$ in Equation 6.1), weighted by a constant c. The following calculation is done per color channel:

$$C_{rContrast} = C_{rVA} \cdot c + 0.5 \cdot (1 - c). \tag{5.1}$$

The constant c is a value between 0 and 1, independent of the pixel values in the image. This operation can also be interpreted as histogram remapping: Scaling the color values with c shrinks the histogram and therefore reduces the contrast. At the same time this operation reduces the intensity of each value by $(1 - c)$ percent. We can now just add $(1 - c)$ to shift all values, so the maximum intensities are preserved. However, this would mean darker regions would be perceived a lot brighter after the contrast reduction. In order to preserve the average intensity in the image, we only add $0.5 \cdot (1 - c)$.

Compressing Luminance

We can perform a more advanced contrast reduction by doing a histogram compression of luminance values. Linear changes of the three channels of RGB colors do not yield

Figure 5.3: (a) Reduced VA. (b) Reduced contrast.

linear contrast changes. The lightness value (L $\in [0, 100]$) in the CIELAB space, on the other hand, represents the perceived luminance of a pixel and is perceptually uniform. Therefore, we modify the L value of a pixel in CIELAB space to reduce contrast. We compress the histogram of lightness values L_I using a factor $0 < p < 1$ to control how much the histogram should be compressed:

$$L = L_I \cdot p + 50 \cdot (1 - p). \tag{5.2}$$

Of course, the p value can be adjusted during the simulation. This histogram compression results in a perceptual contrast reduction of the whole image (see Figure 9.2c).

5.1.3 Apply Color Shift

In this next step, we apply a color shift to the image (see Figure 5.4) to simulate tinted vision, which is a common symptom of cataracts (as mentioned in Section 3.4.4). There

Figure 5.4: (a) Reduced Contrast. (b) Color shift, calculated with Equation (5.3).

are multiple ways to perform a color shift and different color spaces to choose from for this operation. In the following section, we will discuss a color shift using a simple color interpolation and an improved version, simulating a filter, that blocks parts of the incoming light.

Color Interpolation

Because the tinted color that is often experienced by people with cataracts results from a physical phenomenon (i.e., the absorption of parts of the incident light falling onto the retina, caused by opacities in the lens) we chose to do our calculations in the linear RGB color space instead of a perceptual color space. Other eye diseases that cause changes in color vision might require other color spaces for the respective color shift calculations, depending on what causes the color shift. In our cataracts example, we simulate a yellowish/brownish tint by applying a color shift to the contrast-reduced image

$C_{rContrast}$ in the direction of a predefined target color C_{target}, analogous to the contrast reduction step:

$$C_{colorShift} = C_{rContrast} \cdot t + C_{target} \cdot (1 - t). \tag{5.3}$$

The amount of the color shift is controlled by the parameter t. Both the target color C_{target} and the parameter t can be adjusted. Figure 5.4 shows the result of this operation with target color $C_{target} = (1.0, 0.718461, 0.177084)$ and parameter $t = 0.8$. Note that this form of color shift further reduces the contrast of the image, since this is equivalent to an interpolation between the current image $C_{rContrast}$ (with already reduced contrast) and the target color. Therefore, this color interpolation can be used to perform a color shift and contrast reduction (like described in Section 5.1.2) at the same time and omit a separate contrast reduction step. However, in this case the amount of contrast reduction would be determined by the color shift, and would not be separately adjustable. To perform only a color shift (as experienced by people with cataracts) we need a different approach, which we present in the following section.

Simulated Color Filter

To avoid reducing the contrast when applying a color shift, we can also perform a color shift by simulating a filter that reduces the amount of light in parts of the visible spectrum that is absorbed or blocked by the cataract opacities. For each color channel we calculate the color shift as

$$C_{colorShift} = C_{rContrast} - C_{rContrast} \cdot C_{filtered}, \tag{5.4}$$

or

$$C_{colorShift} = C_{rContrast} \cdot (1 - C_{filtered}), \tag{5.5}$$

where $C_{filtered}$ represents the amount of filtered light per color channel that does not reach the retina.

Cataract opacities scatter, absorb and reflect different amounts of each wavelength of the visible light, depending on the opacity. Therefore, the exact amount of transmitted light per wavelength is hard to determine. It is easier to get a description of the experienced color tint from people with cataracts. Since the components of the color that creates this tint represent the amount of transmitted light per wavelength (C_t) and are therefore complementary to the amount of light that is reflected or absorbed by the cataract opacities ($C_{filtered}$), we can simulate the color shift as

$$C_{colorShift} = C_{rContrast} \cdot C_t. \tag{5.6}$$

This calculation is done per color channel with the respective components of the pixel colors $C_{rContrast}$ and transmitted light C_t and does not reduce contrast.

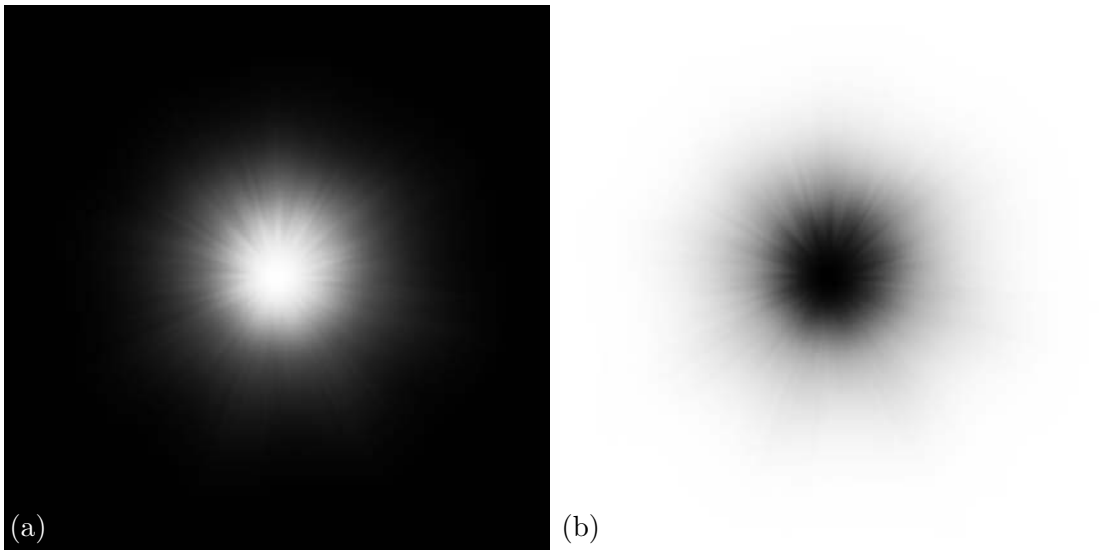

Figure 5.5: Textures used to create shadows for (a) cortical cataracts and (b) posterior subcapsular cataracts, by scaling the image values with the alpha value (between 0 and 1) of this texture.

5.1.4 Simulate Dark Shadows

Cataracts lead to a clouding of the eye lens. While for nuclear cataracts, this clouding is uniform over the whole lens, cortical cataracts also produce dark shadows in the periphery of the lens, and posterior subcapsular cataracts create a dark shadow in the center of the lens. We can simulate these shadows with an alpha texture (see Figure 5.5) that we use to darken the image, either in the periphery (for cortical cataracts) or in the center (for posterior subcapsular cataracts), by linearly interpolating between the image color $C_{colorShift}$ of the image after the color shift and a shadow color C_{shadow}:

$$C = C_{colorShift} \cdot \alpha + C_{shadow} \cdot (1 - \alpha), \tag{5.7}$$

where α has values between 0 and 1.

Different illumination levels cause the pupil of the human eye to get wider or narrower, allowing more or less light to enter the eye. This also affects the area of the lens that is exposed to light entering the eye. For some forms of cataracts, like cortical or posterior subcapsular cataracts, which exhibit a nonuniform clouding of the lens, the area of the pupil that is exposed to light affects the way vision is impaired.

This means the amount to which dark shadows appear in the visual field of the user also depends on the light intensity in the scene. The dilating and contracting of the pupil when looking at dark areas or into bright lights determines how much of the areas of the lens that create dark shadows are exposed to light. For cortical cataracts, the clouding of the lens creates dark shadows in the periphery, but the center of the field of view is less

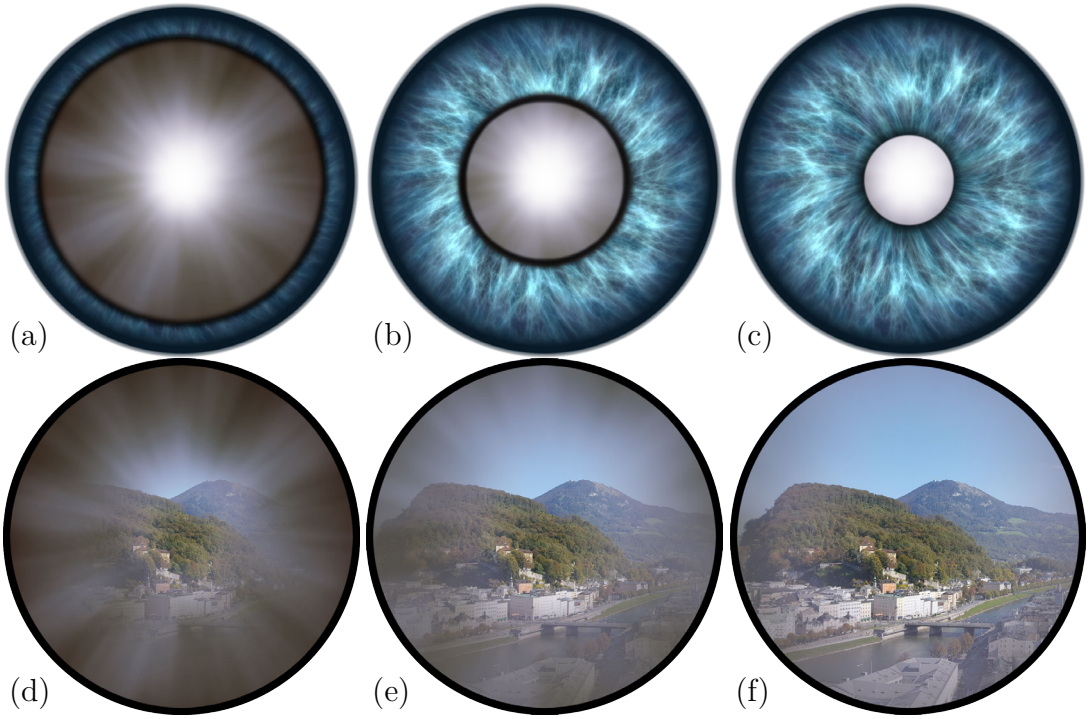

Figure 5.6: Changes in pupil size (a,b,c) can affect the influence of dark shadows, experienced (d,e,f) with cortical cataracts, on human vision. For demonstrative purposes other effects were omitted in this image. (a,d): Vision with large pupil. (b,e): Vision with smaller pupil. (c,f): Vision with very small pupil, where the darkening of the shadows is hardly noticeable anymore.

affected (see Figure 5.6). This means when the pupil is dilated, light enters the eye also through parts that are heavily clouded, and the shadows in the periphery become more apparent for the person. When looking into bright lights, the pupil contracts and light can only enter the eye through the central area of the lens. This area is less clouded, and dark shadows in the periphery are less visible or might disappear altogether. We can simulate the dilation and contraction of the pupil by scaling the texture that creates these peripheral or central shadows for cortical or posterior subcapsular cataracts respectively, according to the light intensity of the image area the user is looking at. Hence, we need to calculate a brightness value for each frame.

Average Brightness

We calculate the average intensity value of the current field of view and use it to scale the texture so it gets bigger when the user looks at bright areas. For cortical cataracts, this extends the less clouded area in the center of the field of view. When the user looks at dark areas, we scale the shadow texture smaller, pushing more of the peripheral shadows into the center of the field of view. The influence of posterior subcapsular cataracts

Figure 5.7: (a) Color shift. (b) Dark shadows for cortical cataracts in the center of the visual field.

increases when the pupil becomes smaller, since less of the unaffected area of the lens is exposed to light in this case. Consequently, the dark shadows in the center of the field of view (see Figure 5.7) become more prominent and more disturbing. We implement this effect the same way as for cortical cataracts, by scaling the texture that creates the shadows. The extent of this effect can be adjusted by setting min and max values for the scale.

Gaze-Tracked Brightness

We can improve the above-described approach by calculating a gaze-dependent brightness value. We take a cutout of the rendered image, centered around the current gaze point, and calculate the average intensity or luminance in this window. To avoid sudden changes of effect sizes, a Gaussian distribution can be used to calculate weights to give pixels at

or near the gaze point a higher importance than pixels farther away.

5.1.5 Simulate Sensitivity to Light

The second way in which light affects the vision of people with cataracts is the clouded lens that scatters light in many directions onto the retina. Images become blurred and bright lights become especially problematic, because they create intense blinding effects. A computer screen cannot display the same range of different brightness levels as we experience in the real world. To simulate very bright objects, we need to use effects that simulate what happens in the eye when light hits the retina. This does not necessarily give us physically correct results, but rather a visualization of the relative brightness of objects, which enables us to depict real-world light phenomena [Epia]. We can simulate blinding effects by post-processing the image to apply a bloom or glare effect.

Figure 5.8: (a) Dark shadows for cortical cataracts. (b) Sensitivity to light, experienced as bloom effect of a larger light source in the upper left corner of the image.

Bloom

A bloom can be realized with a Gaussian blur applied to light sources or bright areas in an image. Unreal Engine's built-in bloom effect uses multiple Gaussian blurs with different radii to increase the visual quality of the effect [Epia], but this needs more computation time.

In Unreal's built-in effect, a threshold determines how bright a pixel has to be to be affected by a bloom. This threshold should be set to a value below the intensity of the light sources in the scene, but above the rest of the geometry. This avoids the blooming of white walls or other white objects that are not light sources. The intensity and width of such an effect can be adjusted. This simple bloom effect (see Figure 5.8(b)) can already give a good impression of glare effects caused by cataracts, but is not a perceptually perfectly accurate depiction of these effects. More advanced approaches of creating blinding effects can involve complex simulations of particles in the eye and dynamic effects, like taking the oscillation of the pupil into account, as described in the work of Ritschel et al. [RIF+09], but are challenging to use in very performance-intensive real-time applications like VR simulations and need adjustments, as discussed in the following, so they can be used in these cases.

Perceptual Glare

To simulate a more perceptually accurate sensitivity to bright light sources such as sunlight or bright lamps, we can apply a glare effect, similar to the work of Ritschel et al. [RIF+09]. This effect is based on the anatomy of the human eye, which has many different layers of tissue, containing particles that can potentially scatter light (see Figure 5.9). We consulted an optometrist and adapted the effect proposed by Ritschel et

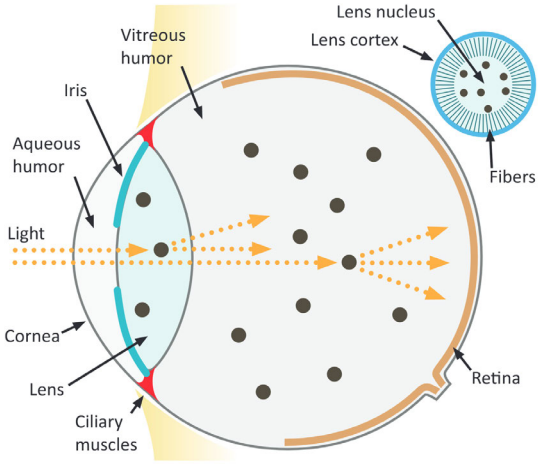

Figure 5.9: "*Anatomy of the human eye. The upper-right inset shows the lens structure.*" Reprinted from Ritschel et al. [RIF+09].

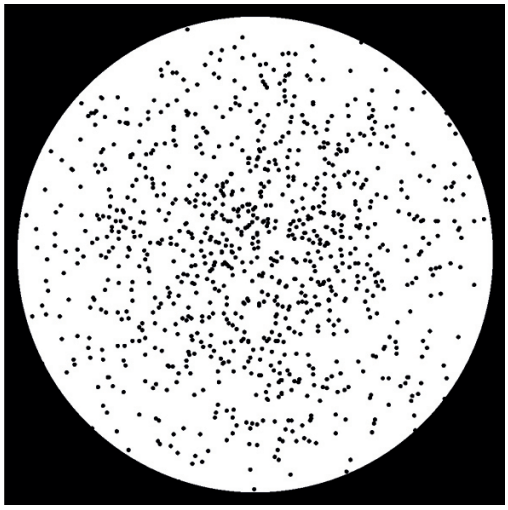

Figure 5.10: Simulated particles at random positions with aperture defined by pupil size, projected onto 2D plane. Reprinted from [LWK20].

al. Based on medical expert knowledge, we identified the relevant areas of the eye that can cause noticeable light scattering in eyes with cataracts. Consequently, the vitreous humor and the collagen fibrils of the cornea were not taken into account in our version of this effect. Our model just includes the size of the pupil and the static particles in the lens and in the cornea.

These particles are simulated by generating a user-defined number of circular particles at random positions and projecting them onto a plane (see Figure 5.10). The pupil size is treated like a camera aperture, changing the amount of light that can enter the eye, and consequently the amount of straylight that can occur. The resulting image is then converted to the spectral domain to obtain a spectral point-spread function, which can then be used as a glare kernel (see Figure 5.11).

The pupil size can be predefined or constantly measured at run-time, using an eye tracker, and adapt the simulation accordingly. However, computing the glare kernel every frame to simulate the slight pulsation of the pupil is expensive and therefore not practical for an interactive VR or AR application. In order to simplify this approach, we assume a static pupil size, which means we have to compute the glare kernel only once and then use it in our simulation. The kernel is applied to the image using a convolutional *Fast Fourier Transformation* (FFT) bloom, where both image and kernel are transformed to the frequency domain and multiplied. The result is then transformed back into linear RGB image space. Since we need two FFTs per eye (forward and inverse), this results in four FFT transformations per frame, which is very costly and not well suited for real-time VR or AR applications. Therefore, we apply our bloom effect according to the viewing direction in a smaller window (in our case, a 1024×1024 window). This results in reasonable run-times and the borders of this window are hardly visible for the

user, since they are almost outside the visible field of view. The resulting glare effect (Figure 9.2e) can be adjusted by changing various parameters, such as the size of the pupil, the number of particles in the eye, and the radius of the particles. We refer to our paper on gaze-dependent simulation of light perception in VR [LWK20] for more details on this perceptual glare.

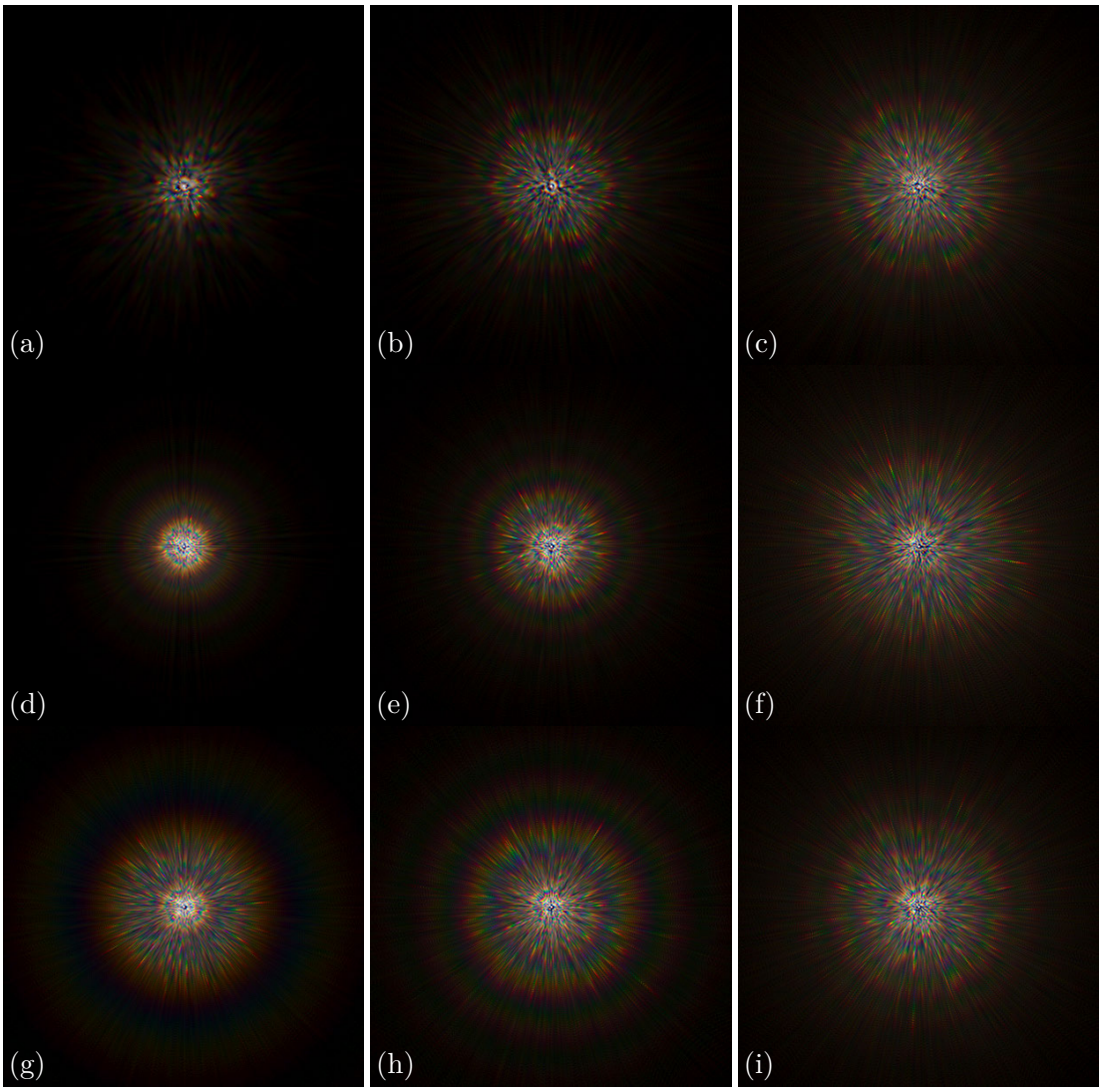

Figure 5.11: Glare kernels used for glare effects. Different pupil sizes: (a) $2mm$, (b) $5mm$, and (c) $8mm$. Different number of particles: (d) 10, (e) 100, and (f) 1000 particles. Different particle radius, using a scale of: (g) 1/3, (h) 2/3, and (i) 1 (representing an average particle radius of $0.74\mu m$).

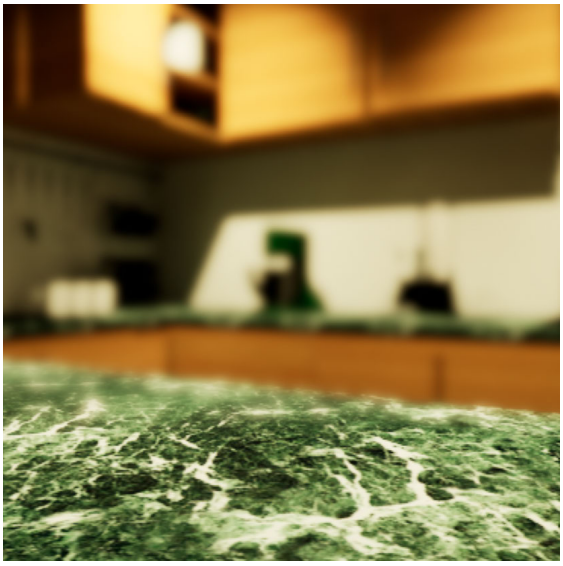

Figure 5.12: Simulation of nuclear cataract with myopia, using a depth-of-field effect.

5.2 Simulating Refractive Errors

People with refractive errors experience blurred vision, most commonly due to a deformation of the eye ball (i.e. an increase or decrease in axial length) which reduces their VA (see Section 3.4.1 for more details). For video–see-through AR and 360° images, we can simulate the reduced VA caused by refractive errors as a Gaussian blur over the image. This approximates the reduced perception of shortsighted people well, although neglecting that very close objects, right in front of a person's face, should be rendered sharp. Our VR simulation already takes the distance of objects into account and uses a depth-of-field effect, as described in Section 5.1.1, which can be used to simulate myopia and its inverted version for hyperopia or presbyopia. For a depth-of-field effect in AR, we could use the information from the depth cameras of the headset, if available. Figure 5.12 shows an example for a refractive error. To simulate a specific severity of these conditions, we need to calibrate our simulation per user to a predefined level of reduced VA. (This can be done by using our symptom calibration methodology for VA, described in Section 6.3. Note that we cannot simply use hard-coded values without calibration to specify a certain level of reduced VA, since the vision capabilities of a user, the resolution of the display as well as the placement of the HWD on the head of a user influence how much their VA is reduced.)

5.3 Simulating Cornea Disease

Cornea disease can have different causes (see Section 3.4.2), which result in different symptoms for affected people. Using and extending parts of our presented effects pipeline, we try to replicate the vision of a patient with cornea disease, who described it as

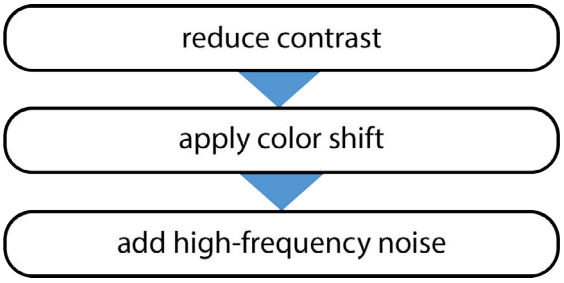

Figure 5.13: Adapted effects pipeline to simulate cornea disease.

"looking through opal glass," by applying the effects shown in Figure 5.13. We reduce the contrast of the image (see Section 5.1.2) by interpolating between the image and a uniform gray image (0.5, 0.5, 0.5 in RGB), and apply a slight color shift by interpolating between the image from the previous step and an adjustable target color (as described in Section 5.1.3). Then we use a high-frequency noise texture, softened by interpolation with a white color image to create an Unreal material representing opal glass. We can then interpolate between this material and the contrast-reduced and color-shifted image to achieve a simulation of cornea disease as shown in Figure 5.14. All interpolation weights and colors are adjustable via parameters to allow fine-tuning of the simulation, in order to create different depictions of cornea diseases, according to patient descriptions or expert knowledge from ophthalmologists.

Figure 5.14: Simulation of cornea disease applied to a 360° image view.

5.4 Simulating Age-Related Macular Degeneration

Most symptoms of age-related macular degeneration (AMD) affect the center of the visual field (see Section 3.4.3 for more details). Depending on the type of AMD (wet or dry), affected people experience slightly different symptoms, including blurry vision, reduced brightness, loss of central vision and distorted vision.

We simulate **wet AMD** by combining a distortion, radial desaturation, contrast reduction and semi-transparent texture to darken the central field of vision, as shown in Figure 5.15. First, we distort UV coordinates with the use of a water texture to create random distortions and then add multiple overlapping, parameterized circular distortions, which cause inward or outward bulges, using Unreal's smoothstep function [Epib] to calculate the extent of the distortion of a pixel:

$$UV_i += s \cdot [(P - UV_i) \cdot smoothstep(A, B, |(P - UV_i)|)]. \tag{5.8}$$

P is the center position of the distortion, which determines the direction in which the UV coordinates UV_i of a pixel are offset. The size of this offset depends on the distance $|(P - UV_i)|$ of the current pixel (i.e., its UV coordinate UV_i) to the center P, and s can be used to manually control the strength of the UV offset. A and B are predefined boundaries that specify the range of values for interpolation with $smoothstep()$. Values below A are clamped to 0 and values above B are clamped to 1.

A radial desaturation is used to create a washed-out image in the center of the field of view. To achieve this, a grayscale version of the image is created by calculating the luminosity of the pixels. Then the original image is interpolated with this grayscale image, weighted by a radial gradient exponential. We use the same contrast reduction as for cornea disease (see Section 5.1.2) and add a circular gradient texture (colored gray) via alpha-blending. All parameters controlling the extent and characteristic of each of these effects are adjustable.

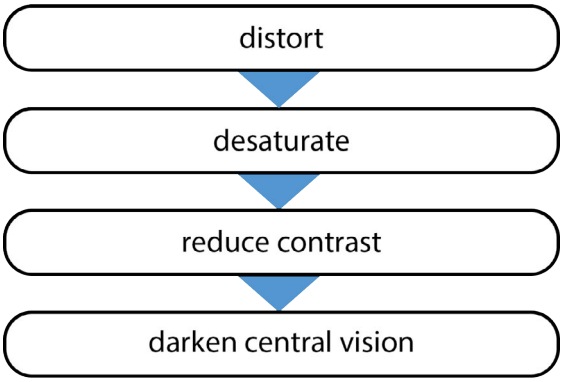

Figure 5.15: Adapted effects pipeline to simulate wet or dry AMD.

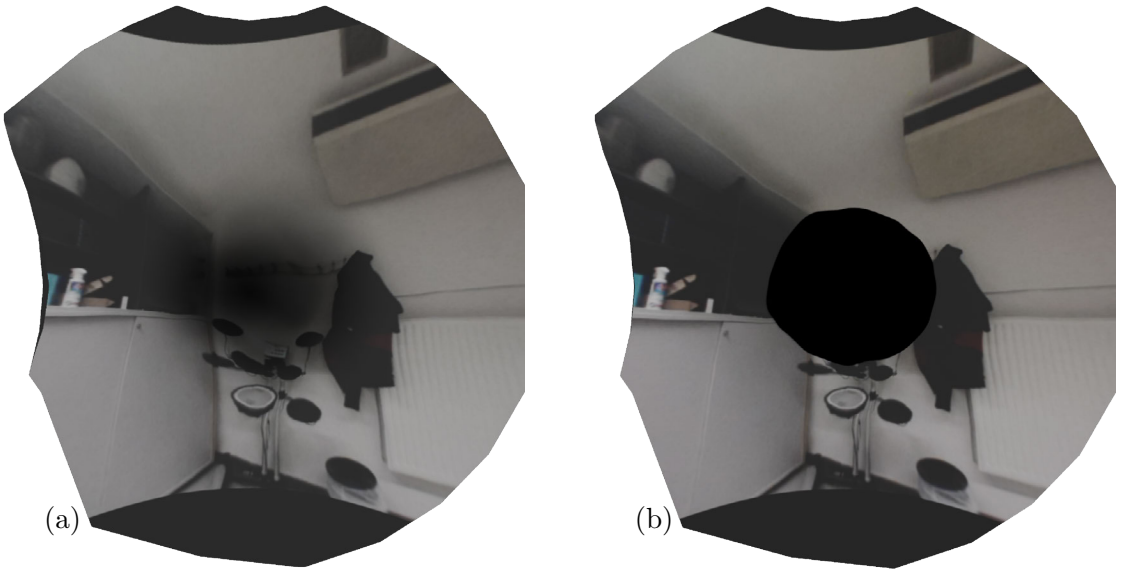

Figure 5.16: Examples of (a) wet and (b) dry AMD, simulated with our framework.

We simulate **dry AMD** in a similar fashion, with slightly modified parameter values. Dry AMD causes a central loss of vision due to failing photoreceptors in the macular area. The main difference to our simulation of wet AMD is that we simulate this central vision loss with a black texture, with clear edges, drawn over the central area of the field of view, instead of blending a gray gradient texture on top. This simulates areas of loss of tissue, called *geographic atrophy*, a symptom of dry AMD.

Figure 5.16 shows examples for our simulation of wet and dry AMD in AR. We developed this simulation based on related work [BM08, LSB12, AFF15, VCH16] and expert knowledge from ophthalmologists, but have not yet evaluated its accuracy in a study.

5.5 Gaze-Dependent Effects

To correctly simulate vision affected by gaze-dependent symptoms, we need to track the gaze of the user, not just to calculate a gaze-dependent brightness, but also to adjust effects that should just appear in a certain area of the visual field of a person. We can, for example, move the texture that is used to simulate the dark shadows produced by cortical or posterior subcapsular cataracts, according to the gaze of the user. This can be done with different eye trackers. Figure 5.17 shows an example of the eye tracking software from Pupil Labs [Pup].

To avoid any noticeable delay of the effects, the eye tracker needs to be fast enough to recognize saccades (quick eye movements from one fixation to another). Therefore, the eye tracker should at least have 200 Hz cameras. Slower cameras might cause a noticeable delay of the movement of the effects. However, even with a certain delay, gaze-adjusted

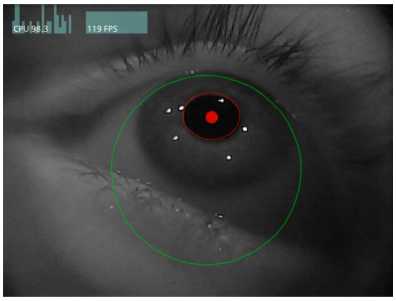

Figure 5.17: Eye tracking with the pupil labs [Pup] eye tracker.

effects are perceived as more realistic as without eye tracking.

There are some additional factors to consider when using eye tracking: The performance and accuracy of the tracker might decrease for people wearing glasses, or it might not work for them at all. Everything that can create reflections could potentially disturb the eye tracker, for example eye lashes with mascara on them.

5.6 Summary

Many immersive vision impairment simulation have some shortcomings. Some are only designed for VR and don't support AR [JAR05, VCH16, MKD16, SES18, WAAB18, KCL+18, ZL19, ANK+20]. Often times simulations of vision impairments are simplified depictions of vision with a certain eye disease, using just one or two effects [JAR05, AFF15, VCH16, CBW+17, JO18, JSCWBC20], instead of multiple effects to simulate different symptoms of a complex eye disease pattern. Gaze-dependent effects are rarely integrated, since most related works do not use eye tracking (exceptions are for example Jones and Ometto [JO18], Jones et al. [JSCWBC20] or Wu et al. [WAAB18]) and to the best of our knowledge no related work on simulating vision impairments takes hardware limitations and vision capabilities of users into account to create a similar impression for every user.

In this chapter, we have introduced our effects pipeline, which we used to implement the most complete simulation of cataracts in VR and AR to date, by combining multiple effects to simulate the most common symptoms of cataract vision. In particular, three different types of cataract, as well as other eye diseases like refractive errors, cornea disease or AMD, can be simulated through an appropriate combination of individual effects, the severity of symptoms can be interactively modified, and the simulation reacts to eye tracking. This allows a realistic simulation of these types of visual impairment in diverse immersive settings. For the first time, we also support simulating the influence of light on the visual perception of people with eye diseases.

We tested our effects pipeline in two user studies. First, we created a simulation of cataracts in VR, using a depth-of-field effect (Section 5.1.1) to reduce the VA, an interpo-

lation with gray (Section 5.1.2) to reduce the contrast, a color interpolation (Section 5.1.3) to create a color shift, a simulation of dark shadows using the average brightness in the image (Section 5.1.4) and a bloom effect (Section 5.1.5) to simulate sensitivity to light. We evaluated this simulation in a user study with healthy individuals, also testing the influence of different lighting setups on the perception under simulated cataracts. This study is presented in Chapter 8. We then used the same effects pipeline, but with a Gaussian blur (Section 5.1.1), compressing luminance (Section 5.1.2), simulating a color filter (Section 5.1.3), using a gaze-tracked brightness value (Section 5.1.4) and a perceptual glare (Section 5.1.5) to simulate the respective symptoms in AR. We conducted a study with cataract patients to evaluate and adjust this simulation, which is presented in Chapter 9.

CHAPTER 6

Symptom Calibration

This chapter is based on the following publications:

- Katharina Krösl, Dominik Bauer, Michael Schwärzler, Henry Fuchs, Georg Suter and Michael Wimmer. "A VR-based User Study on the Effects of Vision Impairments on Recognition Distances of Escape-Route Signs in Buildings" in *The Visual Computer* 34(6-8), 911-923, 2018
- Katharina Krösl, Carmine Elvezio, Matthias Hürbe, Sonja Karst, Michael Wimmer and Steven Feiner. "ICthroughVR: Illuminating Cataracts through Virtual Reality" in *2019 IEEE Conference on Virtual Reality and 3D User Interfaces (VR)* (pp. 655-663). IEEE, 2019

In order to use vision impairment simulations, like the cataract simulation described in Section 5.1, to evaluate accessibility, measure recognition distances or readability of signage, we need to take vision capabilities of users into account and apply a methodology that allows us to calibrate simulated symptoms of vision impairments to the same level of severity for different users. In this section, we discuss vision capabilities of users, present a suitable calibration methodology and illustrate this methodology on two examples (calibrating reduced visual acuity (VA) and reduced contrast).

6.1 Vision Capabilities of Users

Let's assume we want to measure recognition distances of signage or evaluate other accessibility aspects under a certain form of vision impairment by conducting a user study with participants with normal vision and simulated vision impairment. We have to be able to create the same visual impression for every user study participant. Only then is it possible to statistically analyze and generalize findings from a user study. Several independent variables need to be controlled. For vision impairment simulations, such

independent variables are the actual vision capabilities of a user study participant and the hardware constraints imposed by the virtual reality (VR) headset. As explained in Section 1.2, finding participants with the exact same type and severity of vision impairment can be difficult or even impossible, which means this variable cannot be controlled through careful selection of participants. To overcome this problem, we can restrict our participant pool to people with normal sight. However, even people with normal sight can be expected to have different levels of VA and contrast sensitivity, since *normal sight* is not defined by one distinct value, but by a certain range. Hence, it is difficult to control these variables. However, we can take them into account when simulating a vision impairment, to create the same baseline for every user study participant. For our presented cataract simulation, we can do this for example by calibrating the reduced VA and the reduced contrast to the same levels for all participants.

If we assume our users to have normal sight, we do not necessarily need to calibrate other effects like dark shadows, color shift or an increased sensitivity to light, because we would only expect significantly different perception of these effects from users that already have an eye disease.

6.2 Calibration Methodology

In order to calibrate simulated symptoms of vision impairments to the same level of severity, taking different vision capabilities of users into account, we impose the following restrictions:

- All users have to have normal sight (or corrected sight, wearing glasses or lenses) and no conditions that influence their vision.
- The level of severity we calibrate to has to be worse than the vision of each participant.
- The level of severity we calibrate to has to be worse than the vision impairment induced by the VR hardware.

These restrictions allow us to calibrate vision capabilities, such as VA or contrast sensitivity, to a certain reduced level that is perceived similar by every user study participant, by conducting vision tests in VR. Note that we calibrate each simulated symptom separately with all other simulated symptoms turned off. We chose this approach since simulations of different symptoms can affect test results for other symptoms—eg., a reduced VA might also affect the contrast vision of a user and the other way round (see Section 10.2 for a more detailed discussion of this issue).

6.2.1 Vision Tests in VR

The basic concept is to define a level of reduced VA or contrast that is known to be a more severe vision impairment than the mild impairment induced by the VR headset.

For this chosen level of impairment, we know what vision tests people with such vision impairment still pass and at what distance, size or contrast of the optotype they fail the test. So we create an eyesight test in VR that shows optotypes where people with this vision impairment are supposed to fail. Each user takes this eyesight test. During the test, the simulated impairment is increased as long as the user is able to pass the test. At the time a user fails the test, we know exactly which level of simulated impairment we need in order to calibrate the vision of this particular user to the predefined level. Some users with very good vision might require a higher severity of simulated impairment to fail the test at the same stage as others.

Following this methodology yields parameter values (severity levels of simulated impairments) per user, which can be used to create the same perceived level of vision impairment for every user. This methodology is illustrated in the following two sections on the examples of VA and contrast sensitivity.

6.3 Calibrating Reduced Visual Acuity

According to the methodology described above, we can use an eyesight test in VR to calibrate the simulation for all our users to a specific level of reduced VA. There are different eyesight tests that can be adapted for the use in VR, such as the VA test described by the international standard *ISO 8596:2017* [Int17] (see Section 3.2 for details).

In a VR simulation, we do not have an ophthalmologist pointing at one Landolt ring after another on a chart of optoypes. The virtual equivalent to the real-world visual acuity test setting is to place a user in a virtual room with Landolt chart [Int09] lines on the wall at a specific test distance. An alternative, inspired by the Freiburg Vision Test (FrACT) [B$^+$96] is to show five Landolt rings of the same size at the same fixed distance in sequence and not simultaneously.

Instead of changing the size of the rings every five optotypes, we can fix the size (and distance) of the Landolt ring. We select the size and distance of the Landolt ring such that a person who cannot identify the gaps at this fixed size and distance correctly anymore is classified as having a certain reduced VA, eg. 6/38 or 20/125 or 0.16 decimal acuity. Then we add a blur to the image, and increase its effect step wise every 5 rings (without altering size or distance of the rings), until the user can no longer recognize the gaps in the rings and therefore now has a simulated reduced VA of 0.16 decimal. The value of 6/38 or 0.16 decimal, as used in the example above, represents a moderate vision impairment (VA between 6/18 and 6/60) as defined by the WHO [PM12], which is well beyond the VA limit of 0.5 decimal for driving, as prescribed by most international standards [BVT$^+$10]. Figure 6.1 illustrates how such a VA calibration is experienced by the user.

As discussed in Section 3.3, there are a number of factors that influence a person's perception in VR and therefore also have an impact on our calibration procedure and

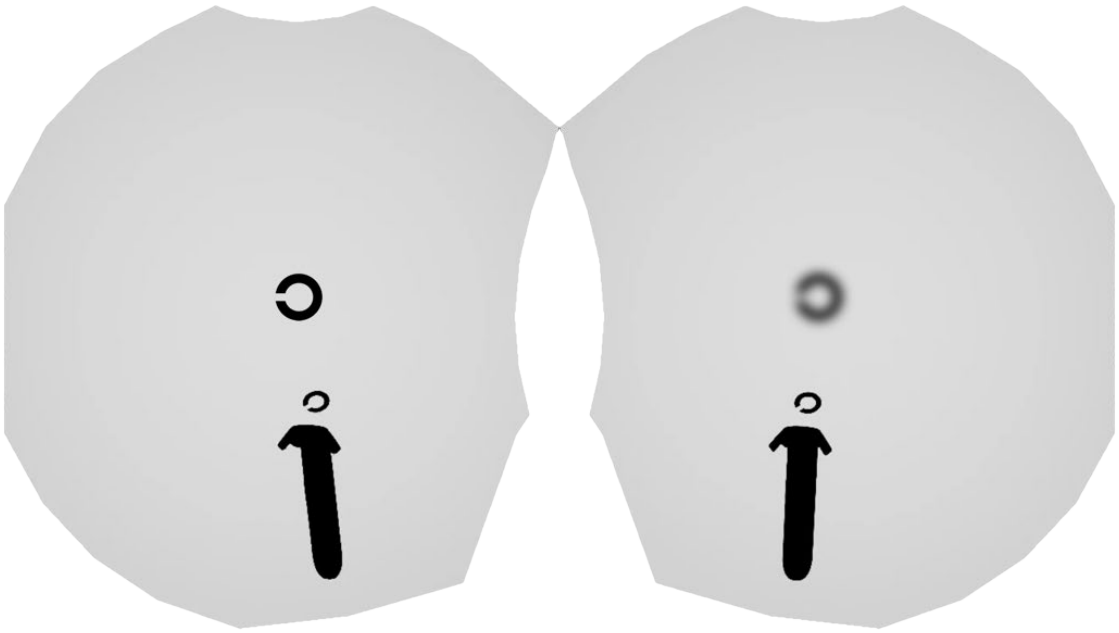

Figure 6.1: Illustration of VA calibration, with (a) unmodified vision at the beginning of the calibration (shown for the left eye) and (b) blurred vision at a later stage during the calibration procedure (shown for the right eye in this image). In our application the optotype that has to be recognized is a Landolt ring, shown at a fixed distance (enlarged in this illustration). Another Landolt ring is displayed directly above the controller. The user has to align the gaps of both Landolt rings by moving their thumb along the trackpad on the controller to turn the Landolt ring that is displayed directly above it and then confirm by pressing the trigger. If three out of a set of five Landolt rings are aligned correctly, the blur applied to the image is increased.

the resulting blur factors. Even if users claim to have normal sight, some might still have a reduced VA without knowing it. Furthermore, since normal sight describes a certain range of VA (see Section 3.1), the actual VA can vary between normal-sighted users. The resolution of the display and discretization of the images also influence a user's ability to perceive details shown at small sizes. Additionally, the head-worn display (HWD) introduces a fixed focal distance to the eyes, which can create a vergence-accommodation conflict that can have negative effects on a user's vision [Kra15]. A possible misplacement of the HWD can also reduce the perceived sharpness of the images and therefore the VA. All these circumstances create an already reduced VA for the user once they put on the HWD. From this unknown level of reduced VA, caused by any or multiple of the factors mentioned above, we start decreasing a user's vision further, by applying and increasing the Gaussian blur until a certain size of the Landolt C (at a certain test distance) cannot be correctly recognized anymore. This size and distance of the last recognizable size of optotypes directly correspond to a certain level of VA in the real world, according to established medical eyesight tests. Note that because we use the HTC Vive with

Steam VR in UE 4 in a room-scale setup, distances and sizes in VR match real-world measurements.

This methodology allows us to have people with different levels of VA participating in an experiment that assumes participants with similar levels of VA.

6.4 Calibrating Reduced Contrast

We can use the same methodology as for calibrating reduced VA also to calibrate the perceived loss of contrast. The *Pelli–Robson contrast sensitivity test* [PRW88] allow us to test the contrast vision of user. For this test, optotypes are displayed at a large size (equivalent to 6/18 or 20/60 acuity) in groups of three with decreased contrast for each group (see Figure 6.2). According to the test protocol [PRW88] of this standardized test, the participant has to correctly recognize two out of three optotypes to proceed with the next group. If the participant cannot recognize two out of three optotypes correctly anymore, the contrast sensitivity (CS) is recorded as the *log CS* value of the last correct group.

To calibrate to a specific level of contrast loss, we display groups of three optotypes, one after the other, and decrease the contrast after each group until the optotypes cannot be recognized correctly anymore. The contrast is reduced by applying the following calculations to the image during this calibration procedure:

$$C_{rContrast} = C_{original} \cdot c + W \cdot (1 - c). \tag{6.1}$$

In this equation, c is a constant specifying the amount of contrast reduction. The Pelli–Robson contrast sensitivity test [PRW88] uses log contrast sensitivity and reduces the contrast after each group of three letters by a factor of 0.15 log units. We can set c to a value representing a reduction of 0.15 log unit or any other amount, depending on how much contrast reduction we want to have per three optotypes. The log contrast sensitivity values $logCS$ on the Pelli–Robson chart can be transformed to percentage contrast sensitivity pCS (in the range from 0 to 1) with the following equation:

$$pCS = \frac{1}{10^{logCS}} \ . \tag{6.2}$$

Depending on the used contrast simulation method, $C_{original}$ in Equation 6.1 represents either the linear RGB color values if we want to use an interpolation with gray (see Section 5.1.2) for our simulation of reduced contrast, or the luminance values in the CIELAB space for a compression of luminance values (as described in Section 5.1.2). W represents the color white in linear RGB values (1.0, 1.0, 1.0), or in the CIELAB space ($L = 100$). Adding $W \cdot (1 - c)$ to each color channel (or the luminance value) then shifts all values, so the maximum intensities are preserved by this operation. This allows us to reduce the contrast of the optotypes in relation to the background, while keeping the background color white, as it is on the Pelli–Robson contrast sensitivity chart [PRW88]. Keeping the background white is also important to preserve the overall brightness in the

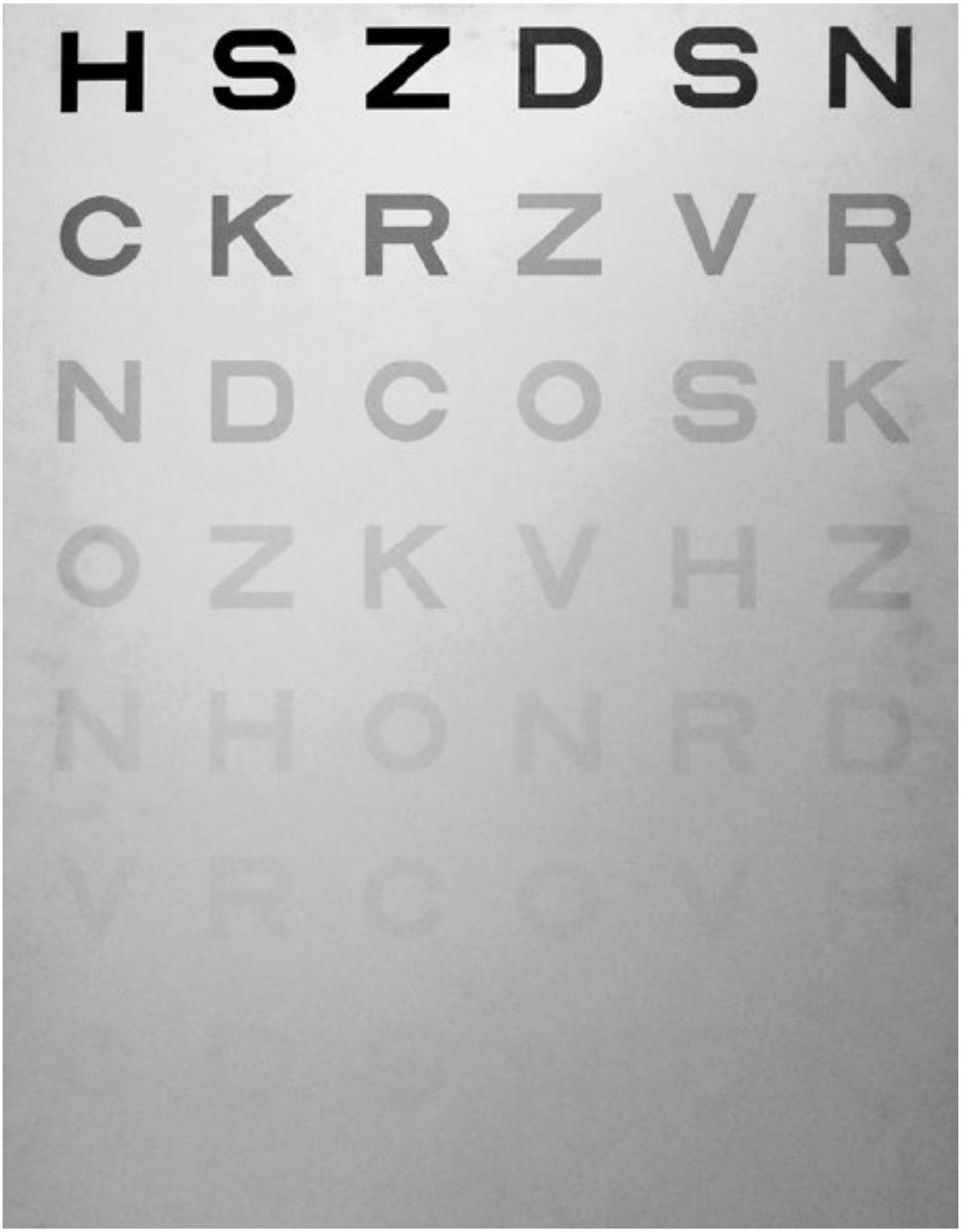

Figure 6.2: The Pelli–Robson chart is used for eye exams to measure contrast sensitivity. Image taken from [PTM+13]

scene, since contrast sensitivity is influenced by the illumination of the background and ambient light in the scene [KKE17] (which is one and the same in our test scene).

Other formulas for contrast reduction (like adaptions of tone mapping algorithms) could be used instead.

As soon as a user cannot recognize the optotypes anymore, the simulation has calibrated the vision of this user to the same perceived level of contrast loss as for every other participant. The constant c of the last group of correctly recognized optotypes can then be used to simulate the same amount of contrast loss.

6.5 Summary

In this chapter, we introduced a new methodology to calibrate simulated vision impairments to the same level of impairment for different users, taking their vision capabilities as well as hardware constraints of the VR headset into account. This allows us to conduct user studies, investigating the effects of vision impairments on perception, with normal-sighted people by graphically simulating such impairments in VR or augmented reality (AR), hence making it much easier to find a suitable number of participants for our experiments.

We evaluated our methodology to calibrate reduced VA in a user study, measuring maximum recognition distances (MRDs) of escape-route signs in buildings under reduced VA. This study is presented in Chapter 7. We also used our methodology to calibrate reduced VA and reduced contrast in our study on the influence of simulated cataract vision on perception, presented in Chapter 8.

CHAPTER 7

Study 1: Reduced Visual Acuity

This chapter is based on the following publication:

Katharina Krösl, Dominik Bauer, Michael Schwärzler, Henry Fuchs, Georg Suter and Michael Wimmer. "A VR-based User Study on the Effects of Vision Impairments on Recognition Distances of Escape-Route Signs in Buildings" in *The Visual Computer* 34(6-8), 911-923, 2018

In this chapter, we investigate the influence of vision impairments on the recognizability of escape-route signs. For this, we use a virtual reality (VR) application (see Figure 7.1) to simulate certain levels of loss of visual acuity (VA). The results of the conducted user study suggest that current norms specifying the positioning of escape-route signage should be adapted for certain buildings like homes for the elderly, where a larger average loss of VA can be expected among the residents than in the general population.

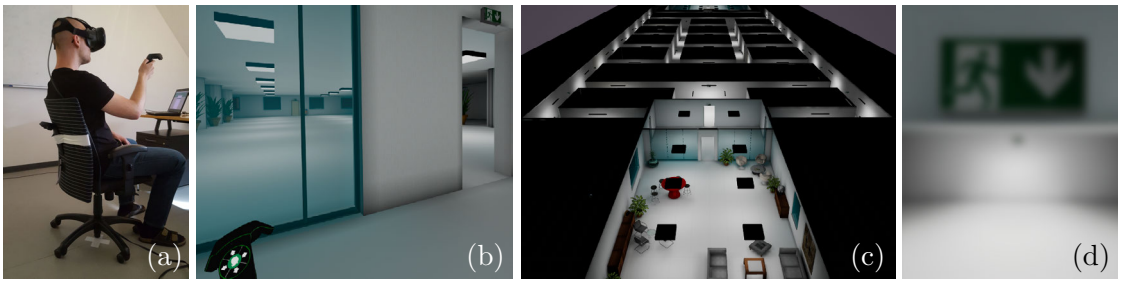

Figure 7.1: VR-based user study: (a) simulated wheelchair reduces motion sickness, (b) participant sees escape-route sign in the upper right, (c) virtual environment for user study, (d) blurred vision caused by simulated reduced visual acuity.

Escape-route signs are planned during building design and construction in a way that ensures people can easily find and follow predefined escape routes in case of an emergency. They are placed according to norms or standards that specify both the maximum recognition distance (MRD) and viewing angles of a sign as well as important areas where they have to be placed. The planned signage is evaluated, and its compliance with the norms is manually checked on site. According to the international standard ISO 3864-1 [Int11], at least 85 percent of all people have to be able to recognize the signs at the given distance and angle. However, in places like retirement homes, where one can expect an increased percentage of people to have impairments that reduce their visual MRD, the information provided by standards and norms might not be sufficient to allow for successful emergency response. To ensure the safety in case of emergency situations in such buildings, it may help to verify that current standards still apply, and, if this is not the case, to adjust them accordingly, decreasing the chances for casualties and also reducing costs in terms of time and money for necessary adaptations later on. Therefore, it is important to investigate and quantify the effects of vision impairments on the recognizability of signage.

In this chapter, we use our new methodology to conduct a valid user study with participants, with normal or corrected vision, that *experience* the same level of reduced VA through our VR simulation. We achieve a similar simulated VA (using a Gaussian blur, as described in Section 5.1.1) for every participant by *calibrating* the impairment to each user in respect to their own vision capabilities (which differ from person to person, also in normal-sighted people) and the limitations of the display system, as described in Section 6.3. Using this methodology, we conducted a user study to measure the MRDs of participants for signs of various sizes and at different viewing angles. We also provide an analysis of the data obtained from these experiments in comparison to the values prescribed by international standards and European norms.

Between MRD measurements, we let participants perform interactive walkthroughs through building models to allow users to experience an emergency scenario like an elderly person, trying to follow an escape route out of the building. For this, we developed a new type of locomotion for VR environments simulating a wheelchair, since this is a common form of movement in our chosen use case: a home for the elderly. Furthermore, our tool chain enables us to create geometrically detailed 3D models of building interiors using a dedicated interior design tool, and employs a physically accurate light-planning software, thus achieving a completely configurable, highly realistic and immersive virtual environment.

The remainder of this chapter is organized as follows: In Section 7.1 we summarize the regulations given by international standards and European norms on escape-route signage. Then we discuss related work regarding locomotion techniques in VR in Section 7.2. Section 7.3 describes our approach to simulate and calibrate reduced VA for each participant in our user study. Details about the user study we conducted are presented in Section 7.4, and the results of the study are listed in Section 7.5. In Section 7.6 we discuss and interpret these results and compare them to the regulations provided by

international standards and European norms. Finally, Section 7.7 gives a summary and conclusion based on the presented findings and an outlook on future work.

7.1 Legal Regulations, Standards and Norms

Laws and regulations are in place for the use and placement of emergency and escape-route signs in buildings. The European norm EN 1838 [DIN13] covers all aspects of emergency lighting: general emergency lighting, anti-panic lighting, emergency lighting for dangerous workplaces and escape-route signs. In terms of vision conditions, EN 1838 notes that factors like eye sight, required illumination level, or adaptation of the eyes differ between individuals. Furthermore, elderly people in general are regarded as requiring a higher level of illumination and a longer time to adapt to the conditions present in emergency scenarios. For escape-route signs to be effective, EN 1838 states that they should not be mounted higher than 2m above floor level, and, where possible, also not higher than 20° above the horizontal viewing direction at the MRD of a sign. The MRD is defined as the maximum distance from which a sign should still be recognized by a normal-sighted observer. This distance is specified by the norm as the sign's height times a distance factor, which is assumed to be 100 for illuminated and 200 for luminescent signs. Let z be the distance factor and h the height of a sign, then the MRD l is calculated as

$$l = z \cdot h. \tag{7.1}$$

According to ISO 3864-1 [Int11] distance factors are calculated based on the angle under which a sign is observed and its brightness. Further factors, identified by the norm, that influence the ability to recognize an escape-route sign are the size of the sign's elements, the contrast of the sign's elements with the background, the illumination conditions, the familiarity of the observer with the sign's elements and the observer's VA. ISO 7010:2011 [Eur12] provides specifications for standardized safety signs, which we also used in our user study. In relation to VA, the informal appendix of ISO 3864-1 suggests to scale the MRD by an observer's decimal VA value. If a person has a VA of 20/20, it is scaled by 1.0. If a person has a VA of 20/80, the distance should be scaled by 0.25. As is pointed out in ISO 3864-1, with increasing recognition distance, the visual angle spanned by a sign element decreases. Thus, an ever-smaller portion of observers can recognize this sign element. The informal appendix of the standard also defines the MRD (as described by EN 1838) to be sufficient for at least 85% of observers.

All regulations and recommendations mention important locations in a building that must be signposted. They also discuss installation height, the MRD depending on the size of a sign and its light intensity, as well as viewing-angle dependent considerations. Based on this information, a lighting designer must place emergency signs appropriately during the planning phase of a building. Since this is a manual procedure, the placement depends on the knowledge and experience of the designer. Particularly when dealing with buildings for special use, e.g., homes for the elderly, a lighting designer has to estimate the influence of eye diseases and other vision impairments on the visibility of escape-route signage and adapt the design accordingly.

7.2 Previous Work on Locomotion Techniques in VR

In order to measure MRDs in VR, it is vital to provide a locomotion technique for continuous movement towards an escape-route sign in a large environment. Hence, all forms of teleportation in VR are not applicable for such measurements.

Research on natural walking [VPK15] in virtual environments has shown positive effects on the immersion in VR. Redirected walking techniques [SBS+12], manipulate the mapping between physical and virtual motions to enable users to navigate through vast virtual environments. However, these techniques require significantly more physical space than the tracking space of a typical HTC Vive setup.

Other walking approaches, like *change blindness illusions* [SCK+11], self-overlapping architecture [SLF+12] or flexible spaces [VKBS13], manipulate the architectural layout of a VR environment to fit into the tracked space. Although these techniques work well to create an immersive experience [VPK15], the need for specific layouts or manipulations of the VR environment prohibits the evaluation of escape route signage of models of real-world buildings.

Locomotion devices [VKBS13] like shoe-based devices, omnidirectional treadmills or robotic elements allow navigation through arbitrary building models without any manipulations of the building architecture or the need for a large physical workspace, but the acquisition of this specialized hardware increases the costs of a project significantly.

Other inexpensive locomotion techniques that require a lot of physical movement, like jumping up and down to run in VR, would be too tiresome if performed for 30 minutes. Techniques that simulate walking while the person does not move in the real world – such as pressing buttons on a controller or navigating via joystick – are known to cause motion sickness for many people due to the discrepancy between visual and vestibular cues.

Therefore, we implemented a form of locomotion that provides continuous movement and also minimizes this discrepancy: a wheelchair simulation. Nybakke et al. [NRI12] compared different locomotion techniques in a series of search tasks in VR. They found that people performed best with real walking as compared to virtual translation via joystick with real rotation while standing. The performance with real movement in a motorized wheelchair was intermediate and only slightly better than rotating a swivel chair and using a joystick for translation. Chowdhury et al. [CFQ17] did a study on information recall in a VR disability simulation and concluded that their wheelchair interface (using a real non-motorized wheelchair) with an Oculus head-worn display (HWD) induced the highest sense of presence in the virtual environment, when compared to non-VR or game-pad navigation. Since real walking is not possible in VR environments that exceed the physical tracking space and a real wheelchair results in additional costs, we designed our wheelchair simulation similar to the swivel chair model of Nybakke et al. [NRI12].

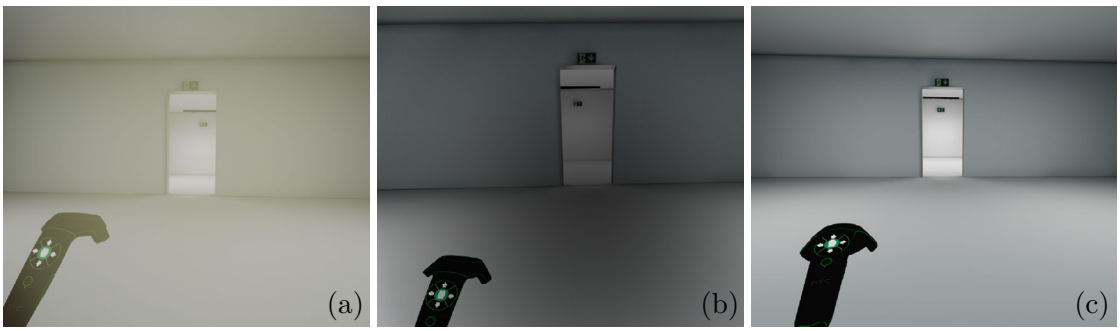

Figure 7.2: Vision impairments visualized in our simulation: (a) nuclear cataract, (b) mild form of macular degeneration, (c) normal sight.

7.3 Simulation

In Section 5.1.1 we presented a simulation of reduced VA, applying a Gaussian blur to the image, which we use for this study. Similar to Lewis et al. [LSB12] we can also apply post-processing effects to simulate common eye diseases like cataracts or macular degeneration, but we combine these effects with our calibrated reduced VA to adapt the simulation of these eye diseases for every user. Figure 7.2 shows our first attempts at simulating cataracts and macular degeneration. We use post-processing effects provided by Unreal Engine 4, to create a yellow tint and contrast-reduction, for cataract vision. To simulate different forms of macular degeneration we combine a blurred image with a darkened version of the same image, using an alpha mask that favors the dark image in the center and the other image on the outside, creating a smooth transition between them. These simulations are easy to implement, but do not represent these vision impairments very well. We use more sophisticated methods (as presented in Chapter 5) to simulate cataracts and macular degeneration in our subsequent studies.

7.3.1 Calibration for Reduced Visual Acuity

Different (even normal-sighted) people have different VA. Furthermore, the display device may limit the maximum achievable VA. Therefore, we devised a calibration procedure to calibrate all users to the intended VA of an experiment, as explained in Chapter 6.

For this user study, the user first performs an eyesight test on the target display device, which allows us to estimate the extent of the VA reduction, caused by the VR headset. Afterwards, we calibrate the correct strength of the blur needed to achieve the desired reduced VA for our MRD tests.

Eyesight Test

For calibration, we use a setting in a virtual room (see Figure 7.3) with Landolt chart lines at 4m distance. Five of these Landolt Cs are displayed at a time. The user's task is to indicate the correct angle of the gap in each Landolt C using a controller, in our case

Figure 7.3: Virtual room used for eyesight tests and calibration of reduced VA.

by pressing the corresponding position on the Vive-controller touch pad. The test then follows the test protocol as outlined in the international standard *ISO 8596:2017* (see Section 3.2 for details).

Determination of Blur Strengths

Next, we determine the parameters we need in order to calibrate the vision of a user to a reduced level of VA, following the methodology, described in Section 6.3. This gives us a factor f_a^u for the width of the blur needed to calibrate the vision of user u to the reduced VA a (note that in the case of a Gaussian blur, f is simply the standard deviation of the respective Gaussian).

7.3.2 Macular Degeneration and Cataracts

In this study, we use the blur factors determined in the calibration phase in combination with other symptoms to simulate vision impairments like macular degeneration and cataracts to create a similar impression for each participant during the walkthroughs with these impairments. However, it will not be perceived exactly the same by every user, since at this point, we only calibrate one of the symptoms (VA) to the user's actual vision and combine it with a fixed level of other symptoms (e.g., contrast loss), using the same value for everyone. In future work, more calibration steps could be added to also calibrate other symptoms that influence contrast, color perception, or field of vision, for example.

7.4 User Study

We chose to apply our new methodology to determine the MRD for escape-route signs. As already mentioned, this is a scenario where visual impairments have so far not been taken into account properly. In a user study, we present participants with two tasks of different complexity: first, indicating when an escape-route sign becomes recognizable when moving straight towards it, and second, finding a given escape route in a building in a simulated emergency situation. The first task constitutes the actual quantitative experiment, while the second task serves to make the study more interesting for participants, and presents first experiments towards studying participant behavior in simulated emergency situations in future work. We also restrict the formal analysis to the study of VA, while in the second task, we also include symptoms of other visual impairments. Since the more complex simulations of eye diseases, used in our second task, need further evaluation and consultations of experts (like ophthalmologists) before meaningful measurements can be derived from them, we do not include data from the second task in our current statistical analysis.

To avoid fatigue, which can be caused by a vergence-accommodation mismatch when using a HWD, we designed our study to not exceed 30 minutes per participant.

7.4.1 Participants

For this work, we conducted a user study with 30 participants (10 female, 20 male) between 23 and 42 years of age. Demographics ad well as prior VR experience and information regarding the users' vision were assessed via questionnaire. All but one participant had experience with computer games in general, and two thirds had already tried a VR headset before participating in our study. 50% of our participants have normal vision. The other, mostly shortsighted participants (some having astigmatism) were wearing either glasses or contact lenses – with the exception of two shortsighted participants who did not wear any sight-correcting aid during the experiments. No participant reported having any other other vision impairments. We did not test our participants for any vision impairments they might not be aware of, such as mild color

vision deficiencies, but suggest doing this for similar studies in future work. One of our participants got motion sick and could not complete the study. Some of the other participants reported minor feelings of dizziness after the study, but overall, the feedback (gathered from informal interviews) of our implemented locomotion technique was very positive. Most participants stated they liked our wheelchair simulator and had fun using it to navigate through the building model.

7.4.2 Experiment Protocol

Each participant starts with the calibration phase as described in Section 7.3. We calibrated for two VA conditions: *weak blur*, corresponding to 5 angular minutes, and *strong blur*, corresponding to 8 angular minutes. We then carry out two rounds of experiments in order to test for learning effects. In each round, we perform the actual MRD experiment with no, weak and strong blur conditions. For each condition, we show 3 escape-route signs of 15cm height and 3 of 30cm height. The angle between sign and observer is set to 0, 30 and 60 degrees, respectively. In total, we obtain 36 measurements for each observer (18 per round of experiments). Interspersed with the MRD experiment, we let the participant do walkthroughs through the test environment with the task of finding the exit, with different vision impairment symptoms. In the first round, the first two conditions (no blur, weak blur) serve to acquaint the participant with the experimental environment. The experiment protocol is as follows:

1. Calibration phase
    - Eyesight test
    - Determine blur factor: weak blur
    - Determine blur factor: strong blur
2. First round of test runs
    - Recognition distances measurements: no blur
    - Walkthrough: no blur
    - Recognition distances measurements: weak blur
    - Recognition distances measurements: strong blur
    - Walkthrough: weak blur
3. Second round of test runs
    - Recognition distances measurements: no blur
    - Walkthrough : cataract (with weak blur)
    - Recognition distances measurements: weak blur
    - Recognition distances measurements: strong blur
    - Walkthrough: macular degeneration (with weak blur)

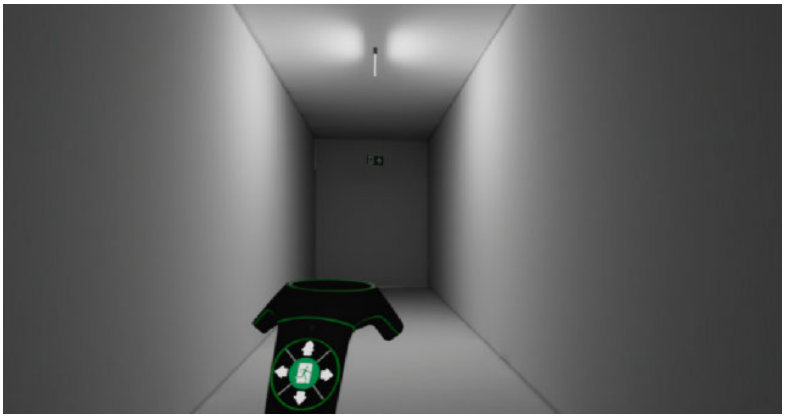

Figure 7.4: Corridor used for the measurements of MRDs. The luminaires and the lightmap for this scene have been exported from HILITE [VRV].

In this study all participants experienced all conditions in the same order. In order to reduce any possible bias, it is common to use a Latin square design for the order of experiments. This is especially important for studies which collect subjective feedback from their participants via interviews or questionnaires. In our study only objective measurements are taken during the experiments. It is reasonable to assume that a participant's vision does not improve over one test session when performing the MRD test multiple times. However, we cannot fully dismiss the possibility that the order of effects could bias the results. Participants might need some time to get comfortable with the MRD test in VR and therefore perform better in later test. This is why we tested for a learning effect (see Section 7.5.4), but did not find any evidence for it.

7.4.3 Task Description

Our experiments consist of two different tasks: MRD measurements and walkthroughs.

Maximum Recognition Distance Measurements

In our study, we aim to determine the maximum distance a user can be away from an escape-route sign such that they can still recognize the direction the sign is pointing to. This is measured by placing the user at the beginning of a 40m long corridor (shown in Figure 7.4) with an escape-route sign at the far end and asking them to advance in the direction of the sign. As soon as they recognize its label, the user indicates the recognized direction by pressing on the corresponding direction of the Vive-controller touch pad. This can be up, down, left or right. The controller vibrates if the input was wrong. In that case, the user has to proceed by moving further towards the escape-route sign until they correctly recognize the displayed direction on the sign and press on the correct position of the touch pad. After a correct input, the scene is reset for the next sample, and the user starts again at the end of the corridor.

Walkthroughs

Between the MRD measurements, the participant is presented with a more realistic escape scenario. The user moves in a large building consisting of multiple furnished rooms and corridors with luminaires and escape-route signs, as can be seen in Figure 7.5 and Figure 7.6. For each walkthrough, a different path is signposted with escape-route signs, and the task for the user is to follow this path out of the virtual building. We aimed for a high level of realism for our VR environments, using realistic geometry and physically plausible lighting, as described in Section 7.4.4. Walkthroughs are performed with different conditions: with clear vision, with a weak blur, with simulated cataract and with simulated macular degeneration.

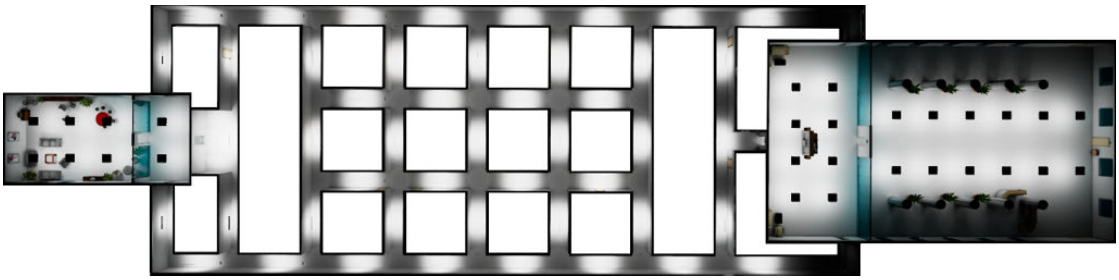

Figure 7.5: Overview of the test environment for interactive walkthroughs.

Figure 7.6: Screenshots of our virtual environment for interactive walkthroughs.

These walkthroughs serve two purposes: First, to provide a break between numerous recognition distance tests and increase the variety of tasks, which makes the whole experiment more interesting for the participants and keeps them motivated and concentrated. Second, to gather more information about the behavior of users in virtual escape scenarios, we also measure the time participants take for each walkthrough, and record their movements. This data could be evaluated in future work to give an impression of the impact of vision impairments on a person's way-finding capabilities, e.g., for architectural design, or for educational or demonstrative purposes to raise awareness for visually impaired people. This application could also be used in emergency training or to evaluate the quality of escape routes.

7.4.4 Experiment Implementation

A primary objective of our project is to improve escape-route signage in homes for the elderly, but simulating navigation of elderly people in VR is a complicated topic and challenge in itself. Elderly people are usually not as fast as the younger population and often have to use canes, walkers or wheelchairs. By simulating a wheelchair in VR, we target the most constraining form of movement for elderly people. At the same time we manage to keep the discrepancy between visual and vestibular cues to motion low, while providing continuous movement (which allows measuring MRDs) in arbitrary large virtual environments.

Wheelchair Simulation

We implemented a wheelchair simulation similar to Nybakke et al. [NRI12], but with an HTC Vive, using a form of torso-directed travel [SFC+10]. Our physical wheelchair consist of a swivel office chair with a Vive controller mounted on its back and a 3D model of a wheelchair that users see in VR (see Figure 7.7). When turning the real-world office chair, the rotation is tracked by the Vive controller on its back and translated to a rotation of the user and the virtual wheelchair in the VR environment. With the trigger of the other Vive controller, users are able to control the speed of the forward movement. Typical mechanical wheelchairs have a maximum speed of about 1.8 to 2.2 meters per second, so we decided to restrict the maximal movement speed of our simulated wheelchair to 1.8 meters per second. Although turning an office chair has a different haptic feeling than counter-rotating the wheels of a real wheelchair, our simulator is a cheap and easy-to-build emulation that lets participants experience a VR environment from the visual perspective of a person in a wheelchair.

Except for one participant, who got motion sick shortly after the start of the experiment and had to abort, all other participants reported no uncomfortable motion sickness or the need to take a break or preliminarily terminate the experiment. Some participants mentioned slight dizziness after the end of the experiment, which is not uncommon after the use of any VR application. Although our informal interviews already gave a good indication that our wheelchair simulator is a suitable solution for the task at hand, providing continuous movement while avoiding any severe motion sickness, we plan to

conduct structured interviews in future research and let participants fill out a Simulator Sickness Questionnaire (SSQ) [KLBL93] to further support this claim.

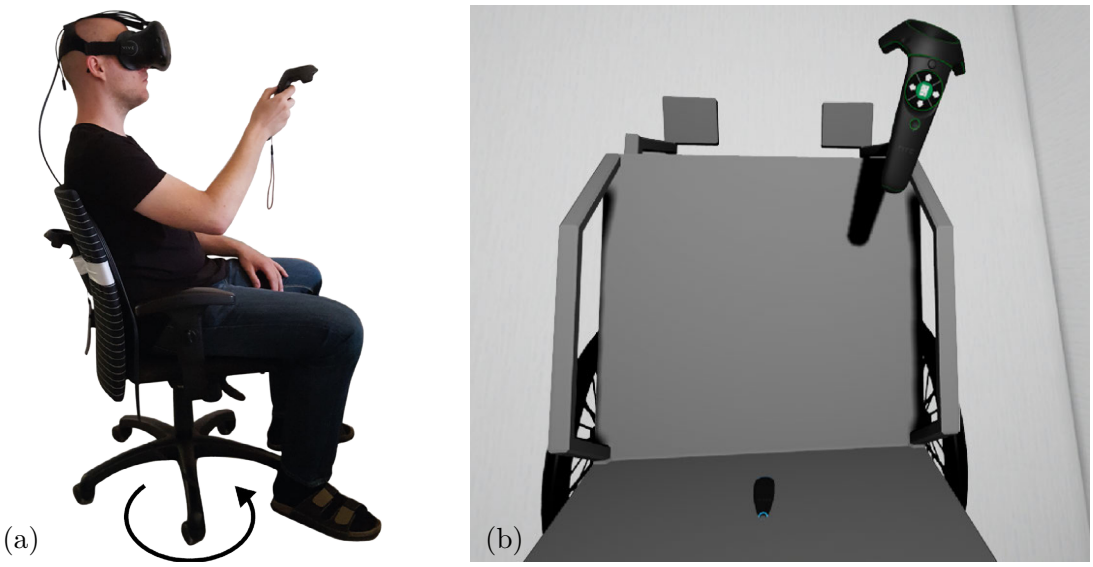

Figure 7.7: (a) Physical model of our wheelchair simulator and (b) virtual model of the wheelchair from the user's perspective (looking down).

Realistic Environments

Simulating emergency situations in VR places high demands on the quality of the virtual environment, both in terms of modeling and realistic rendering. While the MRD task only requires a simple scene, even there the lighting simulation should be accurate to reproduce illumination of the signs comparable to international standards or norms. The walkthrough scenario, on the other hand, should also present a realistically modeled building. To achieve high realism in both modeling and rendering, we implemented a tool chain consisting of a 3D interior design software (*pCon.planner* [Eas]), a light-planning software (*HILITE* [VRV]) and a game engine (*Unreal Engine 4* [Epic]). Using an interior design software allows us to model rooms with realistically looking furnishings. After importing these 3D scenes into HILITE, we are able to insert luminaires and render the scenes with physically plausible lighting, using a realistic material model [LTM+14] and the many-light global-illumination solution of Luksch et al. [LTH+13]. Figure 7.8 shows the use of measurement surfaces in HILITE, which allow us to ensure a minimum brightness for the illumination of escape-route signs, as required by norms or international standards like ISO3864-1.

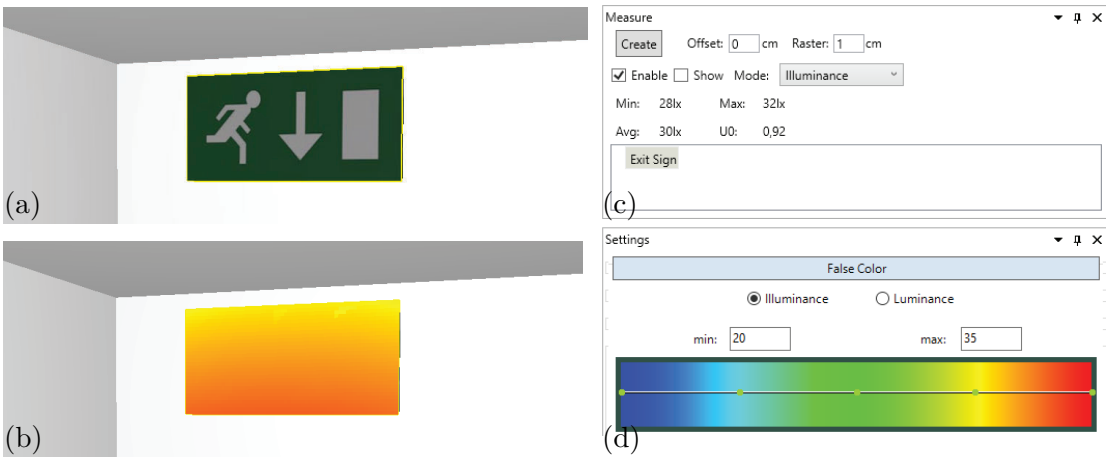

Figure 7.8: Light simulation with HILITE [VRV]: (b) measurement surface with false color visualization ((d) color scale from blue to red: 20 to 35 lux), positioned at the location of (a) an exit sign ensures that (c) norm requirements are fulfilled.

7.5 Results

The results of our user study comprise data collected from MRD measurements as well as a questionnaire completed by each participant. Furthermore, we investigated the influence of hardware limitations of our test setup on the VA of our user study participants.

7.5.1 Hardware Limitations of VR Displays

While for desktop displays the user can be placed at the appropriate distance such that any desired VA can be reached, the distance for VR displays is fixed. Therefore, at a certain size the significant details of the optotypes are smaller than a pixel and can not be properly rendered and displayed. The HTC Vive HWD we use has a resolution of 2160 x 1200 pixels. Even though most of our participants have corrected or normal sight, this resolution made it impossible for any of our participants to recognize a visual angle smaller than 2.5 angular minutes (corresponding to 0.4 decimal acuity or 0.4 LogMAR). Figure 7.9 shows the distribution of measured visual acuity of all participants.

According to the International Council of Ophthalmology [Col02], VA higher than or equal to 0.8 decimal acuity (0.1 LogMAR), corresponding to a maximum perceivable angle of 1.25 angular minutes, is considered normal vision. This means that just by putting on the VR headset, a person with normal sight will experience a loss of VA that is already considered to be a mild vision impairment. Consequently, we were not able to measure MRDs with normal sight and have to take the specifications given by existing norms as base for our comparisons. However, it is still feasible to use a HTC Vive for our study, since most elderly people suffering from vision impairments have a more severe reduction in VA than the one induced by the HWD.

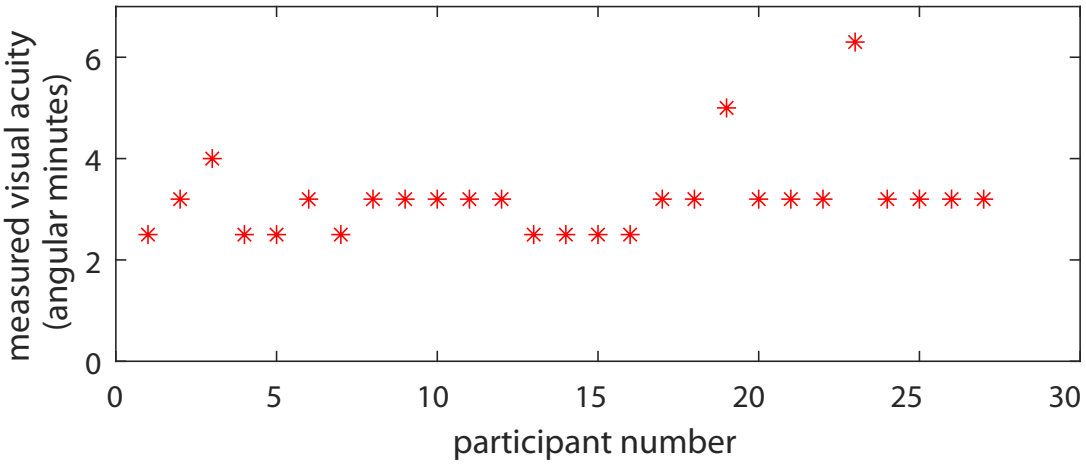

Figure 7.9: Distribution of the visual acuity measured during our eyesight test without blurring the participant's vision.

7.5.2 Measured Recognition Distances and Angles

Table 7.1 shows the average measured MRD over all observations for each test, as well as the corresponding standard deviation (see also boxplot visualization in Figure 7.10). We can see that a doubling of the size of an escape-route sign also on average approximately doubles its MRD. Increasing angles between the surface normal of a sign and the viewing direction of a user decrease the MRD. Our data suggests that this decrease is nonlinear, which is consistent with the observations of Xie et al. [XFG+07]. However, more measurements of different angles would be necessary to determine the exact nature of this angle-dependent decrease in MRDs and the influence of a reduced VA on it.

sign		**first run**						**second run**					
size	**rotation**	**no blur**		**weak blur**		**strong blur**		**no blur**		**weak blur**		**strong blur**	
		$\bar{x}$	σ	$\bar{x}$	σ	$\bar{x}$	σ	$\bar{x}$	σ	$\bar{x}$	σ	$\bar{x}$	σ
	0°	10.3m	2.9m	7.8m	1.5m	6.2m	1.7m	10.0m	1.6m	8.5m	2m	5.7m	1.4m
15 cm	30°	9.6m	1.8m	7.8m	2.2m	5.2m	1.3m	9.3m	2.4m	7.5m	1.6m	5.1m	1.1m
	60°	7.0m	1.6m	6.0m	1.6m	3.7m	1.0m	7.3m	1.6m	6.0m	0.9m	3.9m	1.0m
	0°	20.9m	4.1m	16.6m	3.4m	10.3m	2.3m	20.3m	2.6m	16.7m	3.8m	10.7m	2.5m
30 cm	30°	20.2m	3.2m	15.5m	2.6m	10.1m	2.7m	20.2m	4.1m	15.7m	3.1m	10.7m	2.6m
	60°	14.6m	3.9m	11.1m	2.4m	7.6m	1.9m	14.5m	2.3m	11.9m	2.1m	8.3m	2.6m

Table 7.1: Measured data during the first and second test run. The table shows mean $\bar{x}$ and standard deviation σ over all observations per test (rounded to the 1st position after decimal point).

Our results in Table 7.2, comparing no blur to weak blur and weak blur to strong blur, show that the amount of blur significantly reduced the MRD participants achieved.

Table 7.2

sign		first run		second run	
size	**rotation**	**no, weak**	**weak, strong**	**no, weak**	**weak, strong**
15 cm	0°	0.00088	0.00008	0.00034	<0.00001
	30°	0.00003	<0.00001	0.00026	<0.00001
	60°	0.00082	<0.00001	0.00002	<0.00001
30 cm	0°	0.00004	<0.00001	0.00002	<0.00001
	30°	<0.00001	<0.00001	<0.00001	<0.00001
	60°	0.00006	<0.00001	0.00005	<0.00001
effect size		~ 0.90	~ 1.30	~ 0.93	~ 1.27

Table 7.2: P-values (rounded to the 5^{th} position after decimal point) of Welch's t-test, pairwise comparing measurements of test runs (after outlier removal) with **no** blur, **weak** blur and **strong** blur. The data show significant differences between all the compared distributions. P-values are below ~ 0.00208 ($0.05 \div 24$), the standard $\alpha = 0.05$ cutoff value with Bonferroni correction for 24 tests. Effect sizes calculated with *Cohen's d* suggest a large effect.

7.5.3 Outlier Detection

To prevent technical errors from compromising our data, we need to find outliers in our measurements and remove them from the dataset. First, we look at the blur factors that have been calculated for each participant for *weak blur* (corresponding to a visual angle of 5.0) and *strong blur* (corresponding to a visual angle of 8.0) during the calibration phase. The data show one participant with very low blur factors for weak blur and strong blur and corresponding high recognition distances for all measurements, compared to other participants. We assume that the low blur factors were caused by a technical problem and decided to remove all data from this participant from the data set. For another participant, blur factors for weak and strong blur had the same value, which also indicates a technical error during the calibration phase. Therefore, the data from this participant were removed from the dataset as well. One of our participants had to stop the experiment after the first few measurements due to motion sickness, so we also excluded her data from our analysis.

Although we asked our participants to avoid random guessing during the MRD measurements, some very high values in the measurements suggest that some participants guessed correctly, leading to an outlier in the observations. Another cause for outliers are cases where participants were inattentive or accidentally pressed the wrong button. Pressing the wrong button leads to a short vibration of the controller indicating a wrong input. The participant then needs to advance further towards the sign until they can recognize the direction and press the correct button. However, if a participant accidentally presses

the wrong button without noticing, they might think that they got the direction wrong, even if just their input was wrong, and might move a lot closer to the sign than necessary. To exclude single observations from the data set that are considered as outliers, we calculate the standard deviation for each test and remove all observations that deviate more than 3 standard deviations from the mean.

7.5.4 Validity Checks

We performed several tests to validate the correctness of our data. For our statistical analyses of these tests we used a standard t-test or Welch's t-test, which is more reliable for samples that have unequal variances and unequal sample sizes. Using one of these tests, we test the null hypothesis that samples come from populations with equal means. The null hypothesis is only rejected at the standard 5% significance level.

Learning Effect

Each participant performed our MRD tests with no blur (only the mild vision impairment introduced by the Vive headset), with a weak blur, and with a strong blur. After some time (∼10-15 minutes) spent navigating through a building in VR, the MRD tests were performed for a second time.

Our measured MRDs during the first and second test run show similar distributions (see Fig. 7.10). We also performed a paired-sample t-test, since we obtained two measurements for each test case with each person (one in the first and one in the second test run). Our null hypothesis tests if samples come from populations with equal means. If the resulting p-values show a statistically significant value (a value below the 5% significance level), the null hypothesis is rejected. The results in Table 7.3 show that we cannot reject the null hypothesis, since all p-values are greater than 0.05. This means that we found no evidence for any significant difference between measurements of our first and second test run and thus no evidence for a learning effect.

size	rotation	no blur	weak blur	strong blur
15 cm	0°	0.856	0.169	0.197
	30°	0.075	0.400	0.860
	60°	0.102	0.784	0.372
30 cm	0°	0.944	0.894	0.266
	30°	0.709	0.707	0.061
	60°	0.324	0.104	0.063

Table 7.3: Welch's t-test, comparing both MRD test runs, yields no p-values (rounded to 3rd position after decimal point) under $\alpha = 0.05$. We conclude that there is no significant difference between both distributions, and therefore no evidence for a learning effect.

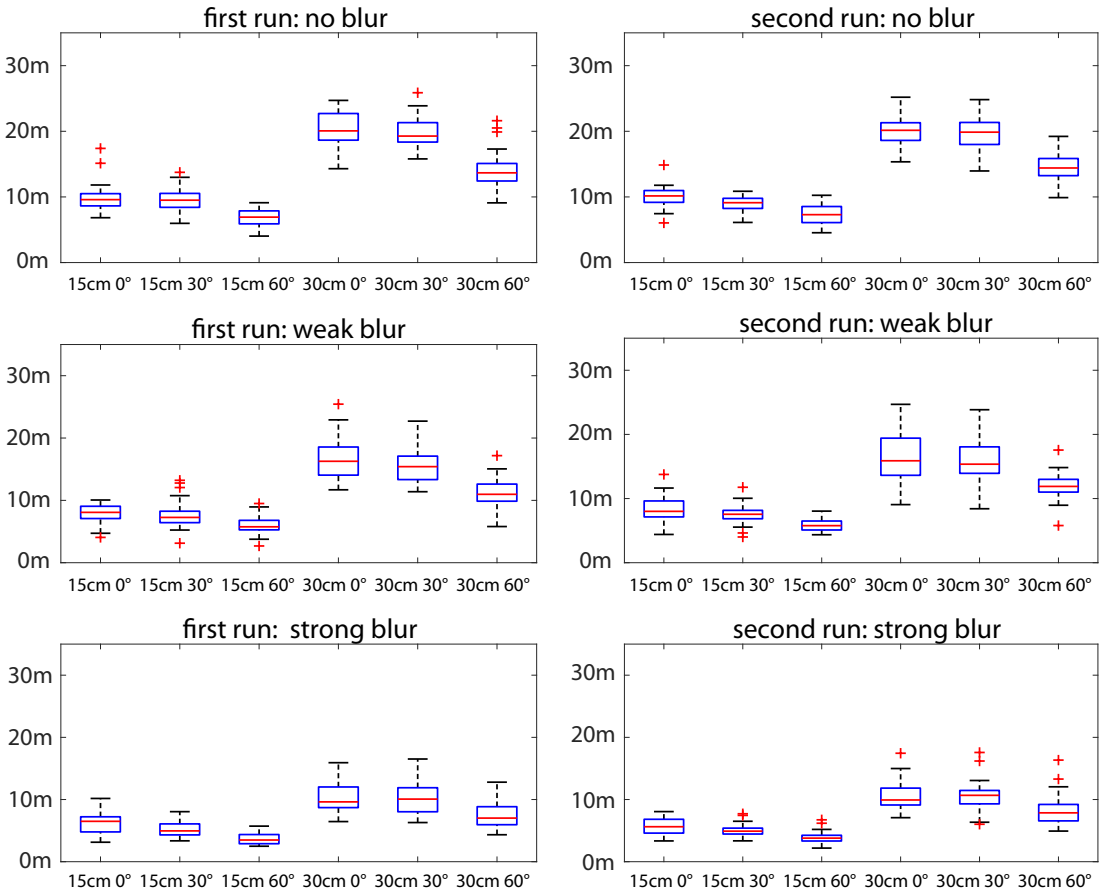

Figure 7.10: Data from two runs of MRD tests with no blur (except for the reduced VA caused by the low resolution of the HWD, resulting in a smallest recognizable detail of size 2.5 arc minutes), weak blur (5.0 arc minutes) and strong blur (8.0 arc minutes).

Comparison of Normal Sight and Corrected Sight

We compared the MRD measurements of people with normal sight to those of people wearing contact lenses or glasses to correct shortsightedness and/or astigmatism, in order to show that there are no significant differences and all participants perform similar when calibrated to the same level of VA. The visualization in Figure 7.11 shows the similarities and differences of the compared distributions.

We used Welch's t-test (unpaired two-sample t-test for distributions of unequal sample sizes), testing the null hypothesis that our two data vectors (*normal sight*, *corrected sight*) are from populations with equal means. P-values greater than 0.05 mean that the null hypothesis can not be rejected at the default 5% significance level, or in other words, that there is no evidence for significant differences between MRDs of people with normal sight and people with corrected sight.

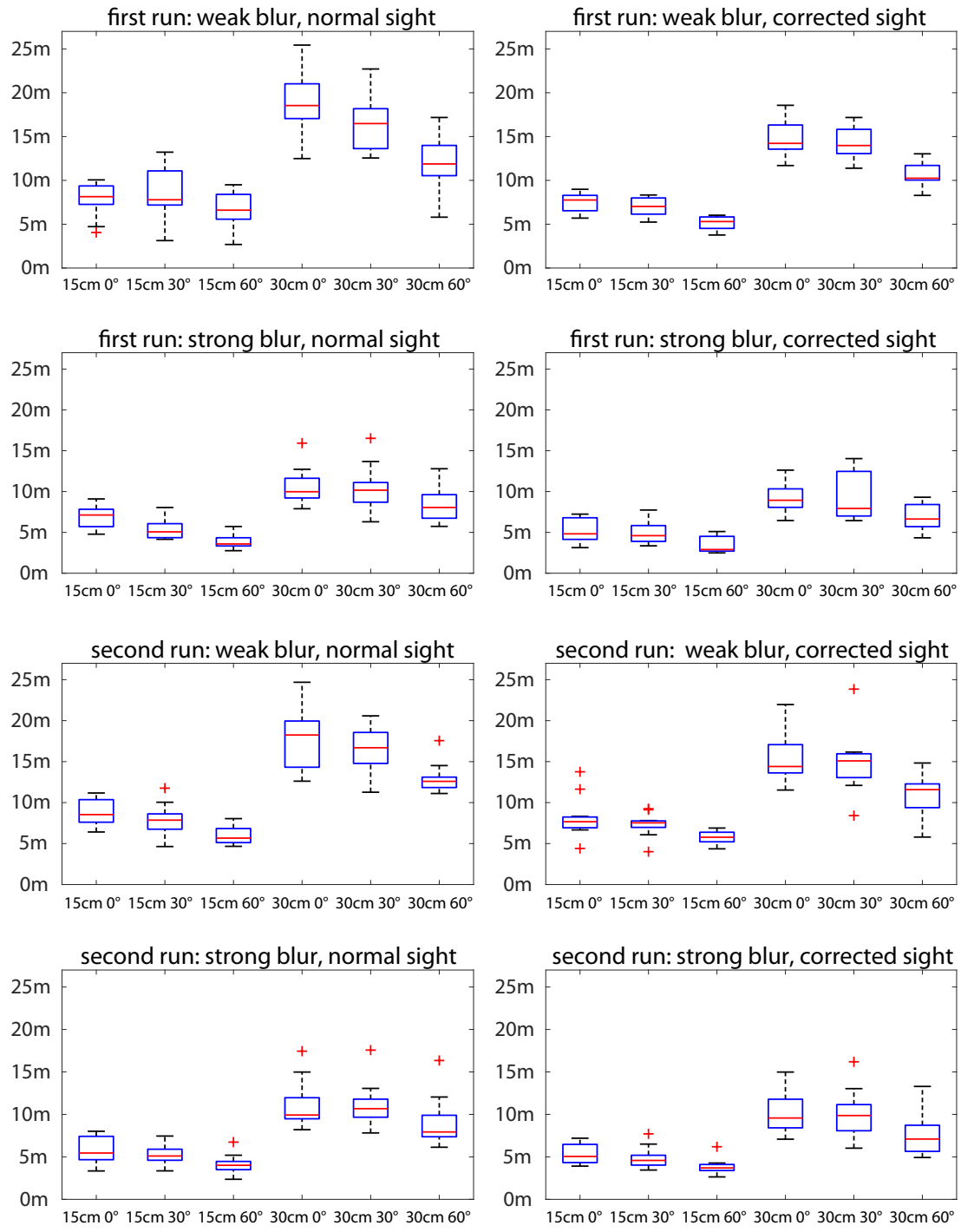

Figure 7.11: A Comparison of measured recognition distances of people with normal sight and people with corrected sight. See also Table 7.4.

sign		first run		second run	
size	**rotation**	**weak blur**	**strong blur**	**weak blur**	**strong blur**
15 cm	0°	0.46992	0.01118	0.407	0.55751
	30°	0.06462	0.36062	0.4249	0.53602
	60°	0.00993	0.33835	0.64268	0.50937
30 cm	0°	0.00122	0.13326	0.12975	0.4025
	30°	0.03462	0.40906	0.21391	0.33536
	60°	0.27634	0.07809	0.05311	0.20502

Table 7.4: P-values (rounded to the 5^{th} position after decimal point) of Welch's t-test, comparing measurements of people with normal sight to people with corrected sight (wearing contact lenses or glasses). 4 (out of 12) t-tests of the first test run show significant differences between the compared distributions (p-values are below the standard $\alpha = 0.05$ cutoff value), while none of the 12 t-tests on data from the second run show any significant p-values to reject the null hypothesis.

The results of this statistical analysis yield four p-values below 0.05, as shown in Table 7.4. We can see that our analysis of the first run of measurements under weak and strong blur shows a significant difference between normal-sighted people and people with corrected sight for half the tests with weak blur and one of the tests with strong blur. However, when analyzing the measurements of our second run, the performed t-tests show no evidence for a significant difference in recognition distance and angle for people with normal sight and people with corrected sight. Therefore, we can conclude that there is no systematic error in our system. The 4 (out of 12) t-tests that show significant differences between the compared distributions could be false positives, the consequence of a too small sample size or other, yet unknown parameters. Further analyses and experiments are needed to identify the cause of these results in future work.

A Bonferroni correction, taking all 24 tests into account, would allow us to compare p-values to a cut-off value of ~ 0.00208 ($0.05 \div 24$) and only recognize values below 0.00208 as significant enough to reject the null hypothesis. Please note that even though a Bonferroni correction reduces the probability for false positives, it also increases the probability for false negatives, which in our case might hide potentially significant values that suggest a rejection of the null hypothesis However, applying the Bonferroni correction on our data, we still get one test (weak blur, $30cm$ sign at 0°) which yields a significant value in the first test run.

Influence of Gender or Previous VR Experience

When comparing the MRD test results of people with prior VR knowledge to the results of people without prior VR knowledge (see Table 7.5), our performed statistical tests yield p-values below 0.05, with the exception of one test. We observe one p-value of 0.015 for

the no blur condition in the second test run. This value is above the the standard $\alpha = 0.05$ cutoff value, but below a Bonferroni corrected cutoff value of ~ 0.00208 (for 24 tests). As shown in Table 7.1, the results of the no blur condition in the second test run have the highest standard deviation of all the MRD tests, which is to be expected, since there was no calibration done in the no blur condition. Hence, individual vision capabilities of users are likely to influence the results. Since the overall trend and Bonferroni corrected tests show no significant values, we conclude that our analysis yields no meaningful evidence to assume a significant difference between the distributions of recognition distances of people with prior VR experience and people without.

Similarly, we could not find any evidence for an influence of gender on the performance in our test (see Table 7.6).

	sign		**first run**			**second run**	
size	**rotation**	**no blur**	**weak blur**	**strong blur**	**no blur**	**weak blur**	**strong blur**
15 cm	0°	0.288	0.695	0.920	0.996	0.482	0.624
	30°	0.230	0.973	0.754	0.261	0.112	0.820
	60°	0.100	0.767	0.875	0.139	0.544	0.784
30 cm	0°	0.401	0.565	0.625	0.329	0.687	0.948
	30°	0.095	0.488	0.554	**0.015**	0.281	0.581
	60°	0.512	0.158	0.227	0.136	0.150	0.838

Table 7.5: Welch's two-sample t-test yields almost no p-values (rounded to the 3rd position after decimal point) below the standard $\alpha = 0.05$ cutoff value. We observe one value of 0.015 for the no blur condition in the second test run, which is however below a Bonferroni corrected cutoff value of ~ 0.00208 (for 24 tests).

	sign		**first run**			**second run**	
size	**rotation**	**no blur**	**weak blur**	**strong blur**	**no blur**	**weak blur**	**strong blur**
15 cm	0°	0.628	0.871	0.952	0.728	0.276	0.432
	30°	0.187	0.540	0.565	0.686	0.333	0.767
	60°	0.449	0.660	0.135	0.836	0.797	0.377
30 cm	0°	0.424	0.519	0.271	0.471	0.649	0.871
	30°	0.874	0.664	0.485	0.066	0.705	0.872
	60°	0.353	0.851	0.956	0.114	0.924	0.918

Table 7.6: Welch's two-sample t-test yields no p-values (rounded to the 3rd position after decimal point) below the standard $\alpha = 0.05$ cutoff value and therefore no evidence for a significant difference of MRDs between people of different gender.

7.6 Discussion

The *International Council of Ophthalmology* [Col02] defines normal vision as range from 0.8 to 1.6 decimal acuity (dA), which means people with normal sight are able to recognize

a visual angle as small as 1.25 to 0.625 angular minutes (see Section 3.1 for more details on VA measurements). Our weak blur *wb* represents a vision impairment corresponding to a minimum recognizable visual angle of 5.0 angular minutes, which is a reduction of the VA by at least a factor of $f = 4$ (from a normal decimal acuity of $dA_{normal} = 0.8$):

$$f = \frac{dA_{normal}}{dA_{reduced}} , \tag{7.2}$$

$$dA_{reduced} = \frac{1}{wb[arcmin]} . \tag{7.3}$$

EN 1838:2013-07 [DIN13] states that the MRD of an escape-route sign of size $15cm$ is $15m$, which according to ISO 3864-1 [Int11] is true for 85 percent of all people. Looking at the results of our study, as shown in Table 7.7 and Figure 7.12, we observe that a VA reduced by a factor of 4 (weak blur) translates to a reduction of the MRD by a factor of approximately 2.25 to 2.27 (calculated from the average of both test runs for $15cm$ signs and $30cm$ signs respectively). Our strong blur, corresponding to a VA of 8.0 angular minutes, represents a reduction of a factor of 6.4 in VA. The results show that this VA reduces the MRD by a factor of 3.5 (for 15 cm signs) or 3.4 (for 30cm signs).

MRD values valid for 85%							
sign		**first run**		**second run**		**average**	
size	**rotation**	**weak blur**	**strong blur**	**weak blur**	**strong blur**	**weak blur**	**strong blur**
15 cm	0°	6.4m	4.4m	6.9m	4.1m	6.7m	4.3m
	30°	6.2m	4.2m	6.1m	4.0m	6.1m	4.1m
	60°	4.6m	2.8m	5.0m	3.0m	4.8m	2.9m
30 cm	0°	13.5m	8.5m	13.0m	8.9m	13.2m	8.7m
	30°	13.1m	7.1m	13.2m	8.2m	13.1m	7.6m
	60°	9.4m	5.8m	10.5m	6.2m	9.9m	6.0m

Table 7.7: Measured MRDs (rounded to the 1st position after decimal point) that are valid for 85 percent of the participants of our user study. (Average of both runs calculated before rounding.)

In future work we would like to conduct a study with more tests of different levels of VA to obtain a more detailed quantification of the influence of vision impairment on the recognizability of escape-route signs. However, our results already suggest that a reduced VA has a significant impact on the MRD of escape-route signs, which differs from the recommendations or assumptions of current norms and standards. The specifications of EN 1838 do not provide guidelines on how to take vision impairments into account, nor on how to consider the dependency of the MRD on the viewing angle. Compared to the informal appendix of ISO 3864-1, which assumes a reduction of the MRD by a factor

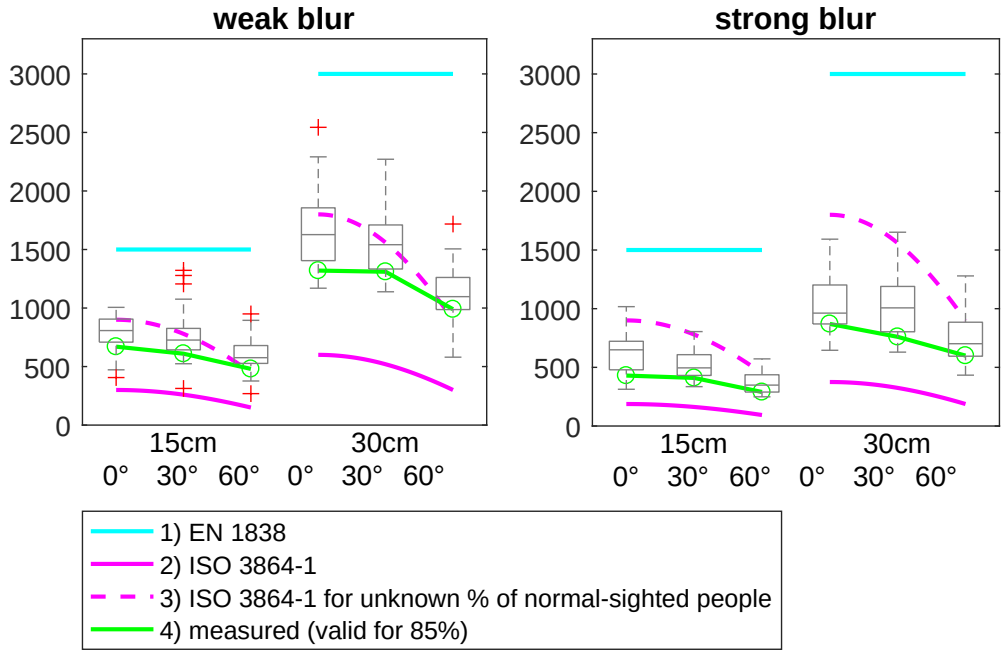

Figure 7.12: The comparison shows the MRDs for 15cm and 30cm size signs and rotations according to 1) EN 1838 (not taking VA into account), 2) ISO 3864-1 (directly scaled by calculated VA) underestimating MRDs, and 3) ISO 3864-1 (calculated for an unknown percentage of normal-sighted people, reducing normal MRDs by 40 percent) overestimating MRDs when compared to 4) our measured results (with simulated reduced VA), which are valid for 85% of our study participants. The distributions of our measurement are depicted as boxplots.

equal to the decimal acuity of the observer, our results show a lower impact on the MRD. Figure 7.12 shows that ISO 3864-1 underestimates the MRDs recorded during our study, while EN 1838 generally overestimates the MRDs. The appendix of ISO 3864-1 further states that if the amount of normal-sighted people is unknown, the distance factor as calculated for normal-sighted people for illuminated escape route signs should be reduced by 40 percent. As our results show (see Figure 7.12), this is insufficient for people that are only able to perceive a minimum visual angle of 5.0 or more. Considering that about half the population of the USA over the age of 75 suffered from some form of cataract in 2010, and the total number of cases is expected to double until 2050, according to the NEI [NEIb], it is reasonable to assume that the informal recommendation (reducing the distance of escape route signs by 40 percent) of ISO 3864-1 is insufficient. Therefore, we recommend further in-depth studies on the impact of vision impairments on the recognition distance to derive more specific information to be included in norms and standards. Additionally, a more conservative recommendation for the distance between escape-route signs in places like homes for the elderly, where a high percentage of residents are expected to suffer from vision impairments, may be advisable.

7.7 Summary

In this chapter, we have presented the first step towards the evaluation and quantification of the effects of vision impairments on recognition distances of escape-route signs, which got little attention in scientific research until now. We have found that informal recommendations for the placement of escape-route signs are insufficient for buildings where a larger number of residents with vision impairments can be found, and provide first steps towards adapting international standards and norms.

There are several avenues for future work in this direction. Many aspects we have already discussed could be studied in more depth: taking more levels of VA into account, or investigating why some conditions show differences between corrected and normal-sighted participants. While we have taken care to provide a realistic lighting simulation, we do not yet account for environmental conditions specific for emergency situations, like flickering light, smoke and haze. This is especially interesting when doing more formal studies for the walkthrough settings, where the additional question arises whether a sign is noticed by the user at all (independent of whether the content of the sign is recognized). VR headsets with eye-tracking could be helpful in answering this question. In the current study, we only focused on unlit signs, while many modern buildings feature incandescent emergency signs. We would also like to investigate further the influence of the angle under which a sign is seen, on recognizability, especially for grazing angles.

Simulating eye disease (e.g. cataracts, diabetic rethinopathy, age-related macular degeneration, etc.), that cause a person to experience multiple vision-degrading symptoms, and investigating their effects on MRDs or visual perception in general, can help us understand the impact of vision impairments better. Given a realistic simulation of a specific eye disease pattern, we can use our realistic environments with the physically plausible lighting simulation and evaluate lighting setups and their impact on vision under these simulated impairments, consequently giving us insights into which kind of illumination might positively affect the perception of people with vision impairments. We test this theory in the next chapter on the example of simulated cataract vision and present the results of our second study.

CHAPTER 8

Study 2: Cataracts in VR

This chapter is based on the following publication:

Katharina Krösl, Carmine Elvezio, Matthias Hürbe, Sonja Karst, Michael Wimmer and Steven Feiner. "ICthroughVR: Illuminating Cataracts through Virtual Reality" in *2019 IEEE Conference on Virtual Reality and 3D User Interfaces (VR)* (pp. 655-663). IEEE, 2019

Vision impairments, such as cataracts, affect the way many people interact with their environment, yet are rarely considered by architects and lighting designers because of a lack of design tools. To address this, we developed a method to simulate vision impairments, in particular cataracts, graphically in virtual reality (VR), using eye tracking for gaze-dependent effects. In this chapter, we use our approach to simulate cataract vision in VR, with the effects pipeline, we introduced in Chapter 5, and our methodology to conduct user studies for evaluating architectural design concepts with regard to vision

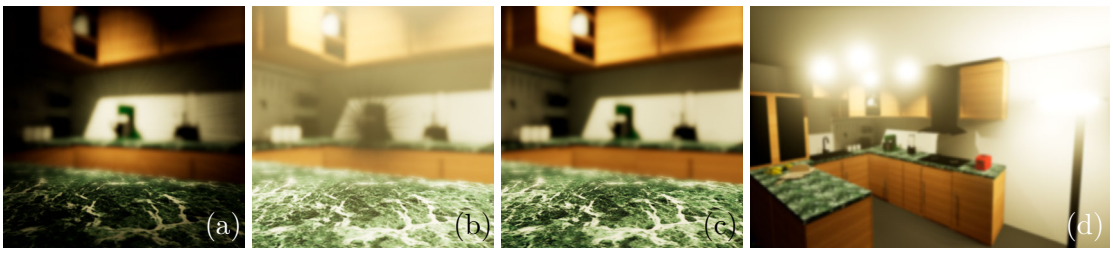

Figure 8.1: In our virtual reality simulation of cataracts, users experience (a) cortical cataracts, (b) posterior subcapsular cataracts and (c) nuclear cataracts, and the influence of different lighting setups on their perception with these simulated vision impairments in (d) a virtual environment.

impairments. Together with experts in ophthalmology, we developed simulations of different forms of cataracts, using eye tracking for gaze-dependent effects. We use these simulations to demonstrate how our approach creates new possibilities to investigate maximum recognition distances (MRDs) of escape-route signs, prescribed by international norms and standards, for people with different types of cataract.

We conducted a VR user study to investigate the effects of lighting on visual perception for users with cataracts. While existing approaches mostly provide only simplified simulations and are primarily targeted at educational or demonstrative purposes, we account for the user's vision and the hardware constraints of the VR headset. This makes it possible to calibrate our cataract simulation to the same level of degraded vision for all participants. In the previous study (Chapter 7), we tested our methodology (presented in Section 6.3) to calibrate the vision of users to a specific level of reduced visual acuity (VA), taking into account the actual vision of users and the hardware constraints of the VR headset. We extended this methodology to simulate and calibrate not only reduced VA, but also loss of contrast (see Section 6.4). We now combine both of these calibrated impairments with a simulation of dark shadows, a color shift, and a simulation of light sensitivity and use the effects pipeline presented in Chapter 5. In combination, these symptoms create a form of impaired vision corresponding to a disease pattern associated with cataracts.

In contrast to previous work on cataract simulation [JAR05, WCCC10, LBCM11, LSB12], we achieve a more detailed and adjustable simulation of this eye disease by simulating and combining multiple symptoms and are able to simulate different forms of cataracts: nuclear cataracts, cortical cataracts, and subcapsular cataracts, as shown in Figure 8. Our simulation adapts to different lighting conditions to simulate effects like dilation or contraction of the pupil, making it possible for the first time to conduct experiments on the effects of illumination on perception under simulated cataract vision.

Our study results show that we are able to calibrate the vision of all our participants to a similar level of impairment, that MRDs for escape route signs with simulated cataracts are significantly smaller than without, and that luminaires visible in the field of view are perceived as especially disturbing due to the glare effects they create. In addition, the results show that our realistic simulation increases the understanding of how people with cataracts see and could therefore also be informative for health care personnel or relatives of cataract patients.

This chapter is organized as follows: Section 8.1 briefly summarizes how we simulate, calibrate, and combine different cataract symptoms to form certain disease patterns of cataracts. We describe our user study in Section 8.2 and present its results in Section 8.3. We then discuss and summarize the results in Section 8.4 and point out limitations of our work and possible approaches for improvement. Finally, Section 8.5 gives a summary and conclusion of this chapter and an outlook on future work.

simulation of	study 1	study 2	*comment*	study 3
reduced VA (Sec. 5.1.1)	Gaussian blur (Sec. 5.1.1)	depth of field (Sec. 5.1.1)	*also for refractive errors, UE effect*	Gaussian blur (Sec. 5.1.1)
reduced contrast (Sec. 5.1.2)		interpolation with gray (Sec. 5.1.2)		compressing luminance (Sec. 5.1.2)
color shift (Sec. 5.1.3)		color interpolation (Sec. 5.1.3)	*reduces contrast further*	simulated color filter (Sec. 5.1.3)
dark shadows (Sec. 5.1.4)		average brightness (Sec. 5.1.4)	*works without eye tracker*	gaze-tracked brightness (Sec. 5.1.4)
sensitivity to light (Sec. 5.1.5)		bloom (Sec. 5.1.5)	*UE effect*	perceptual glare (Sec. 5.1.5)

Table 8.1: Effects from our effects pipeline (Chapter 5) used per study. In the VR study, presented in this chapter, we used the highlighted effects.

8.1 Simulation

Taking the VA of users and the hardware constraints of the VR headset into account by calibrating our effects appropriately, we used Unreal Engine (UE) 4.0 (on a PC with an AMD Ryzen 7 1800 CPU, 32GB RAM and an NVIDIA GTX 1070 GPU) and an HTC Vive Pro headset with Pupil Labs binocular eye tracker add-on to develop simulations for three different types of cataracts: nuclear cataracts, cortical cataracts, and posterior subcapsular cataracts. We simulate separately each of five symptoms (blurred vision, contrast loss, color shift, clouded lens, and sensitivity to light) and combine them for a simulation of the whole disease pattern.

For this study, we used our effects pipeline (Chapter 5) with the in Table 8.1 highlighted versions of the effects. We reduce the VA of a user with a depth-of-field effect (Section 5.1.1), which can also be used to simulate refractive errors, because it is distance dependent. For a reduction of contrast, we interpolate with uniformly gray color image (Section 5.1.2). To apply a color shift we interpolate with a selected target color (Section 5.1.3), which adds a brownish/yellowish tint to a user's vision. For cortical an posterior subcapsular cataracts, we simulate dark shadows (Section 5.1.4) in the periphery or center of the field of view respectively. We animate this effect to simulate the contraction and dilation of a pupil, according to the average brightness in the field of view of the user. This technique is not gaze-dependent as is just takes the current camera view of the VR headset into account. The advantage is that it also gives nice results in cases where the eye tracker does not work properly, or if no eye tracker is available. The downside of this approach is that light sources entering the field of can

cause sudden changes to the average brightness value, which might lead to more extreme changes in pupil size than appropriate. To simulate an increased sensitivity to bright light, as reported by cataract patients, we apply a bloom effect (Section 5.1.5) around light sources.

We calibrate the VA and contrast for all users to a predefined level, as explained in Chapter 6, taking vision capabilities of users and hardware constraints into account.

8.2 User Study

We conducted a user study with 21 participants, 8 participating in a pilot study and 13 in the final study, which included some adjustments. For more details on demographics see Section 8.3.4.

8.2.1 Methodology and Experiment Design

In study presented in Chapter 7, we conducted MRD tests at the beginning and again at the end of each experiment session with a user. We compared these measurements statistically and could not find any evidence for a learning effect. We use the same experiment setup again for our MRD test in this study, but omit a second round of MRD tests to stay within a maximum time of half an hour per participant. Because we did not expect a learning effect and wanted to keep our participant pool small, we use a within-group design for our user study, so that every participant experiences each of our experimental conditions.

Maximum Recognition Distance Tests

The MRD tests constitute our quantitative experiment. Participants are placed in a virtual corridor with an escape-route sign at the end (Figure 8.2). They then have to advance along the corridor until they can recognize the direction to which the sign is pointing and indicate this through trackpad input on the HTC Vive controller. In this experiment, we are investigating one independent variable (vision) with four conditions (clear vision and three types of cataracts). The task is to recognize the direction on the sign. We took three measurements per condition (and one extra for the subcapsular cataract vision), resulting in 13 trials per participant.

Environment Exploration

In the second experiment, participants are asked to explore a VE and rate its lighting setup. In this qualitative experiment, users are placed in a virtual kitchen with two different lighting setups (see Figure 8.3). The individuals are then asked to try to identify different details in the environment and comment on how well or badly they can recognize objects. We again investigate one independent variable (vision), but with two *experimental objects* (two different lighting setups) and three conditions (cataract

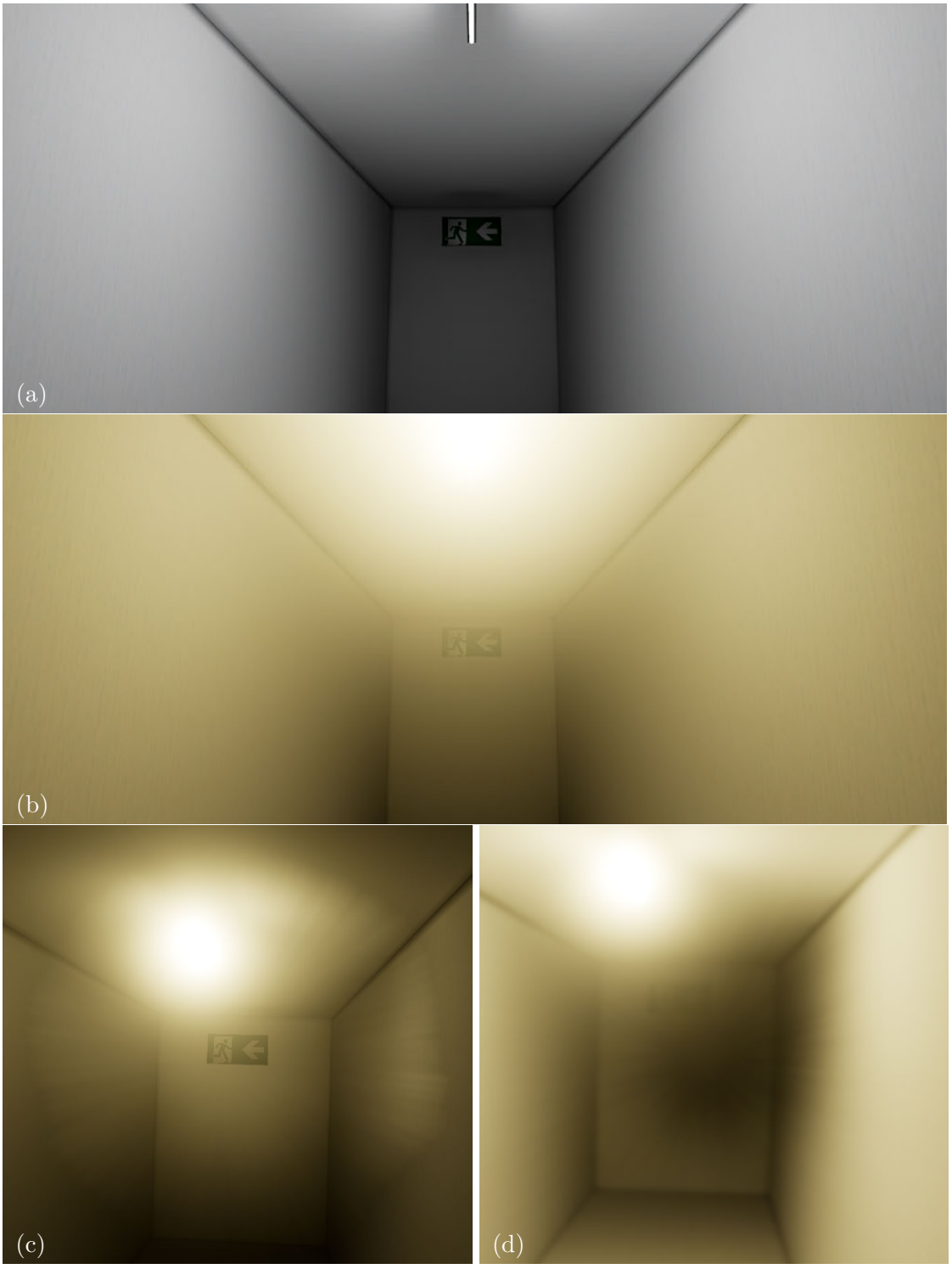

Figure 8.2: Escape-route sign at the end of the corridor during MRD tests with (a) clear vision, (b) nuclear cataract, (c) cortical cataract and (d) posterior subcapsular cataract.

Figure 8.3: virtual environment (VE) with (a) lighting setup 1, consisting of four luminaires on the ceiling and a torchiere in the corner of the room, and (b) lighting setup 2, featuring small spotlights under the kitchen cupboards and on the ceiling.

types). While exploring and comparing both lighting setups with each cataract type, the researchers write down comments by the participants for use in qualitative analysis.

8.2.2 Pilot Study

While we used the same methodology for MRD testing as in our previous work, we also wanted to analyze how various lighting setups would impact a person's ability to recognize objects in the environment. We first conducted a pilot study with eight participants to test the simulation and experiment setup, which led to two changes:

- Participants were told not to "cheat" the eye tracker with fast eye movements after it became apparent that exploiting eye tracker delay made it possible to recognize escape-route signs early.
- Participants wanted to be able to switch back and forth between both lighting setups in the environment exploration experiment, to be able to better compare the lighting setups. This functionality was added after the pilot study.

We did not have any automatic "cheat detection mechanism" in place for our studies. For future work we recommend live evaluation of eye tracking data to compare gaze points to positions users are expected to look at and notify the investigator during the experiment of significant discrepancies between those two. This could help to detect intentional "cheating" of users or simply the need to re-calibrate the eye tracker.

8.2.3 User Study Protocol

The participant was first welcomed by the study coordinator and asked to answer a few demographics and computer literacy questions.

The coordinator then introduced and explained the procedures for the study. After the introduction, the participant was asked to sign a consent form. Then the participant moved into the HTC Vive tracking space and was outfitted with the equipment. Once the participant was ready, the study began, with the following flow:

1. (Calibration) Eye-tracker calibration. To ensure proper functionality, the eye tracker needed to be calibrated for each user. This was done by asking the participant to focus on a green point that would move about their field-of-view, to calibrate different eye-to-screen poses.
2. (Baseline Test) Eyesight test for VA using Landolt Cs to test VA of participants (capped by HTC Vive Pro resolution), as described in Section 6.3.
3. (Calibration) Eyesight test for VA using Landolt Cs to calibrate to predefined level of reduced VA (constant size of Landolt C, step wise increasing the blur applied to the image, using the UE depth-of-field effect).

4. (Calibration) Eyesight test for contrast sensitivity using Pelli–Robson contrast-sensitivity test (as described in Section 6.4), but with Landolt Cs, to calibrate to predefined level of loss of contrast.

5. (Baseline Test) Eyesight test with full nuclear cataract simulation to measure the VA of the combined effects.

6. (Quantitative Experiment) Test MRDss of an escape-route sign, with both clear vision and different cataract simulations (measurements taken for illuminated signs).

7. (Qualitative Experiment) Environment Exploration

   - After the previous step, users are placed in a VE and are asked to look around and perform 2-3 tasks (e.g., reading aloud brand names and looking at a clock). The completion of these tasks was not measured in any way. They merely served to focus the users' attention and let them experience everyday tasks in a kitchen with simulated vision impairments.
   - Two different illumination scenarios (for the same VE) are tested (Figure 8.3).
   - The investigator changed scenarios manually.
   - Participants were asked to compare both illumination scenarios when looking at the scene with (1) cortical, (2) nuclear, and (3) subcapsular cataract.
   - The investigator wrote down observations (while participants—still in VR—were talking and commenting on the quality of the different illumination scenarios).

8. Questionnaire. After the VR experiment, participants were asked to fill out a questionnaire, consisting of questions for each cataract simulation and some additional questions about their experience with the simulation.

Note that the order of conditions during the environment exploration was not taken into account in the evaluation, because participants could ask the investigator to switch back and forth between cataract types and illumination scenarios any time. Furthermore, we did not conduct any analyses regarding learning effects, because participants were presented with different random tasks by the investigator. The user was asked to look at different details in the environment and tell the investigator what they could recognize (e.g. read the brand name of a box on the shelf, count the cups next to the sink, look at the clock and report the time). These tasks only served to make participants look more closely at the VE before giving their subjective opinion on which lighting system they preferred with which type of cataract. In future work, one could also implement search tasks and measure completion times for a quantitative analysis.

8.3 Results

During our user study, we measured VA without and with simulated cataracts. Then we conducted our quantitative experiment and measured MRDs under different vision conditions. The environment-exploration experiment yielded qualitative feedback on two different lighting setups, experienced with all three types of cataracts. Through our questionnaire and a look at the data recorded by the eye tracker, we gained additional insights for our analysis.

8.3.1 Eyesight Tests in VR

We tested the VA of all participants when they first put on the Vive Pro headset used in our study. We used an eyesight test using Landolt rings as described in Section 6.3. After reducing their VA and contrast in our calibration procedure, we tested their VA again with simulated nuclear cataract (combining the effects listed in Table 8.1). The results are of these experiments are shown in Figure 8.4. We do not show the few outliers we removed here as they fall significantly outside of range, and did not occur due to normal operating procedure, but were caused by errors such as a faulty VA calibration. Even without simulated vision impairment, none of the participants managed to achieve a higher decimal VA than 0.5 (or 6/12), which is considered "mild vision loss" according to the *International Council of Ophthalmology* [Col02]. Hence, the HTC Vive Pro headset alone induces a mild vision loss of 0.5 decimal VA. This is slightly better than previously reported for the original HTC Vive (0.4), presumably because of the higher resolution of the HTC Vive Pro.

While VA varied without simulating vision impairment (with a variance of ~ 0.0093), for nuclear cataracts, we achieved simulated VA levels with a very small variance of ~ 0.0004. (Note that outliers were removed for the variance calculations of VAs.) Considering that eyesight tests (in VR or in reality) are never completely accurate (patients are asked to guess when they can no longer recognize the stimulus), this gives us a realistic baseline to investigate MRDs with cataract vision.

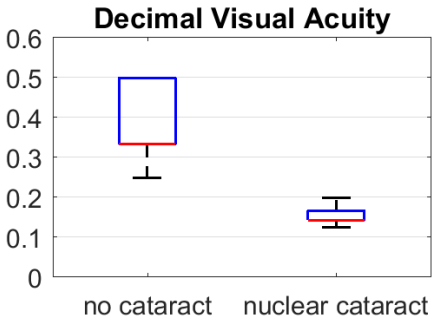

Figure 8.4: Decimal VA measured without (left: 0.25 to 0.5 VA), and with (right: 0.125 to 0.2 VA) simulated nuclear cataracts.

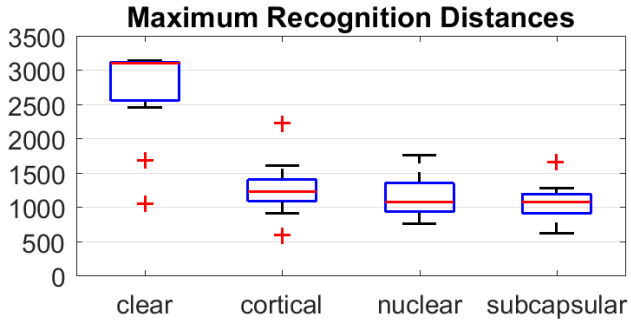

Figure 8.5: MRD (in cm), measured with clear vision, and simulated cortical, nuclear, and subcapsular cataracts.

8.3.2 Measured Maximum Recognition Distances

In our quantitative experiments, we measured MRDs under different visual conditions as described in Section 8.2.1. These tests were error-prone, as participants sometimes touched the the trackpad of the Vive controller too far on the rim and the controller would not register their input. This led users to believe their input was wrong and made them move much closer to the escape-route sign than necessary (before realizing how to properly press the trackpad), yielding a very small MRD value in the results. Since these input problems caused at least one skewed MRD value for almost every participant, we decided to take the median of each group of samples (1 group = 3 samples under 1 condition) instead of all samples or the mean of these groups. Figure 8.5 shows the distributions of median values per vision condition. The first boxplot represents the measurements with clear vision and no simulated cataracts. Participants achieved higher MRDs than we anticipated and sometimes recognized the sign's direction from the starting point. For future studies, we recommend placing the starting point much farther from the sign to avoid capping the MRD values.

Knezevic [Kne08] states that "*[i]f two statistics have non-overlapping confidence intervals, they are necessarily significantly different.*" Figure 8.5 shows that MRDs with cataract vision are significantly lower than with clear vision. Paired t-tests comparing the distribution of MRDs of clear vision to MRDs of each cataract type also show that these distributions are significantly different, rejecting the null-hypothesis at a 0.05 significance level, with $p < 0.001$ and effect sizes of 2.43, 2.46 and 2.56, calculated with *Cohen's d* for MRDs with cortical, nuclear and subcapsular cataracts, respectively. Our statistical evaluation yields that a sample size of four or five participants is required to achieve a statistical power of 0.9 for these tests. All of our tests have a power of ~ 1 with our sample size of 13 participants. With outliers removed, the p-values are still below 0.001. The outliers that are shown as red plus-signs in Figure 8.5 can be attributed to three participants. After investigating our data, we found that for at least one of these three participants our VA calibration procedure did not work, causing errors in the remaining measurements of this participant. We have not determined the causes for the other two

outliers.

8.3.3 Environment Exploration Results

During our qualitative experiment (Section 8.2.1), participants were asked to comment on the illumination in the scene and their perception with the three different cataract simulations. For each cataract type, they were shown lighting setup 1 (Figure 8.3a) and then lighting setup 2 (Figure 8.3b), and could switch back and forth between them. They were asked to compare the second to the first lighting setup, first with cortical cataracts, then with nuclear cataracts, and finally with subcapsular cataracts.

Figure 8.6 shows that most participants rated the second lighting setup worse when compared to the first, with cortical or nuclear cataracts. Some participants complained in the second setup that they did not like having this many spotlights in their field of view, since the simulated glare was blinding their vision. Interestingly, three taller participants preferred the second lighting setup over the first one, since they experienced a smaller grazing angle to the spotlights and therefore a less severe blinding effect. Most participants also mentioned that the first setup illuminated the whole scene better, instead of primarily illuminating the work surface. Overall, participants liked a well-illuminated work space (as in the second setup), but in general disliked luminaires in their field of view, due to blinding effects.

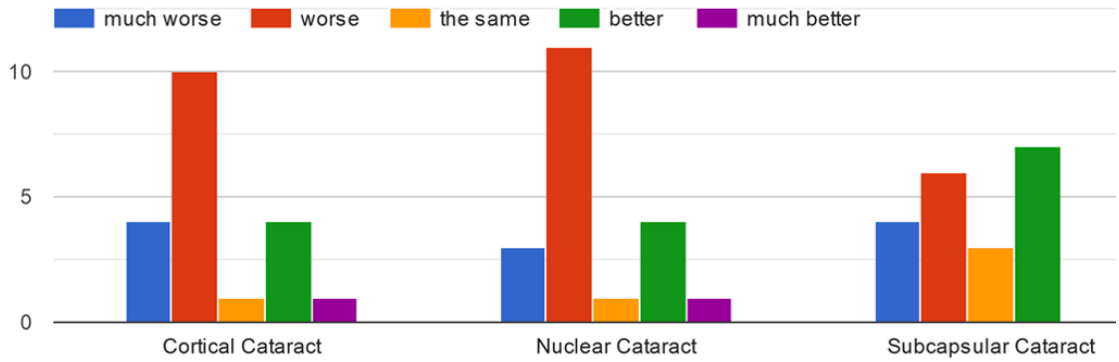

Figure 8.6: Answers to the question, "Compared to the previous illumination, does this second one feel better or worse regarding perception? (Is it easier or harder to see objects?)".

8.3.4 Questionnaire Data

We had 21 user study participants in total, 8 of them for the pilot study and 13 for the final user study. The participants' ages ranged from 24 to 56 years old, with $\sim$ 85% male and $\sim$ 15% female. 19% wore glasses and another 19% wore contact lenses during the experiments, mostly due to myopia. Since we expected glasses to interfere with the eye tracker, we were specifically looking for people with normal sight or wearing contact

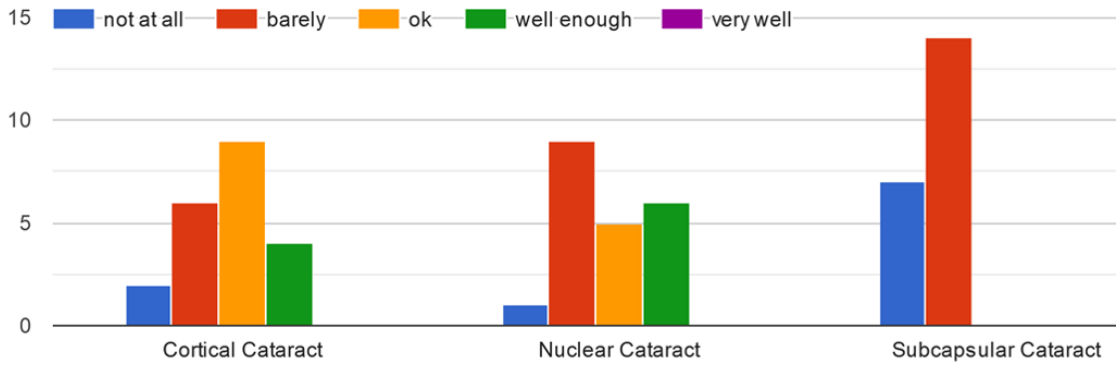

Figure 8.7: Answers to the question, "How well did you feel you were able to read the escape-route signs with cortical cataracts, nuclear cataracts or subcapsular cataracts?".

lenses for our study, but did not exclude any participants who volunteered to take part in our study (even when they were wearing glasses). All participants were proficient in using computers and except for one participant, all had had at least some previous experience with VR. After the experiments, participants were asked to answer a questionnaire about their experience with the simulation. Figure 8.7 shows that all participants felt they could barely read escape-route signs with subcapsular cataracts or not at all. Our data (see Figure 8.5) does not show such an apparent performance difference between different cataract types. All participants answered the question of whether they thought they gained a better understanding for the problems people with cataracts face every day, after testing this simulation, with "yes."

8.3.5 Eye Tracking Data

During the whole study (for the MRD tests as well as the environment exploration), we recorded the eye movements picked up by the eye tracker. The more data it recorded for a participant, the better it worked. When using the eye tracker with users wearing glasses, the performance and accuracy of the tracker, as well as the amount of recorded data, decreased. Another interesting observation we made was that for one participant in our user study, dark mascara irritated the eye tracker, causing it to sometimes track eye lashes instead of the pupil (Figure 8.8).

8.4 Discussion

The results of our VA tests in VR suggest that our simulation is able to calibrate the vision of every participant with simulated cataracts to a similar level of impairment. This is achieved by using a calibration step for VA (as introduced in Section 6.3) and our novel calibration for loss of contrast (Section 6.4). Both calibration procedures are based on a medical test and follow the respective protocols as outlined in the international standard ISO 8596 [Int17] and the work of Pelli et al. [PRW88]. For future work, it may

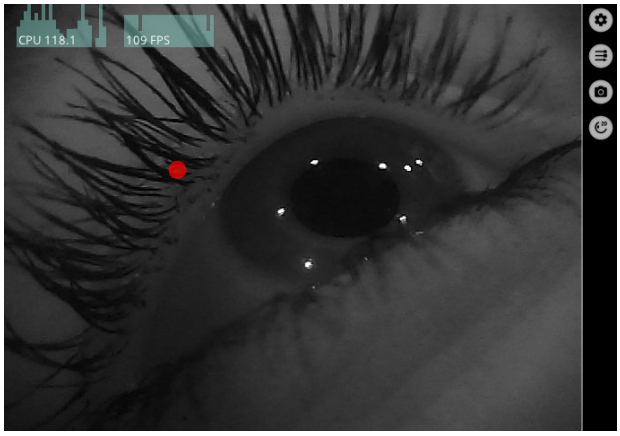

Figure 8.8: Eye tracker showing poor performance for user with dark mascara, mistaking eye lashes for pupil.

be worth considering deviating from these protocols and instead using a psychophysical approach to possibly increase the accuracy of these tests.

Regarding the color shift and bloom effect, we at this point cannot claim that our simulation correctly simulates exactly how cataract vision appears. The different symptoms of cataracts, including tinted vision and glare, vary among affected patients. In the next chapter (Chapter 9) we present a study with cataract patients to better verify the faithfulness of each of our simulated symptoms, comparing simulated cataract vision seen with an unaffected eye with actual cataract vision in the other eye.

The results of our quantitative experiments show that people with simulated cataracts achieve significantly lower MRDs than people with clear vision. For future work, conducting a user study with a larger number of participants and more measurements per vision condition could allow us to also investigate possible differences between types of cataracts.

In our qualitative experiment, we found that different lighting setups achieve different quality ratings when experienced with cataract vision. Our present methodology can allow architects or lighting designers to qualitatively evaluate their designs by importing them into UE and conducting experiments with our cataract simulation. To demonstrate this approach, we did a brief experimental evaluation of two different lighting setups (Figure 8.3) for a 3D model of a kitchen with our system. During these tests, looking at direct lights was reported as especially uncomfortable.

Our current integration of the Pupil Labs eye tracker has a noticeable delay, but still made it possible to show gaze-dependent effects. Even if our simulation is not perfect yet, participants were impressed by the simulated cataract vision and our questionnaire shows it succeeded in increasing their understanding of what people with cataracts experience.

8.5 Summary

We have employed our novel methodology for simulating eye diseases (Chapters 5), such as cataracts, and calibrating symptoms (Chapter 6) to the same level for every participant, in a user study, investigating the impact of cataracts on perception. After evaluating our method to reduce VA in our first study (Chapter 7), we now tested our approach for a complete simulation of cataracts in VR, including a calibration for contrast loss. Our experiments showed that our simulated cataract vision significantly influences the MRD for escape-route signs and that different lighting conditions are perceived as more or less comfortable with cataracts. We believe that our methodology could be helpful to architects and designers, when designing spaces that are accessible to people with visual impairments.

To evaluate the realism of our simulation of cataract vision, we need to consult people who know from first hand experience how cataracts can influence someone's vision. In the next chapter we will discuss experiments with cataract patients who have already been operated on one eye and whom we asked to help us adjust our cataract simulation, which they observe with their corrected eye, to match the VE as seen with their not yet corrected eye (without any graphically impaired vision). We also extend our simulation to other visual impairments, such as age-related macular degeneration or cornea disease as presented in Section 5.4 and Section 5.3.

CHAPTER 9

Study 3: Cataracts in AR

This chapter is based on the following publication:

Katharina Krösl, Carmine Elvezio, Laura R. Luidolt, Matthias Hürbe, Sonja Karst, Steven Feiner and Michael Wimmer. "CatARact: Simulating Cataracts in Augmented Reality" in *2020 IEEE International Symposium on Mixed and Augmented Reality (ISMAR)*, IEEE, 2020

Cataracts are not only the leading cause for blindness worldwide, they impact the vision of 65.2 million, putting them in second place behind refractive errors (presbyopia: 1.8 billion, other refractive errors: 123.7 million) [WHO19]. To address this, we developed

Figure 9.1: Simulation of cataract vision in eye-tracked stereoscopic head-worn display. Study participants were cataract patients with one corrected eye and one uncorrected eye. (a) Posterior subcapsular cataract simulated for corrected left eye and no modification for uncorrected right eye, viewing live stereoscopic video. (b) Cortical cataract with glare simulated for corrected right eye and no modification for uncorrected left eye, viewing 360° image.

a system to simulate cataract vision interactively in virtual reality (VR), using eye tracking to model gaze-dependent effects. In order to evaluate the faithfulness our of our simulation, we developed an augmented reality (AR) version (Figure 9.1) with improved simulated effects and tested it with actual cataract patients. During these experiments, we also used our symptom matching methodology to adjust the simulations as much as possible to match the actual cataract vision of the patient. In this chapter, we present the results from this pilot study, from which we also obtained sets of parameter values that can be used to create a simulation of cataract vision in AR or VR, as experienced by these patients. Our system presents a number of cataract symptoms (in one or both eyes) to a user wearing a stereoscopic head-worn display, integrating them with either the user's live binocular camera view of the real world, previously recorded video footage, 360° images, or live virtual environments. We support a number of modifiable parameters that control the simulated symptoms. Using a binocular eye tracker, gaze-dependent effects of the cataract simulation respond to the user's gaze.

Cataract symptoms are highly subjective and can vary individually depending on the kind and severity of lens opacity. There are different tests available to assess vision capabilities (e.g. visual acuity (VA), contrast sensitivity, color perception), which are are standardized and performed under a predefined setting with predefined lighting conditions. However, individual demands on visual function and its impact on quality of life also differ vastly, depending on the individual lifestyle. Someone with poor contrast sensitivity might not notice anything, while an artist might have a huge impact with only mild changes in contrast vision. According to an ophthalmologist we talked to, some people are happy with 50% VA, while others have high demands, and complain with 100% VA (according to the test), because they cannot see where their golf ball is going. This is why we believe AR can offer new possibilities to understand vision impairments and their impact on quality of life better, because symptoms can be experienced in an everyday life setting, instead of just obtaining measurements from medical test. To achieve realistic simulations, we need to contact affected people and investigate how exactly their vision is affected by a certain vision impairment or eye disease. Therefore, we designed a pilot study to evaluate our cataract simulation with people who actually have cataracts. Our participants recently had cataract surgery on one eye, and were awaiting surgery on their other eye, and thus could do a side-by-side comparison of our simulation, seen through their post-operative eye, with their own cataracts. In subsequent remote experiments, we showed our simulation through video calls to people who had cataract surgery a few months before and asked them to compare our simulation to related work.

Our system simulates and includes parameterized control for the characteristics and intensity of reduced VA, reduced contrast, a color shift, dark shadows and an increased sensitivity to light. To maximize the potential applicability of our system, we worked closely with ophthalmologists to refine both this set of symptoms and their depiction. Their expertise informed our development process and provided valuable insights that helped us understand how these diseases impact a person's vision, allowing us to identify and represent the core symptoms.

9.1 Simulation

The system we use in this study is an advanced version of the one used in our previous VR study (see Section 8.1), using our effects pipeline (Chapter 5) with the effects highlighted in Table 9.1. The system was extended to work in AR and on 360° images. Figure 9.2 shows the results of an AR image after each stage of the effects pipeline.

Our implementation is built using Unreal Engine 4.0 and runs on a PC with an AMD Ryzen 7 1800 CPU, 32GB RAM, and an Nvidia GTX 1070 graphics card. Stereoscopic output is displayed on an HTC Vive Pro headset with built-in RGB stereo cameras to support video–see-through AR, outfitted with a Pupil Labs binocular eye tracker with 200Hz update-rate cameras.

simulation of	**study 1**	**study 2**	**study 3**	***comment***
reduced VA (Sec. 5.1.1)	Gaussian blur (Sec. 5.1.1)	depth of field (Sec. 5.1.1)	Gaussian blur (Sec. 5.1.1)	*more accurate for cataracts*
reduced contrast (Sec. 5.1.2)		interpolation with gray (Sec. 5.1.2)	compressing luminance (Sec. 5.1.2)	*perceptual contrast reduction*
color shift (Sec. 5.1.3)		color interpolation (Sec. 5.1.3)	simulated color filter (Sec. 5.1.3)	*simulates physical phenomenon*
dark shadows (Sec. 5.1.4)		average brightness (Sec. 5.1.4)	gaze-tracked brightness (Sec. 5.1.4)	*reduces artifacts*
sensitivity to light (Sec. 5.1.5)		bloom (Sec. 5.1.5)	perceptual glare (Sec. 5.1.5)	*based on medical expertise*

Table 9.1: Effects from our effects pipeline (Chapter 5) used per study. In the AR study, presented in this chapter, we used the highlighted effects.

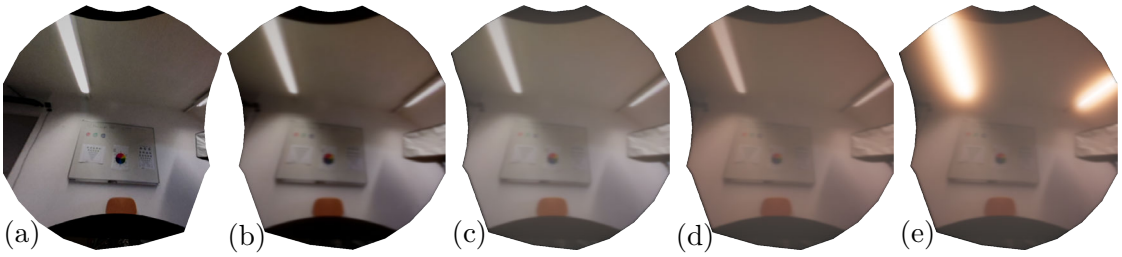

Figure 9.2: Application of the effects pipeline. (a) Original AR video with (b) reduced VA, (c) reduced contrast, (d) applied color shift, and (e) glare effect.

9.1.1 Reduce VA

In cataracts, reduction of VA is caused by an accumulation of yellow-brown pigment or protein in the lens as well as by the axial growth of the lens. Therefore, the VA of people with cataracts mainly depends on the visual angle of an object in the field of view and does not necessarily improve with short or far distance. Hence, a Gaussian blur (Section 5.1.1) simulates the reduced VA caused by cataracts more accurately than the previously used depth-of-field effect. Another reason for choosing a Gaussian blur over a depth-of-field effect is the choice to design an AR simulation that also works on prerecorded videos or 360° images, where depth information might not be available. Figure 9.2b shows the effect of this Gaussian blur on an AR image.

9.1.2 Reduce Contrast

In our previous study we reduced contrast by interpolating between a pixel color and a gray value in linear RGB space. However, transformations in a linear color space do not correspond to perceived contrast changes. To achieve a perceptual contrast reduction, we perform a compression of luminance values (Section 5.1.2) in the CIELAB color space, which is based on human perception and has perceptual uniformity[1]. A contrast-reduced AR image is shown in Figure 9.2c.

9.1.3 Color Shift

We applied a color shift by interpolating between the pixel color of the image and a predefined *target color* in the linear RGB color space, in our previous study. This is a fast and easy way to perform a color shift, but it has the disadvantage of also reducing contrast in the process. The yellowish/brownish tinted vision that people with cataracts sometimes experience is caused by particles in the lens that absorb parts of the incoming light falling onto the retina. Hence, the resulting color shift that a person with cataracts experiences can be simulated as color filter by multiplying the image color with the complementary color of the cataract particles, as described in Section 5.1.3. The result of this color shift can be seen in Figure 9.2d.

9.1.4 Dark Shadows

People with cortical or posterior subcapsular cataracts experience dark shadows in the periphery or center of their field of view (depending on the cataract type), due to protein aggregation or damage to fibers in the lens, which form an opacity that casts these shadows. Our simulation uses the in Section 5.1.4 described approach to simulate these dark shadows with a semi-transparent shadow texture overlaid over the image (see Figure 9.3). To simulate the influence of the contraction and dilation of the pupil, the shadow texture is scaled according to a gaze-tracked brightness value, as described in Section 5.1.4.

[1]This means the Euclidean distance between two colors (differing in color value or luminance), represented as 3D locations in the color space, is proportional to their perceived distance.

Figure 9.3: (a) Unmodified 360° image (left) and dark shadows of cortical cataract added to the VA-reduced, contrast-reduced, and color-shifted image for the right eye. (b) Posterior subcapsular cataracts with glare simulated for the right eye.

9.1.5 Simulate Sensitivity to Light

To simulate the intense blinding effects, often experienced by people with cataracts, we implemented a perceptual glare effect (see Figure 9.2e) based on work by Ritschel et al. [RIF+09] to replace the simple bloom we used during our previous study, as described in Section 5.1.5. Based on expert knowledge from consulting an optometrist, we were able simplify their approach and omit the simulation of particles in regions of the eye that have no significant influence. We also modified it for VR or AR applications, and further cut down rendering time of this effect for our pilot study by reducing the number of necessary *Fast Fourier Transforms* to only two instead of four, since we apply the cataract simulation, including this glare effect, to only one eye.

9.1.6 Adjustments for an AR Study

In recreating the approach used in our previous VR study, we needed to make a number of modifications to properly adapt the visualizations for video–see-through AR (see Figure 9.2), and to prepare the system for an AR pilot study whose participants are patients who have undergone cataract surgery on one eye and will soon have cataract surgery on the other eye. In our in-person experiments, we ask participants to view one channel of the video stream, captured by the built-in Vive Pro stereoscopic RGB cameras, and modified with our simulation, with their post-operative corrected eye. With their preoperative other eye, which still has cataracts, they will view the unaltered video stream. This allows them to compare our simulation (as seen with the corrected eye) to their own cataract vision (when looking at the unaltered video).

To better compare both images, users need to close one eye at a time if both images were displayed. However, this is not very comfortable and the resulting facial movement could easily move the headset a bit, affecting the calibration of the eye tracker. Therefore, we provide a comparison mode, where we render the view for only one eye at a time and show a black screen to the other eye. We let users switch between left and right eye, using the Vive controller trigger. While users switch back and forth, we are able to adjust the parameters of our effects according to their feedback. At the conclusion of the experiment, all adjusted parameters are saved and can be used as a parameter set to simulate the cataract vision of that participant as closely as we could match it. Our study yielded three parameter sets from the in-person experiments and two parameter sets from remote experiments, where participants looked at both images (left and right) while one was being modified with our simulation.

9.2 User Study

To develop our simulation, we consulted experts from the field of ophthalmology and optometry. To evaluate our simulation and the methodology behind it, we consulted cataract patients, who are uniquely qualified to tell from first-hand experience what vision with cataracts looks like and who are able to do a side-by-side comparison of our simulation to their own cataract vision. We conducted a pilot study that was registered and approved by the ethics committee of the Medical University Vienna (EK 1737/2019) and adhered to the tenants of The Declaration of Helsinki. To gather additional feedback, we decided to conduct remote experiments, showing our simulation to participants on a 2D screen via video call. Our primary goal for this pilot study (and the subsequent remote experiments) was to test how well our methodology works for parameter adjustment of simulated symptoms, during the experiments. Furthermore, we wanted to investigate how realistic each of our simulated symptoms can be in comparison to the effects of real cataracts on vision. Finally, we wanted to determine the overall realism of the simulation.

To answer these research questions, we formulated two hypotheses:

- *H1*: The experiment design allows the adjustment of simulated cataract symptoms to match the corresponding symptom of each participant's own cataract vision.
- *H2*: Participants do not observe a great difference between their vision with their own cataract and the simulated cataract, when compared while looking at the environment through the video–see-through AR headset.

9.2.1 Study Design

We designed a qualitative study with a very specialized population: cataract patients after their first operation on one eye and before the operation on their other eye. This allows us to compare the clear vision of a corrected eye viewing the environment through our cataract simulation to the vision of a cataract-affected eye viewing the unmodified environment. Since cataract patients often get surgery on their second eye a few days or weeks after their first operation, there is a very limited time frame in which they qualify as participants for our study. Furthermore, cataracts predominantly affect elderly people [WHO19] and this age group is, in general, not as technically knowledgeable as younger adults. Consequently, finding volunteers for such a study, in which participants cannot expect any benefits or compensation, was challenging because of the lack of motivation: Many initially recruited participants dropped out right before starting the single-session experiment.

These circumstances made it difficult to recruit the larger number of participants we had hoped to have for quantitative analyses. Instead, we decided to work with fewer participants and try to obtain more qualitative feedback, during semi-structured interviews. We use a between-subjects design for our study and no randomization or counterbalancing was done, since each patient experienced a simulation adjusted to their own specific vision impairments.

9.2.2 Participants

We recruited five participants, three male and two female, aged 63, 64, 74, 64, and 71, for our study. Three of them were cataract patients, recruited at the Department of Ophthalmology and Optometry, Medical University Vienna, after their first cataract surgery. Inclusion criteria involved good best-corrected VA (6/6 or 20/20 vision) in the post-operative eye, whose procedure was performed within two weeks prior to study inclusion, diagnosed cataract scheduled for surgery in the other eye, and no ocular disease responsible for vision impairment other than cataract.

The two other participants were acquaintances of the research team, who were recruited subsequent to our pilot study for remote experiments. They had cataract surgery about two months before the remote experiments.

Most of our participants had only a mild degree of vision impairment secondary to cataract because surgery was available to the population from which we recruited before severe symptoms could develop. We would like to emphasize that our five patients are not representative of all different manifestations of cataract. However, a clouded lens results in distinct symptoms (e.g., a change in color vision), so participants were expected to give us valuable feedback on the realism and adaptive options of our simulation.

Participants for in-Person Experiments

The following three patients participated in our study for the in-person experiments:

P1 (male, 63 years old) was shortsighted (-6 diopters[2]) with astigmatism ($+3/90°$) and diagnosed with cataract in both eyes. An introcular lens was chosen that left him with a refractive error of -3 diopters in the left, post-operative eye. The right eye, that served as reference was also shortsighted (-5.5 diopters) with astigmatism ($+2.75/89°$) and had early signs of cataract with a VA of 20/30. This patient participated in our study one week after his first cataract surgery.

P2 (female, 64 years old) was also shortsighted (-5 diopters) before surgery and had her refractive error corrected during surgery on the left eye. An examination of the background of this eye showed *drusen*, a sign of aging or dry age-related macular degeneration, which could potentially impact the VA. The patient's first cataract surgery was just two days prior to our study. Her right eye was also shortsighted (-7.25 diopters), had astigmatism ($+2.75/86°$) and early stage cataract, with 20/30 vision.

P3 (male, 74 years old), was shortsighted (-3.25 diopters) in his left eye before surgery and his refractive error was corrected with the implanted intraocular lens. Cataract surgery was performed eight days before his participation in our study. His right eye had early-stage cataract, and was farsighted ($+1.75$ diopters) with a VA of 20/25.

[2] see Section 3.1 for more details on diopters and relation to VA

Participants for Remote Experiments

The following two participants agreed to participate in our remote experiments:

P4 (female, 64 years old), was farsighted (+2.25 diopters) in her left eye before surgery and her refractive error was corrected during surgery, which was performed about two months before the remote experiment. Her right eye still had early-stage cataract, with no noticeable symptoms at this time.

P5 (male, 71 years old) was farsighted (+0.1 diopters) before surgery, and his refractive error was corrected during surgery about three months prior to the remote experiment. His right eye had early stage cataract.

9.2.3 Pilot Study Protocol

The in-person experiments were conducted in our lab, after cataract surgery on the first eye, with participants P1, P2 and P3.

1. Patient information and consent form.
   Before the experiment, the study, its purpose and the study protocol are explained in detail and written informed consent is obtained. Patients are also advised to refrain from fast head movements to avoid VR sickness that could be caused by the lag of the AR video.

2. Calibrate eye tracker in VR.
   The patient puts on the VR headset and looks at a black dot that is displayed in the headset and moves around in circles, in order to calibrate the Pupil Labs binocular eye tracker.

3. AR simulation.
   The video stream of the surrounding environment, captured by the Vive Pro cameras, is displayed unaltered in the headset. Then the view for one eye is turned off. Using the Vive controller, the user is able to switch between eyes (one is always looking at a black screen, the other at the AR video) to simulate closing alternating eyes.

4. Iterative parameter adjustment.
   The participant is asked to compare the vision of their preoperative eye with cataract (looking at the unaltered video stream) to the vision with their post-operative eye on the AR video and tell the researchers about the differences. The researchers then activate and adjust one effect at a time and apply it only to the former unmodified clear vision of the post-operative eye. Meanwhile, the patient switches back and forth between the view of the left and right eye to compare both AR videos. Each effect is adapted according to the patient's feedback to achieve a simulation that matches the patient's cataract vision as closely as possible.

Figure 9.4: 360° image[3] shown to participants.

5. 360° image.
   After the parameter adjustment in AR, patients are also shown a 360° image (Figure 9.4) and are again asked to point out differences between simulated cataract vision and actual cataract vision in the other eye. Parameters are further adjusted if necessary. This 360° image view serves as a fallback in case the parameter adjustment in AR does not work well. Especially for patients who have just a mild form of cataract, the quality of the AR video might be too low for them to easily tell differences between the view with their post-operative eye and the view with their cataract.

6. Environment exploration and semi-structured interview.
   While the patients look around and explore (either in AR or in the 360° image), they are asked to rate the (adjusted) parameters and the overall impression of the simulation in terms of realism (on a Likert scale from 1 to 7) and are asked a few questions regarding the simulation, in a short semi-structured interview (which may continue after the patient takes off the headset).

7. Questionnaire.
   Patients are asked to fill out or dictate answers to several questions regarding demographics as well as their own severity of symptoms and experience living with cataracts.

Breaks are possible at any time on demand and are recorded. Eye tracking re-calibration is done if necessary. The experiment is stopped if a patient starts to feel uncomfortable.

[3]Image taken from https://hdrihaven.com/

Figure 9.5: 360° image[5] of a low-light scene shown to participants.

9.2.4 Remote Experiments Protocol

We conducted further experiments with participants P4 and P5. For these experiments we used Jitsi[4] to stream live images and communicate with participants via voice chat. For these experiments, participants are specifically asked to compare the presented cataract simulations to their memory of their cataract vision before the surgery.

1. Patient information and consent form.
   Before the experiment, the study, its purpose and the study protocol are explained in detail and written informed consent is obtained. Participants are told that they will be shown different cataract simulations and need to advise the researchers on how to adjust each of them and rate their quality in the end.

2. Related work simulations.
   Two images are shown in a side-by-side view, with and without simulated cataract. We use 2D images of related work by the National Eye Institute [Nata], images of the VR simulation by Väyrynen et al. [VCH16] and images of the AR simulation of Ates et al. [AFF15]. (Since Ates et al. did not provide the original image in their publication, we took their image of simulated protanopia and reconstructed the colors with the *match color* operation in Photoshop.)

3. Severity adjustment.
   The participant is asked to compare both images and tell the instructor to adjust

[4]https://jitsi.org/
[5]Image taken from https://hdrihaven.com/

the cataract simulation until it best reflects their memory of their cataract vision before surgery. Adjustment is done by adjusting the opacity of the cataract image when blending it over the original. (Since the cataract simulation of Ates et al. consists only of a Gaussian blur, the respective built-in effect in Photoshop is used to simulate their version of cataract vision.) The unmodified original image is always shown next to it as reference.

4. *CatARact* simulation in 360° image mode.
   The video displayed in the Vive Pro (for both eyes) is mirrored on the desktop and streamed via Jitsi video call to the participant. The position of the head-worn display (HWD) is fixed and shows a static part of a 360° image (Figure 9.4), to create a fair comparison to the related-work images, and avoid revealing which one is our simulation). A second image (Figure 9.5) is used to test a low-light scene.

5. Iterative parameter adjustment.
   The participant is asked again to compare two images. One stays unmodified and the other is adjusted with our simulation, one effect at a time, each tweaked with input from the participant until it best matches their memory of their cataract vision before surgery.

6. Final ratings and semi-structured interview.
   Images of all four adjusted simulations with reference images are shown to the participant at the same time. The participant now has to rate the quality of each simulation in terms of realism (on a Likert scale from 1 to 7) and is asked further questions about their experience with cataracts.

7. Questionnaire.
   Patients are asked to fill out a short questionnaire regarding demographics as well as their own severity of symptoms and experience living with cataracts and send it via email to the research team.

9.3 Results

We first conducted our pilot study with in-person experiments. After evaluating the results, we conducted two more remote experiments to gain further insights and compare our simulation to related work.

9.3.1 Pilot Study

Figure 9.6, 9.7 and 9.8 show examples of simulated cataract vision after parameter adjustment for P1, P2, and P3, respectively, compared to their unaltered views. For each participant, we only simulated their individual symptoms experienced with their cataract-affected eye. For example, P3 did not experience any blinding or glare effects and none of the three participants in our pilot study experience dark shadows, which are caused by cortical or posterior subcapsular cataracts. All three participants experienced

reduced VA and color shift with their cataract vision. P3 did not notice any difference in contrast vision, when comparing his post-operative eye to his cataract vision.

Figure 9.6: Simulated cataract vision (left) of P1 and unmodified 360° image (right).

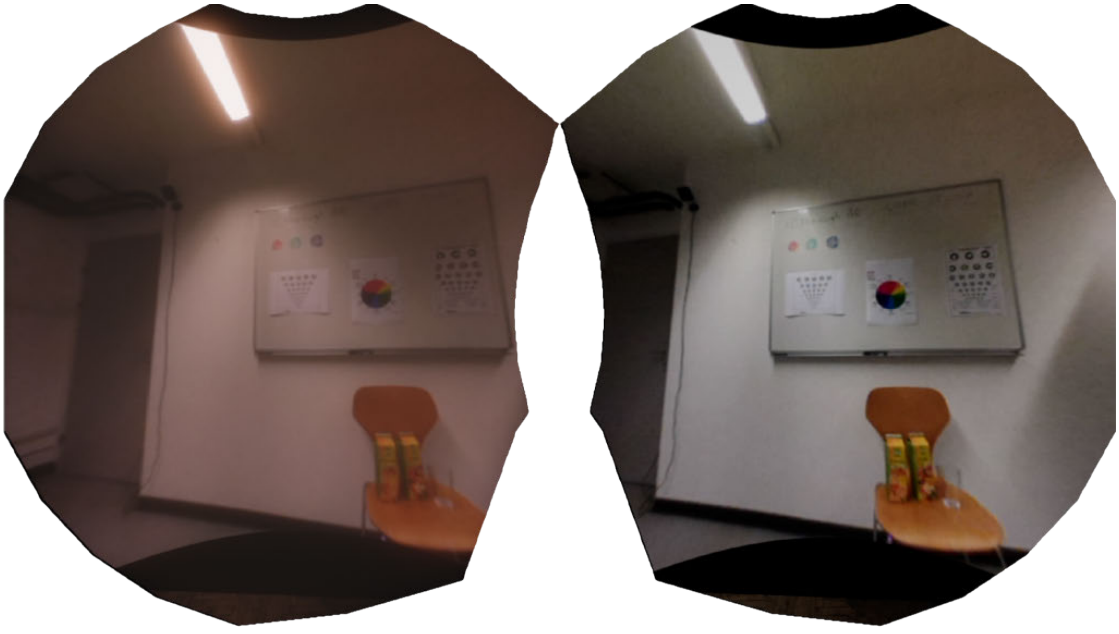

Figure 9.7: Simulated cataract vision (left) of P2 and unmodified live AR video (right).

Figure 9.8: Close-up of simulated cataract vision (top/bottom left) of P3 and unmodified AR video (top right) and 360° image (bottom right).

After adjusting parameters, participants were asked to compare the simulated effects to their own cataract vision, by using the trigger on the Vive controller to switch between left and right view (noting again that the other eye would always see a black screen). The participants had to rate the similarity of simulated symptoms and the symptoms of their own cataract on a 7-point Likert scale. Figure 9.9 shows the results of these comparisons. All symptoms were rated as more similar than not, except for glare, which was rated as 7 by P1 and as 2 by P2 (in terms of similarity). With an average score of ~ 3.7, the overall impression of the simulated cataracts was that they were not perceived as very similar to the vision participants experienced with their own cataracts. P3 was overall very satisfied with the simulated cataract, which involved just the simulation of reduced VA and a color shift, because he did not experience any other symptoms.

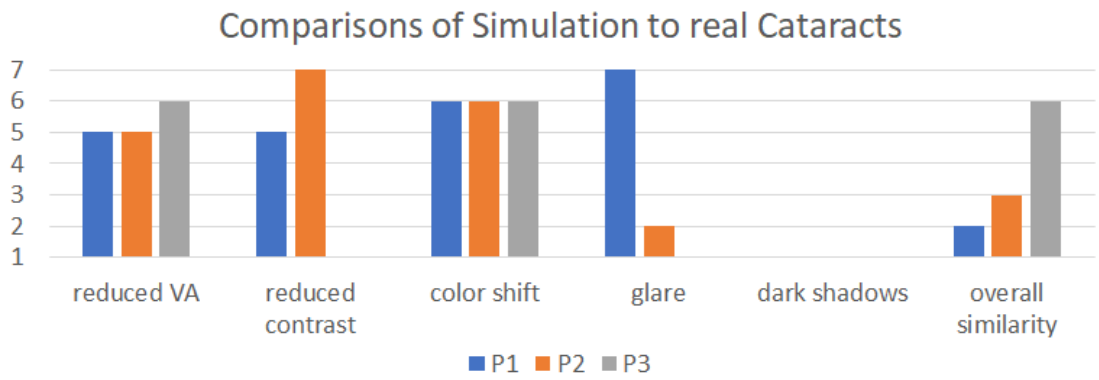

Figure 9.9: Participants P1, P2 and P3 compared each simulated effect, as well as the overall impression of our simulation, to their own cataract vision on the preoperative eye, on a 7-point Likert scale (from 1 — does not look similar, to 7 — looks exactly alike).

Observations and Qualitative Feedback

For P1, it took a long time to adjust the parameters for all effects in the AR mode. At some points, P1 mentioned seeing changes in the view of the right eye (which was never changed) or changes when no parameters were modified. The visual impression for this patient seemed to vary over time. The experiment was continued in the 360° image view, where he had an easier time distinguishing between his own cataract and the simulation and could give more precise feedback, which allowed adjusting the parameters with less variance. Although P1 rated each of our effects above average up to very good (see Figure 9.9), he rated the overall impression of the simulation as 2 out of 7.

P2 participated in our study just two days after her first cataract surgery. She often tilted her head backwards in order to be able to look downwards. (This behavior can be explained by her astigmatism, where looking down makes it easier for her to recognize objects.) Unfortunately, her neck became sore, which resulted in an early termination of the experiment before the 360° image view could be tested. This participant did not experience very disturbing glare effects with her cataract, which could explain why she gave a rather low rating for our glare effect. She mentioned impaired vision especially in dark environments.

P3 noticed only a slight blurriness and color shift in his vision when his cataracts started to become noticeable. Therefore we focused on these effects with this participant. He also told us that he first noticed his eyesight was deteriorating when driving a car, because his peripheral vision had gotten worse.

9.3.2 Remote Experiments

P4 rated the result of our simulation of the low-light scene, including reduced VA, reduced contrast and glare, as 7 on the Likert scale, since it best resembled her experienced cataract vision, especially with the blinding effects (see Figure 9.10). She also liked (6 on

Figure 9.10: Simulated cataract vision (left) of P4 and unmodified 360° image (right).

Figure 9.11: Simulated cataract vision (left) of P5 and unmodified 360° image (right).

the Likert scale) our simulation of the interior scene, since it showed the faded colors well, which she had experienced. The participant further rated the adjusted image of Väyrynen et al. [VCH16] as 7 regarding the blinding effect as well as the adjusted image of Ates et al. [AFF15] regarding the blur alone. She did not like the adjusted image of the NEI [Nata] (rated as 2), since she could not recall experiencing such color changes.

P5 also preferred our simulated cataract for the low-light scene (rated as 7), and the indoor scene (rated as 6) shown in Figure 9.11. The simulation included reduced VA and contrast, a very subtle glare, as well as a dark shadow in the center of the field of view. P5 rated the simulated effects of Ates et al. and the NEI [Nata] as 7 and 6 respectively (even though he mentioned not having experienced any color shift). Furthermore, he could not recall experiencing intense blinding effects as simulated by Väyrynen et al. (no rating).

9.4 Discussion

Our simulation uses the effects pipeline presented in Chapter 5 with the effects highlighted in Table 9.1. We used a Gaussian blur instead of a depth-of-field effect, because this simulates the reduced VA, resulting from a clouded lens caused by cataracts, independent of the viewing distance, which in this case is more accurate. We used a histogram compression of luminance values instead of an interpolation with a fixed gray value, resulting in a perceptually correct contrast reduction. Our new color shift also more accurately simulates the physical process of light passing through a tinted lens than the color-interpolation used in our previous study. When simulating dark shadows, we enhanced the technique described in Section 5.1.4 by making the influence of light (and therefore interactive scaling of the shadow textures) dependent on the distance of a light source to the center of the gaze. This more accurate, since light sources create more glaring effects when we look at them directly, and it also reduces artifacts caused by light source suddenly entering our field of view on the side. Furthermore, we exchanged a simple bloom effect by an implementation of a glare, based on human perception and medical expertise. In addition to VR, we can also apply our simulation to an AR video stream or a 360° image and apply it selectively on one or both eyes, which allowed us to present a new methodology to adjust and evaluate simulated symptoms with real patients. In contrast to our previous study, which included only people with healthy eyesight, we now tested our methodology with a very specialized population— cataract patients between surgeries. This allowed us to gain insight into the complexity and subjectivity of visual perception with cataract vision.

9.4.1 Interpretation of Results

Through our first qualitative pilot study, we learned that parameter adjustment for our simulation is not trivial and multiple factors can influence the perception of patients with their operated eye.

Varying Visual Impressions

For some patients, it can take up to a few weeks for the operated eye to fully heal. An unstable tear film, small injuries of the cornea, elevated intraocular pressure, or mild inflammatory response are frequently seen early after surgery. Each of these conditions could have an impact on VA and might explain the varying visual impressions of P1. In future studies, experiments should be conducted a few weeks after the surgery if possible (noting that our protocol did not allow postponing surgery on the other eye). Additionally, auto-focus AR eyeglasses, as described by Chakravarthula et al. [CDAF18], could be used to compensate for a remaining reduced VA that could not be fully corrected through cataract surgery, as in the case of P1.

Ratings

The individual components (effects) are rated by participants during environment exploration, while experiencing the simulation as a whole (including all adjusted effects combined). Individual effects got good, but not perfect, ratings. We suspect that these small differences of each effect (comparing simulated to real symptoms) add up, which explains why the overall simulations received lower ratings than the individual effects. Our glare effect was rated very good (7 on a 7-point Liker scale) by P1, but did just get a rating of 2 by P3. In our work on gaze-dependent simulation of light perception in virtual reality [LWK20], we also ran a user study using a version of this perceptual glare effect. Based on the results of that study, we concluded that "[...]*perception is highly subjective. Therefore, it is difficult to generate a generally acceptable model.*". We believe that a more detailed adjustment of the individual glare parameters (which is already possible with our simulation, but time consuming during a user study experiment) could improve the realism of our glare. However, more research is needed to improve individual effects and we argue that working together with patients is the right approach, since they are the only ones who can provide a ground truth for our simulations.

Blur

In this study, we applied our blur uniformly to the whole image to simulated reduced VA. For future work we plan to blur the periphery of a user's visual field independently to an adjustable amount, so we can simulate early cataract symptoms like blurry peripheral vision, as described by P3.

Subjective Feedback

Even when conducting a study with a very specialized population such as cataract patients between surgeries, who can simultaneously compare our simulation to their cataract vision, it may be useful to conduct medical vision tests (e.g., for VA or contrast sensitivity) in the simulation. This would help acquire additional objective feedback: Vision impairments such as cataracts can be experienced very differently and it can be hard to explain how cataract vision looks or even accurately describe the difference between cataract and clear

vision when comparing both. As an extreme example, Pamplona et al. [PPZ+11] describe a procedure for capturing and modeling the visual effects of a participant's cataract-affected eye with a smartphone augmented with special optics, and then rendering an image with the model (without real-time constraints).

9.4.2 Limitations

We note that all our participants had a refractive error beside their cataracts, which potentially interfered with their visual perception. In addition, our calibrations might not reflect the impact of a clouded lens alone. However, refractive errors can easily be corrected with glasses or contact lenses, which could be worn with the VR HWD.

Mitigating the Effects of COVID-19 on Research

After the presented pilot study, we planned to conduct a quantitative study with cataract patients, which would also include medical data such as slit-lamp images of eye lenses of patients and Lens-Opacity-Classification-System (LOCS) III gradings of these images. However, the prepared study with already scheduled experiments with patients had to be postponed at the last minute, due to the COVID-19 pandemic [Wor20]. With hospitals that could only be entered by medical personnel or for procedures that could not be delayed, elderly people (our primary target group) who are supposed to stay at home, and social distancing rules in place, it was impossible for us to conduct further in-person experiments. We plan to run our quantitative user study as soon as it is safe to do so for our participants, even though we cannot predict when this will be the case.

In the meantime, we were able to recruit two participants for remote experiments. This allowed us to test an alternative form for conducting such studies, which turned out to be a viable option to gather more information and gain more insight when in-person experiments are not possible. However, we need to keep in mind that simulated symptoms are experienced very differently in a VR HWD as compared to looking at a computer screen. Reducing the content shown on the desktop screen to match the field of view inside an HWD could make these experiments more comparable. However, it might be hard to achieve similar conditions, since the quality of the internet connection can have a significant impact on the visual quality of the images shown and on communication with the researcher. Changes are sometimes only visible after a perceptible delay, which makes parameter adjustments difficult. Even if we are not able to create a controlled test environment and show a high-quality simulation for the whole field of view, this format at least allows us to compare our simulation to related work. We chose images from the National Eye Institute [Nata], Väyrynen et al. [VCH16] and Ates et al. [AFF15] to compare our simulation to, since cataract images as well as the corresponding original images were available (or easy to reconstruct). Since patients in our pilot study mentioned experiencing blinding effects, especially when driving at night, we added a low-light scene for our remote experiments, which turned out to yield the best results.

Evaluation

Even though we could not test every simulated symptom during our in-person experiments (since none of the three participants experienced dark shadows caused by their cataracts), they showed that our symptom-matching methodology, involving comparisons of simulated cataract symptoms to real cataract vision, proves useful. While parameter adjustments cannot be done as accurately in our remote experiments, they enabled us to also test one simulation with dark shadows (for P6), and participants preferred our simulation when compared to related work.

We acknowledge that our pilot study has a very small number of participants. However, our simulation builds upon our previous work[KEH+19], was developed in close collaboration with medical experts, and our experiments yielded encouraging feedback of each individual effect. Even though our study cannot fully validate the accuracy of our simulation, we believe that our methodology and framework already provide timely and valuable insights for the research community and create a base for future studies.

Hardware

Using the low-resolution Vive Pro cameras for our AR simulation is not ideal, as it results in reduced VA for both eyes. We then add additional blur in one eye to reduce the VA further for our cataract simulation, to match the vision of the other (cataract-affected) eye. The limited resolution does not directly interfere with the VA simulation, but as a result, our simulation will match the blurred vision of the cataract-affected eye including the reduced VA caused by the HWD alone. It is unclear at this point if the overall VA experienced with cataracts (when looking at the unmodified AR stream) equals the person's VA in the real world, or if it equals the sum of the VA reduction caused by the HWD and the cataract. Still, we need to use video–see-through AR for our simulation, since it uses post-processing effects that cannot be applied to conventional optical–see-through AR. We have also tried a Stereolabs ZED Mini stereo camera, which has higher resolution and lower latency, but at the expense of a smaller field of view. The Varjo XR-1 video–see-through AR HWD meets our resolution needs, but is an order of magnitude more expensive and weighs much more—an important concern when deploying to an elderly population.

9.5 Summary

In this chapter, we tested our methodology to simulate cataracts in AR and evaluated the realism of our simulation in a pilot study with three participants, each of whom had cataract surgery on one eye, while they still had cataracts in the other eye. Our preliminary results (Figure 9.9) show that the individually adjusted symptoms were deemed to be close to our participants' perception of the environment with cataract vision in the majority of cases. However, the overall impression of our simulation was rated worse than the individual symptoms by P1 and P2. We also conducted two remote experiments,

adjusting our effects with participants via video call and comparing our simulation to images of simulated cataracts in related work. Qualitative feedback and Likert-scale ratings from our participants indicate that our complete simulation of cataract vision is superior to related work, which often only features one or two symptoms.

The individual setting of each parameter adjusted during our experiments was saved for use in future experiments to start with more realistic simulation parameters. By conducting a pilot study, we have shown the feasibility of our methodology and gathered qualitative feedback. Our remote experiments demonstrate an alternative to in-person experiments and served as a way to compare our simulation to related work. We conclude that our methodology proved useful for creating more realistic simulations of cataracts and could also be used for simulations of other vision impairments. In future work, we also want to provide a statistical analysis of quantitative data, evaluating the realism of our simulation. To that end, we already obtained ethics-committee approval for a quantitative study with cataract patients, which will run over a longer period of time and also include patient medical data.

Although there is potential for improvement, this work already has advantages over 2D images, physical goggles or other existing 3D, VR or AR simulations with very simple depictions of cataract vision, due to its immersiveness and complete simulation of cataracts, which was developed together with ophthalmology experts.

CHAPTER 10

Concluding Remarks

10.1 Summary

The key goals of our work are to reduce barriers to empathy, helping people with healthy eyes to understand how the world looks to a person with a visual impairment, and to provide tools to quantify the effects of visual impairments on perception and evaluate architectural and lighting designs for accessibility for people with vision impairments. To that end, we posed the following research questions:

- *Q1: How can we efficiently quantify the effects of a reduced visual acuity (VA) on the recognizably of signage?*
- *Q2: How can architects and lighting designers test their designs for accessibility for people with different vision impairments?*
- *Q3: How can we create realistic simulations of vision impairments, based on the first-hand experience of affected people?*

To address these research questions we have presented a **methodology and system to simulate vision impairments in in virtual reality (VR) and augmented reality (AR)**.

- *(Q1:)* We have demonstrated how to calibrate different symptoms of eye diseases to the same level for different users and conduct user studies to take measurements and quantitatively evaluate the influence of certain symptoms on perception, such as the effect of reduced VA on emergency signage.

- *(Q2:)* Our approach to combine individual symptoms and simulate complex eye disease patterns, together with the ability of our system to import 3D models of architectural scenes, can be used to investigate different aspects of architectural or lighting design and inform architectural planning to create more inclusive designs in the future.

- *(Q3:)* We also showed how to evaluate and adjust vision impairment simulations with patients, using our symptom-matching methodology, to achieve realistic depictions of certain eye diseases.

When designing vision impairment simulations, different factors, like the visual capabilities of users, the resolution of the display and fixed focal distance a possible misplacement of the VR headset and many others factors could influence the perception of people in VR or AR and need to be taken into account as best as possible with today's available head-worn displays (HWDs) and their hardware limitations. There are different approaches to simulating vision impairments, using goggles, modified 2D images, VR or AR simulations. At the time of writing this thesis, most existing approaches did not take hardware constraints or vision capabilities of users into account. Therefore, they are not feasible for user studies where we want to take exact measurements and statistically evaluate results.

We presented a system that offers more complete, accurate and immersive simulations than previous work, combining multiple effects to simulate different eye disease patterns and taking the above-mentioned factors with the most impact on vision into account. Our proposed methodology allows calibrating different effects that simulate symptoms of vision impairments to the same level for every user, by adapting medical eyesight tests and using them in a VR simulation.

In order to achieve gaze-dependent effects, eye tracking is used to calculate brightness values at the gaze point, to adjust different effects, or move effects relative with the gaze of the user. We have shown how an effects pipeline can be built to combine different symptoms to simulate complex eye diseases, such as different types of cataracts, age-related macular degeneration (AMD), or cornea disease, as well as refractive errors.

Our experiments emphasized that current standards and norms for signage should be revised to include people with vision impairments, that different lighting conditions influence the perception of cataract symptoms and that VR and AR systems can be used to create realistic vision impairment simulations together with doctors and patients and help to increase the understanding for challenges people with vision impairments face everyday.

Our simulations can be used to train medical personnel as well as to increase empathy of relatives of patients with vision impairments and raise awareness for vision impairments. While planning the design of a building, architects can use our methodology to make determinations of where to place constructions, such as lighting fixtures, in order to

maximize accessibility for users with limited VA, or to investigate how well different lighting conditions work for people with vision impairments.

10.2 Limitations and Future Work

One of our goals was to create realistic vision impairment simulations. Our experiments showed the flexibility of our framework in supporting the combination of different effects, adjusting the severity of each effect at run-time, allowing us to simulate a variety of different eye disease patterns. While the ophthalmologists we collaborate with see our simulations (with their flexibility and immersive nature) as a clear advancement for helping people to better understand vision impairment, the only way to fully validate the quality and realism of our simulation is to compare the simulated effects to a ground truth. Since the characteristics and severity of some symptoms are hard to assess, patients who have the same eye diseases we aim to simulate are the only ones who can provide us with a comparison to a ground truth (i.e., their own affected vision). The purpose of our third study was to test an improved simulation and our symptom matching methodology in AR and let patients judge the quality of our work and help us to improve it. Unfortunately, our planned study with 30 participants got cut short due to the COVID-19 pandemic and we are only able to present preliminary results on the quality of our simulated effects in this thesis. The few experiments we could run showed that our simulated effects are not yet perfect. We believe that these effects can be improved in future work, by working closely with ophthalmologists and patients, and that our methodology and framework form a solid basis for this future research and are a valuable contribution to the research community.

As discussed in Section 3.3, there are many factors that can influence the visual perception of a person wearing an HWD and we just selected some of these effects, which we deemed to have the highest impact on perception for our vision impairment simulations, to take into account. There are still plenty of other factors that could be investigated, and possibly taken into account when calibrating effects, in future work.

With our symptom-calibration methodology, we are able to calibrate different simulated symptoms, but the calibration is only done for one symptom at a time. We chose this approach because one symptom can influence the perception of another symptom. If we, for example, do a VA test or calibrate VA with already reduced contrast, we will get a different result than when testing or calibrating VA in isolation. Every simulated symptom degrades the vision of a person to some extent. If we combine multiple symptoms and then test a user's vision with the whole simulation, we can get different results for our eyesight tests than when just testing individual symptoms. Consequently, if we reduce the VA of a user to, e.g., 50% and then reduce contrast, add a color shift, simulate dark shadows and sensitivity to light and then perform a VA test in the end, the user might just be left with, e.g., 20% VA. If we change the order of effects and perform the VA reduction last, we can already take into account the amount of VA reduction that happens due to other effects and just reduce the VA further to the predefined value.

However, if we start with a contrast reduction to, e.g., 80%, then add other symptoms such as dark shadows or reduced VA, and then perform a contrast test with the whole simulation, we might get a different overall contrast sensitivity value than the one we initially calibrated the contrast vision to. Since many symptoms can influence each other, we cannot easily simulate a complex eye disease pattern that is specified beforehand by parameters like VA, contrast sensitivity or the amount of tinted vision, since we don't know which symptom affects which vision capability to which amount. We can, however, use our methodology to simulate an eye disease pattern that is perceived similarly by different users, by defining values for individual effects as opposed to values for the whole simulated condition.

Since some effects might be depending more or less on other effects, we need to investigate which order of effects yields a simulation closest to a set of predefined values. We could also iterate over the individual symptoms, re-calibrating them to different values in order to converge to a good approximation of a given eye disease pattern. However, even if the eyesight tests with our final simulation yield the predefined values, we cannot guarantee that we calibrated every symptom correctly, because we cannot rule out that another combination of symptoms could yield the same eyesight test results in the end. This is an open problem that we would like to tackle in future work.

We used our effects pipeline, which we originally developed to simulate different types of cataracts, to create simulations for cornea disease and wet and dry AMD, informed by expert knowledge from ophthalmologists and medical images. However, we did not yet evaluate the accuracy of these simulations with patients. Medical images of eyes with dry AMD show geographic atrophy (areas of loss of tissue) as areas on the macula with clear boundaries. Thévin and Machulla [TM20] argue, however, that a central loss of vision does not necessarily result in perceptually black areas in the center of the field of view (like used in our simulation of dry AMD), since affected people may experience *auto-completion*, a phenomenon where the brain fills in missing information by extrapolating from the surrounding area of the blind spot. We plan to conduct user studies to investigate this further in the future.

The impact of different lighting conditions on the individual perception of a visually impaired eye also presents an interesting research topic for future work. People with vision impairments such as cataracts often experience uncomfortable blinding or glaring effects caused by bright light sources. Although light is needed, very bright light like sunlight can be dazzling. To create truly realistic simulations of vision impairments, these effects should be supported as well. However, the HWDs that we use in our studies limit our ability to simulate very bright, dazzling light, let alone sunlight. Furthermore, even if we could, we would not want to expose our study participants to uncomfortable and potentially harmful light intensity. Instead, we simulated these blinding effects by using a bloom or glare as post-processing effect.

It should also be noted that the lenses and brightness of a particular HWD affect the perception of what is rendered on the display. We used the HTC Vive and HTC Vive Pro for our studies. With other types of displays, we would expect to get different values

from our symptom calibration procedures and might need different calculations for some effects. Our research would benefit from using HWDs with low latency, high resolution cameras, fast eye tracking and ideally a resolution that can match 20/20 vision of the human eye. Hence, we are looking forward to testing our simulations on modern high-end HWDs like the Varjo XR-1.

Our experiments, testing two different lighting setups, showed that bright light sources in the field of view of a user with simulated cataracts can create disturbing glaring effects. Future work should test lighting setups designed by a professional lighting designer, especially featuring indirect illumination, to find suitable lighting designs for people with vision impairments, such as cataracts.

Architects can use our tool to import 3D models of their designs and explore them in VR with different simulated vision impairments. This could help to identify problematic areas, where people with vision impairments might have difficulties to orient themselves, early in the design phase. Our AR mode could be used to test a shell of a building or the finished building later on for accessibility. In future work we would like to run studies with architects to discover how our tool can support them best or in what ways we need to extend or adapt it to meet their needs.

Our presented methodology and the system described in this thesis form the basis for many vision impairment simulations in VR or AR. We are currently working on simulations of other vision impairments and plan to open source our framework with all implemented simulations in the near future.

List of Figures

List of Tables

Acronyms

AMD age-related macular degeneration. 1, 3–7, 14, 15, 25, 27, 28, 34–42, 62–64, 136, 138, 141, 143

AR augmented reality. xi, 3–8, 13–15, 23, 24, 31, 32, 34, 38, 40–43, 45, 46, 49, 58, 60, 63–65, 73, 114–116, 118, 119, 121, 122, 125–127, 129, 130, 132, 133, 135–137, 139, 144, 145, 148

CVD color vision deficiency. 31, 33–35, 40

HWD head-worn display. 4, 6, 7, 12, 14, 15, 23–25, 31, 36–41, 47–49, 60, 70, 78, 81, 87, 91, 124, 131, 132, 136–139, 142, 143

MRD maximum recognition distance. 4, 6, 11, 12, 37, 43, 73, 76–79, 81–91, 93–97, 100, 102, 103, 105–108, 110–112, 143, 144, 147, 148

UE Unreal Engine. 47, 101, 105, 111

VA visual acuity. 2–4, 6, 9, 11–15, 18, 19, 21, 22, 29, 33–35, 37, 38, 41–43, 47–50, 60, 64, 67–71, 73, 75–77, 79–82, 87, 88, 91, 95–97, 100–102, 105–108, 110, 112, 114–117, 120, 125, 126, 129, 130, 132, 135, 137, 138, 141–144, 147

VE virtual environment. 37–39, 102, 104, 106, 112, 144

VR virtual reality. xi, 3, 4, 6–8, 11–15, 23–25, 33, 34, 36–43, 45–49, 57–60, 64, 68, 69, 71, 73, 75, 76, 78, 79, 81, 83–87, 90, 93, 94, 97, 99–101, 106, 107, 110, 112, 114, 115, 118, 121, 129, 131, 133, 135, 136, 139, 141, 142, 148

XR extended reality. 7

Bibliography

[Aar13] Aaron Leventhal. NoCoffee – Vision Simulator for Chrome. `https://accessgarage.wordpress.com/`, 2013. Accessed: 2019-10-30.

[AFF15] Halim Cagri Ates, Alexander Fiannaca, and Eelke Folmer. Immersive simulation of visual impairments using a wearable see-through display. In *Proceedings of the Ninth International Conference on Tangible, Embedded, and Embodied Interaction*, pages 225–228. ACM, 2015.

[AGR+00] Zhuming Ai, Balaji K Gupta, Mary Rasmussen, Ya Ju Lin, Fred Dech, Walter Panko, and Jonathan C Silverstein. Simulation of eye diseases in a virtual environment. In *Proceedings of the 33rd Annual Hawaii International Conference on System Sciences*, pages 5–pp. IEEE, 2000.

[Ame15] American Society of Cataract and Refractive Surgery. In-depth three-year trend report on clinical opinions and practice patterns. Available exclusively to ASCRS members. `http://ascrs.org/three-year-trend-report`, 2015. Accessed: 2019-09-19.

[ANK+20] Drew Alexander, Thuy Nguyen, Patrick Keller, Jason Orlosky, Shilpa Brown, Elena Wood, Onyeka Ezenwoye, and Wanda Jirau-Rosaly. Design of visual deficit simulation for integration into a geriatric physical diagnosis course. In *2020 IEEE Conference on Virtual Reality and 3D User Interfaces Abstracts and Workshops (VRW)*, pages 839–840. IEEE, 2020.

[APLBB18] Jérémy Albouys-Perrois, Jérémy Laviole, Carine Briant, and Anke M Brock. Towards a multisensory augmented reality map for blind and low vision people: A participatory design approach. In *Proceedings of the 2018 CHI Conference on Human Factors in Computing Systems*, pages 1–14, 2018.

[AT07] Samuel Aballéa and Aki Tsuchiya. Seeing for yourself: feasibility study towards valuing visual impairment using simulation spectacles. *Health economics*, 16(5):537–543, 2007.

[AZTZ19] Prithul Aniruddha, Nasif Zaman, Alireza Tavakkoli, and Stewart Zuckerbrod. A parametric perceptual deficit modeling and diagnostics framework for retina damage using mixed reality. In *International Symposium on Visual Computing*, pages 258–269. Springer, 2019.

[B+96] Michael Bach et al. The freiburg visual acuity test-automatic measurement of visual acuity. *Optometry and vision science*, 73(1):49–53, 1996.

[BM08] D Banks and RJ McCrindle. Visual eye disease simulator. *Proc. 7th ICDVRAT with ArtAbilitation, Maia, Portugal*, 2008.

[Bra] Braille Institute of America. VisionSim by Braille Institute. `https://apps.apple.com/us/app/visionsim-by-braille-institute/id525114829`. Accessed: 2019-10-30.

[BVM97] Hans Brettel, Françoise Viénot, and John D Mollon. Computerized simulation of color appearance for dichromats. *JOSA A*, 14(10):2647–2655, 1997.

[BVT+10] Alain M Bron, Ananth C Viswanathan, Ulrich Thelen, Renato de Natale, Antonio Ferreras, Jens Gundgaard, Gail Schwartz, and Patricia Buchholz. International vision requirements for driver licensing and disability pensions: using a milestone approach in characterization of progressive eye disease. *Clinical ophthalmology (Auckland, NZ)*, 4:1361, 2010.

[CARM15] Ethan Coggins, Kevin Andrews, Molly Rossman, and Tony Morelli. Sonicwalker: Virtual reality simulation of non-visual pedestrian city navigation. In *FDG*, 2015.

[CBL19] Kenny Tsu Wei Choo, Rajesh Krishna Balan, and Youngki Lee. Examining augmented virtuality impairment simulation for mobile app accessibility design. In *Proceedings of the 2019 CHI Conference on Human Factors in Computing Systems*, pages 1–11, 2019.

[CBW+17] Kenny Tsu Wei Choo, Rajesh Krishna Balan, Tan Kiat Wee, Jagmohan Chauhan, Archan Misra, and Youngki Lee. Empath-d: Empathetic design for accessibility. In *Proceedings of the 18th International Workshop on Mobile Computing Systems and Applications*, pages 55–60, 2017.

[CDAF18] Praneeth Chakravarthula, David Dunn, Kaan Akşit, and Henry Fuchs. FocusAR: Auto-focus augmented reality eyeglasses for both real world and virtual imagery. *IEEE transactions on visualization and computer graphics*, 24(11):2906–2916, 2018.

[Cen] Centers for Disease Control and Prevention. Germs & Infections. https://www.cdc.gov/contactlenses/germs-infections.html. Accessed: 2020-May-10.

[CFQ17] Tanvir Irfan Chowdhury, Sharif Mohammad Shahnewaz Ferdous, and John Quarles. Information recall in a virtual reality disability simulation. In *Proceedings of the 23rd ACM Symposium on Virtual Reality Software and Technology*, page 37. ACM, 2017.

[Col01] August Colenbrander. Measuring vision and vision loss. *Duane's clinical ophthalmology*, 5:1–39, 2001.

[Col02] A Colenbrander. Visual Standards – Aspects and Ranges of Vision Loss. http://www.icoph.org/downloads/visualstandardsreport.pdf, April 2002. Accessed: 2017-09-09.

[CWS+93] Leo T Chylack, John K Wolfe, David M Singer, M Cristina Leske, Mark A Bullimore, Ian L Bailey, Judith Friend, Daniel McCarthy, and Suh-Yuh Wu. The lens opacities classification system iii. *Archives of ophthalmology*, 111(6):831–836, 1993.

[DIN13] DIN German Institute for Standardization. Lighting applications - Emergency lighting; EN 1838:2013. Standard, DIN German Institute for Standardization, Berlin, Germany, October 2013.

[Don16] Kendall E Donaldson. Current status of bilateral same-day cataract surgery. *International ophthalmology clinics*, 56(3):29–37, 2016.

[Eas] EasternGraphics GmbH. pCon.planner. http://pcon-planner.com/en/. Accessed: 2017-09-04.

[Epia] Epic Games, Inc. Bloom. https://docs.unrealengine.com/en-US/Engine/Rendering/PostProcessEffects/Bloom/index.html. Online; accessed 17 April 2020.

[Epib] Epic Games, Inc. FMath::SmoothStep. https://docs.unrealengine.com/en-US/API/Runtime/Core/Math/FMath/SmoothStep/index.html. Online; accessed 17 April 2020.

[Epic] Epic Games, Inc. Unreal Engine 4. https://www.unrealengine.com. Accessed: 2017-09-04.

[Eur12] European Committee for Standardization. Graphical symbols - Safety colours and safety signs - Registered safety signs (ISO 7010:2011) . Standard, European Committee for Standardization, Brussels , Belgium, July 2012.

[FG12] David R Flatla and Carl Gutwin. " so that's what you see" building understanding with personalized simulations of colour vision deficiency. In *Proceedings of the 14th international ACM SIGACCESS conference on Computers and accessibility*, pages 167–174, 2012.

[GCQ+16] Anhong Guo, Xiang'Anthony' Chen, Haoran Qi, Samuel White, Suman Ghosh, Chieko Asakawa, and Jeffrey P Bigham. Vizlens: A robust and interactive screen reader for interfaces in the real world. In *Proceedings of the 29th Annual Symposium on User Interface Software and Technology*, pages 651–664, 2016.

[GDLC+07] Joy Goodman-Deane, Patrick M Langdon, P John Clarkson, Nicholas HM Caldwell, and Ahmed M Sarhan. Equipping designers by simulating the effects of visual and hearing impairments. In *Proceedings of the 9th international ACM SIGACCESS conference on Computers and accessibility*, pages 241–242, 2007.

[HCZ+19] Menghan Hu, Yuzhen Chen, Guangtao Zhai, Zhongpai Gao, and Lei Fan. An overview of assistive devices for blind and visually impaired people. *International Journal of Robotics and Automation*, 34(5):580–598, 2019.

[HNL80] LEA HYVÄRINEN, RISTO NÄSÄNEN, and PENTTI LAURINEN. New visual acuity test for pre-school children. *Acta ophthalmologica*, 58(4):507–511, 1980.

[HP14] Alex D Hwang and Eli Peli. An augmented-reality edge enhancement application for google glass. *Optometry and vision science: official publication of the American Academy of Optometry*, 91(8):1021, 2014.

[HTBGP18] Alex D Hwang, Merve Tuccar-Burak, Robert Goldstein, and Eli Peli. Impact of oncoming headlight glare with cataracts: a pilot study. *Frontiers in psychology*, 9:164, 2018.

[HVD06] MA Hogervorst and WJM Van Damme. Visualizing visual impairments. *Gerontechnology*, 5(4):208–221, 2006.

[Hyv18] Hyvärinen, Lea. Lea-Test. `http://www.lea-test.fi/index.html?start=en/vistests/instruct/250250/index.html`, 2018. Accessed: 2020-05-09.

[Int09] International Organization for Standardization. ISO 8596:2009 Ophthalmic optics – Visual acuity testing – Standard optotype and its presentation. Standard, International Organization for Standardization, Geneva, CH, July 2009.

[Int11] International Organization for Standardization. ISO 3864-1:2011 Graphical symbols – Safety colours and safety signs – Part 1: Design principles

for safety signs and safety markings. Standard, International Organization for Standardization, Geneva, CH, April 2011.

[Int17] International Organization for Standardization. ISO 8596:2017(en) Ophthalmic optics – Visual acuity testing – Standard and clinical optotypes and their presentation. 2017.

[JAR05] Bei Jin, Zhuming Ai, and Mary Rasmussen. Simulation of eye disease in virtual reality. In *Engineering in Medicine and Biology Society, 2005. IEEE-EMBS 2005. 27th Annual International Conference of the*, pages 5128–5131. IEEE, 2005.

[Jef08] Jeff Dahl. A typical Snellen chart. Originally developed by Dutch ophthalmologist Herman Snellen in 1862, to estimate visual acuity., 2008. [Online; accessed Februry 11, 2020. This file is licensed under the Creative Commons Attribution-Share Alike 3.0 Unported license. https://creativecommons.org/licenses/by-sa/3.0/legalcode].

[JO18] P. R. Jones and G. Ometto. Degraded reality: Using vr/ar to simulate visual impairments. In *2018 IEEE Workshop on Augmented and Virtual Realities for Good (VAR4Good)*, pages 1–4, March 2018.

[JSCWBC20] Pete R Jones, Tamás Somoskeöy, Hugo Chow-Wing-Bom, and David P Crabb. Seeing other perspectives: evaluating the use of virtual and augmented reality to simulate visual impairments (openvissim). *NPJ digital medicine*, 3(1):1–9, 2020.

[KAS+19] George Alex Koulieris, Kaan Akşit, Michael Stengel, Rafał K Mantiuk, Katerina Mania, and Christian Richardt. Near-eye display and tracking technologies for virtual and augmented reality. In *Computer Graphics Forum*, volume 38, pages 493–519. Wiley Online Library, 2019.

[KBS+18] Katharina Krösl, Dominik Bauer, Michael Schwärzler, Henry Fuchs, Georg Suter, and Michael Wimmer. A vr-based user study on the effects of vision impairments on recognition distances of escape-route signs in buildings. *The Visual Computer*, 34(6-8):911–923, 2018.

[KCL+18] Wonjung Kim, Kenny Tsu Wei Choo, Youngki Lee, Archan Misra, and Rajesh Krishna Balan. Empath-d: Vr-based empathetic app design for accessibility. In *Proceedings of the 16th Annual International Conference on Mobile Systems, Applications, and Services*, pages 123–135, 2018.

[KEH+19] Katharina Krösl, Carmine Elvezio, Matthias Hürbe, Sonja Karst, Michael Wimmer, and Steven Feiner. Icthroughvr: Illuminating cataracts through virtual reality. In *2019 IEEE Conference on Virtual Reality and 3D User Interfaces (VR)*, pages 655–663. IEEE, 2019.

[KEH+20] Katharina Krösl, Carmine Elvezio, Matthias Hürbe, Sonja Karst, Steven Feiner, and Michael Wimmer. Xreye: Simulating visual impairments in eye-tracked xr. In *2020 IEEE Conference on Virtual Reality and 3D User Interfaces Abstracts and Workshops (VRW)*, pages 831–832. IEEE, 2020.

[KEL+20] Katharina Krösl, Carmine Elvezio, Laura R Luidolt, Matthias Hürbe, Sonja Karst, Steven Feiner, and Michael Wimmer. CatARact: Simulating cataracts in augmented reality. In *2020 IEEE International Symposium on Mixed and Augmented Reality (ISMAR). IEEE*, 2020.

[KKE17] Arzu Seyhan Karatepe, Süheyla Köse, and Sait Eğrilmez. Factors affecting contrast sensitivity in healthy individuals: a pilot study. *Turkish journal of ophthalmology*, 47(2):80, 2017.

[KLBL93] Robert S Kennedy, Norman E Lane, Kevin S Berbaum, and Michael G Lilienthal. Simulator sickness questionnaire: An enhanced method for quantifying simulator sickness. *The international journal of aviation psychology*, 3(3):203–220, 1993.

[Kne08] Andrea Knezevic. Overlapping confidence intervals and statistical significance. *StatNews: Cornell University Statistical Consulting Unit*, 73(1), 2008.

[Kra15] Gregory Kramida. Resolving the vergence-accommodation conflict in head-mounted displays. *IEEE transactions on visualization and computer graphics*, 22(7):1912–1931, 2015.

[KSF10] Ernst Kruijff, J Edward Swan, and Steven Feiner. Perceptual issues in augmented reality revisited. In *2010 IEEE International Symposium on Mixed and Augmented Reality*, pages 3–12. IEEE, 2010.

[LBCM11] James Lewis, David Brown, Wayne Cranton, and Robert Mason. Simulating visual impairments using the unreal engine 3 game engine. In *Serious Games and Applications for Health (SeGAH), 2011 IEEE 1st International Conference on*, pages 1–8. IEEE, 2011.

[LSB12] James Lewis, L Shires, and DJ Brown. Development of a visual impairment simulator using the microsoft XNA framework. In *Proc. 9th Intl Conf. Disability, Virtual Reality & Associated Technologies, Laval, France*, 2012.

[LSZ+18] Tobias Langlotz, Jonathan Sutton, Stefanie Zollmann, Yuta Itoh, and Holger Regenbrecht. Chromaglasses: Computational glasses for compensating colour blindness. In *Proceedings of the 2018 CHI Conference on Human Factors in Computing Systems*, CHI '18, pages 390:1–390:12, New York, NY, USA, 2018. ACM.

[LTH+13] Christian Luksch, Robert F Tobler, Ralf Habel, Michael Schwärzler, and Michael Wimmer. Fast light-map computation with virtual polygon lights. In *ACM SIGGRAPH Symposium on Interactive 3D Graphics and Games*, pages 87–94, 2013.

[LTM+14] Christian Luksch, Robert F. Tobler, Thomas Mühlbacher, Michael Schwärzler, and Michael Wimmer. Real-time rendering of glossy materials with regular sampling. *The Visual Computer*, 30(6-8):717–727, June 2014.

[LWK20] L. R. Luidolt, M. Wimmer, and K. Krösl. Gaze-dependent simulation of light perception in virtual reality. *IEEE Transactions on Visualization and Computer Graphics*, 2020.

[MB11] R Michael and AJ Bron. The ageing lens and cataract: a model of normal and pathological ageing. *Philosophical Transactions of the Royal Society of London B: Biological Sciences*, 366(1568):1278–1292, 2011.

[MF16] Rhouri MacAlpine and David R Flatla. Real-time mobile personalized simulations of impaired colour vision. In *Proceedings of the 18th International ACM SIGACCESS Conference on Computers and Accessibility*, pages 181–189, 2016.

[MG88] Gary W Meyer and Donald P Greenberg. Color-defective vision and computer graphics displays. *IEEE Computer Graphics and Applications*, 8(5):28–40, 1988.

[MKD16] Tsubasa Maruyama, Satoshi Kanai, and Hiroaki Date. Vision-based wayfinding simulation of digital human model in three dimensional as-is environment models and its application to accessibility evaluation. In *International Design Engineering Technical Conferences and Computers and Information in Engineering Conference*, volume 50077, page V01AT02A064. American Society of Mechanical Engineers, 2016.

[MOF09] Gustavo M Machado, Manuel M Oliveira, and Leandro AF Fernandes. A physiologically-based model for simulation of color vision deficiency. *IEEE transactions on visualization and computer graphics*, 15(6):1291–1298, 2009.

[MVRVDB+09] Ralph Michael, Laurentius J Van Rijn, Thomas JTP Van Den Berg, Rafael I Barraquer, Günther Grabner, Helmut Wilhelm, Tanja Coeckelbergh, Martin Emesz, Patrik Marvan, and Christian Nischler. Association of lens opacities, intraocular straylight, contrast sensitivity and visual acuity in european drivers. *Acta ophthalmologica*, 87(6):666–671, 2009.

[Nata] National Eye Institute, National Institutes of Health (NEI/NIH). NEI Media Library. https://medialibrary.nei.nih.gov/. Accessed: 2020-May-11.

[Natb] National Eye Institute, National Institutes of Health (NEI/NIH). NEI Photos and Images. https://nei.nih.gov/photo. Accessed: 2018-Nov-29.

[Natc] National Eye Institute (NEI). Age-Related Macular Degeneration. https://www.nei.nih.gov/learn-about-eye-health/eye-conditions-and-diseases/age-related-macular-degeneration. Accessed: 2020-Oct-30.

[Natd] National Eye Institute (NEI). Corneal Conditions. https://www.nei.nih.gov/learn-about-eye-health/eye-conditions-and-diseases/corneal-conditions. Accessed: 2019-Dec-18.

[Nate] National Eye Institute (NEI). Eye Conditions and Diseases . https://www.nei.nih.gov/learn-about-eye-health/eye-conditions-and-diseases. Accessed: 2019-Dec-18.

[Natf] National Eye Institute (NEI). Refractive Errors. https://www.nei.nih.gov/learn-about-eye-health/eye-conditions-and-diseases/refractive-errors. Accessed: 2019-Dec-18.

[NEIa] NEI Office of Science Communications, Public Liaison, and Education. At a glance: Cataracts. https://www.nei.nih.gov/learn-about-eye-health/eye-conditions-and-diseases/cataracts. Accessed: 2019-Oct-24.

[NEIb] NEI Office of Science Communications, Public Liaison, and Education. Prevalence of Adult Vision Impairment and Age-Related Eye Diseases in America. https://nei.nih.gov/eyedata/adultvision_usa. Accessed: 2018-Nov-09.

[Nov18] Novartis Pharma AG. ViaOpta Simulator. https://www.viaopta-apps.com/ViaOpta-Simulator.html, 2018. Accessed: 2019-09-19.

[NRI12] Amelia Nybakke, Ramya Ramakrishnan, and Victoria Interrante. From virtual to actual mobility: Assessing the benefits of active locomotion through an immersive virtual environment using a motorized wheelchair. In *3D User Interfaces (3DUI), 2012 IEEE Symposium on*, pages 27–30. IEEE, 2012.

[Par] Parker Cronea. Fuchs' Dystrophy. https://parkercornea.com/fuchs-dystrophy/. Ophthalmic images are © 2009 American Academy of Ophthalmology. Accessed: 2020-May-11.

[PM12] Donatella Pascolini and Silvio Paolo Mariotti. Global estimates of visual impairment: 2010. *British Journal of Ophthalmology*, 96(5):614–618, 2012.

[PPZ+11] Vitor F. Pamplona, Erick B. Passos, Jan Zizka, Manuel M. Oliveira, Everett Lawson, Esteban Clua, and Ramesh Raskar. Catra: Interactive measuring and modeling of cataracts. *ACM Trans. Graph.*, 30(4):47:1–47:8, July 2011.

[PRW88] D.G. Pelli, J.G. Robson, and A.J. Wilkins. The design of a new letter chart for measuring contrast sensitivity. In *Clinical Vision Sciences*. Citeseer, 1988.

[PTM+13] Taís Renata Ribeira Parede, André Augusto Miranda Torricelli, Adriana Mukai, Marcelo Vieira Netto, and Samir Jacob Bechara. Quality of vision in refractive and cataract surgery, indirect measurers. *Arquivos brasileiros de oftalmologia*, 76(6):386–390, 2013.

[Pup] Pupil Labs GmbH. VR/AR. https://pupil-labs.com/products/vr-ar/. Accessed: 2019-Oct-24.

[PYL+16] Shrinivas Pundlik, Huaqi Yi, Rui Liu, Eli Peli, and Gang Luo. Magnifying smartphone screen using google glass for low-vision users. *IEEE Transactions on Neural Systems and Rehabilitation Engineering*, 25(1):52–61, 2016.

[RCW+18] Andreas Reichinger, Helena Garcia Carrizosa, Joanna Wood, Svenja Schröder, Christian Löw, Laura Rosalia Luidolt, Maria Schimkowitsch, Anton Fuhrmann, Stefan Maierhofer, and Werner Purgathofer. Pictures in your mind: using interactive gesture-controlled reliefs to explore art. *ACM Transactions on Accessible Computing (TACCESS)*, 11(1):1–39, 2018.

[RIF+09] Tobias Ritschel, Matthias Ihrke, Jeppe Revall Frisvad, Joris Coppens, Karol Myszkowski, and H-P Seidel. Temporal glare: Real-time dynamic simulation of the scattering in the human eye. In *Computer Graphics Forum*, volume 28, pages 183–192. Wiley Online Library, 2009.

[SBS+12] Evan A Suma, Gerd Bruder, Frank Steinicke, David M Krum, and Mark Bolas. A taxonomy for deploying redirection techniques in immersive virtual environments. In *Virtual Reality Short Papers and Posters (VRW), 2012 IEEE*, pages 43–46. IEEE, 2012.

[SCK+11] Evan A Suma, Seth Clark, David Krum, Samantha Finkelstein, Mark Bolas, and Zachary Warte. Leveraging change blindness for redirection in virtual environments. In *Virtual Reality Conference (VR), 2011 IEEE*, pages 159–166. IEEE, 2011.

[SES18] Simon Stock, Christina Erler, and Wilhelm Stork. Realistic simulation of progressive vision diseases in virtual reality. In *Proceedings of the 24th ACM Symposium on Virtual Reality Software and Technology*, pages 1–2, 2018.

[SFC+10] Evan A Suma, Samantha L Finkelstein, Seth Clark, Paula Goolkasian, and Larry F Hodges. Effects of travel technique and gender on a divided attention task in a virtual environment. In *3D User Interfaces (3DUI), 2010 IEEE Symposium on*, pages 27–34. IEEE, 2010.

[SFF18] Lee Stearns, Leah Findlater, and Jon E Froehlich. Design of an augmented reality magnification aid for low vision users. In *Proceedings of the 20th International ACM SIGACCESS Conference on Computers and Accessibility*, pages 28–39, 2018.

[Sho02] John A Shoemaker. *Vision problems in the US: Prevalence of adult vision impairment and age-related eye disease in America.* National Eye Institute, 2002.

[SLF+12] Evan A Suma, Zachary Lipps, Samantha Finkelstein, David M Krum, and Mark Bolas. Impossible spaces: Maximizing natural walking in virtual environments with self-overlapping architecture. *IEEE Transactions on Visualization and Computer Graphics*, 18(4):555–564, 2012.

[SLI19] Jonathan Sutton, Tobias Langlotz, and Yuta Itoh. Computational glasses: Vision augmentations using computational near-eye optics and displays. In *2019 IEEE International Symposium on Mixed and Augmented Reality Adjunct (ISMAR-Adjunct)*, pages 438–442. IEEE, 2019.

[Sne62] H Snellen. Optotypi ad visum determinandum (letterproeven tot bepaling der gezichtsscherpte; probebuchstaben zur bestimmung der sehschaerfe). *Weyers, Utrecht, The Netherlands*, 1862.

[TM20] Lauren Thévin and Tonja Machulla. Three common misconceptions about visual impairments. 2020.

[VBM99] Françoise Viénot, Hans Brettel, and John D Mollon. Digital video colourmaps for checking the legibility of displays by dichromats. *Color Research & Application: Endorsed by Inter-Society Color Council, The Colour Group (Great Britain), Canadian Society for Color, Color Science Association of Japan, Dutch Society for the Study of Color, The Swedish*

Colour Centre Foundation, Colour Society of Australia, Centre Français de la Couleur, 24(4):243–252, 1999.

[VCH16] Jani Väyrynen, Ashley Colley, and Jonna Häkkilä. Head mounted display design tool for simulating visual disabilities. In *Proceedings of the 15th International Conference on Mobile and Ubiquitous Multimedia*, pages 69–73. ACM, 2016.

[VdB86] TJTP Van den Berg. Importance of pathological intraocular light scatter for visual disability. *Documenta Ophthalmologica*, 61(3-4):327–333, 1986.

[vis] Simulate your Vision For family, friends, and eye doctors... `https://visionsimulations.com`. Accessed: 2019-10-30.

[Vis19] Vision Rehabilitation Services LLC. Cataract simulators. `https://www.lowvisionsimulators.com/products/cataract-simulators`, 2019. [Online; accessed 19-September-2019].

[VKBS13] Khrystyna Vasylevska, Hannes Kaufmann, Mark Bolas, and Evan A Suma. Flexible spaces: Dynamic layout generation for infinite walking in virtual environments. In *3D User Interfaces (3DUI), 2013 IEEE Symposium on*, pages 39–42. IEEE, 2013.

[VPK15] Khrystyna Vasylevska, Iana Podkosova, and Hannes Kaufmann. Walking in virtual reality: Flexible spaces and other techniques. In Luigi Cocchiarella, editor, *The Visual Language of Technique*, pages 81–97. Springer International Publishing, 2015.

[VRV] VRVis Research Center. HILITE. `http://www.vrvis.at/projects/hilite`. Accessed: 2017-02-13.

[WAAB18] Haojie Wu, Daniel H Ashmead, Haley Adams, and Bobby Bodenheimer. Using virtual reality to assess the street crossing behavior of pedestrians with simulated macular degeneration at a roundabout. *Frontiers in ICT*, 5:27, 2018.

[WBW+19] Ryan Wedoff, Lindsay Ball, Amelia Wang, Yi Xuan Khoo, Lauren Lieberman, and Kyle Rector. Virtual showdown: An accessible virtual reality game with scaffolds for youth with visual impairments. In *Proceedings of the 2019 CHI Conference on Human Factors in Computing Systems*, pages 1–15, 2019.

[WCCC10] Joanne Wood, Alex Chaparro, Trent Carberry, and Byoung Sun Chu. Effect of simulated visual impairment on nighttime driving performance. *Optometry and vision science*, 87(6):379–386, 2010.

[WHO19] *World report on vision*. World Health Organization, Geneva, 2019. Licence: CC BY-NC-SA 3.0 IGO.

[Wor20] World Health Organization. "coronavirus disease (covid-19) outbreak". http://www.euro.who.int/en/health-topics/health-emergencies/coronavirus-covid-19/novel-coronavirus-2019-ncov, 2020. [Online; accessed 30-April-2020].

[WWFG16] Fabian Werfel, Roman Wiche, Jochen Feitsch, and Christian Geiger. Empathizing audiovisual sense impairments: Interactive real-time illustration of diminished sense perception. In *Proceedings of the 7th Augmented Human International Conference 2016*, page 15. ACM, 2016.

[XFG+07] Hui Xie, Lazaros Filippidis, Steven Gwynne, Edwin R Galea, Darren Blackshields, and Peter J Lawrence. Signage legibility distances as a function of observation angle. *Journal of fire protection engineering*, 17(1):41–64, 2007.

[ZB10] Michelle Zagar and Scott Baggarly. Low vision simulator goggles in pharmacy education. *American Journal of Pharmaceutical Education*, 74(5):83, 2010.

[ZBB+18] Yuhang Zhao, Cynthia L Bennett, Hrvoje Benko, Edward Cutrell, Christian Holz, Meredith Ringel Morris, and Mike Sinclair. Enabling people with visual impairments to navigate virtual reality with a haptic and auditory cane simulation. In *Proceedings of the 2018 CHI conference on human factors in computing systems*, pages 1–14, 2018.

[ZCH+19] Yuhang Zhao, Edward Cutrell, Christian Holz, Meredith Ringel Morris, Eyal Ofek, and Andrew D Wilson. Seeingvr: A set of tools to make virtual reality more accessible to people with low vision. In *Proceedings of the 2019 CHI Conference on Human Factors in Computing Systems*, pages 1–14, 2019.

[Zim13] Zimmerman Low Vision Simulation Kit. Zimmerman low vision simulation kit. https://www.lowvisionsimulationkit.com, 2013. [Online; accessed 30-October-2020].

[ZKC+19] Yuhang Zhao, Elizabeth Kupferstein, Brenda Veronica Castro, Steven Feiner, and Shiri Azenkot. Designing ar visualizations to facilitate stair navigation for people with low vision. In *Proceedings of the 32nd Annual ACM Symposium on User Interface Software and Technology*, pages 387–402, 2019.

[ZKR+20] Yuhang Zhao, Elizabeth Kupferstein, Hathaitorn Rojnirun, Leah Findlater, and Shiri Azenkot. The effectiveness of visual and audio wayfinding guidance on smartglasses for people with low vision. In *Proceedings of the 2020 CHI Conference on Human Factors in Computing Systems*, pages 1–14, 2020.

[ZL19] Christina Zavlanou and Andreas Lanitis. Virtual reality-based simulation of age-related visual deficiencies: Implementation and evaluation in the design process. In *International Conference on Human Interaction and Emerging Technologies*, pages 262–267. Springer, 2019.

[ZSA15] Yuhang Zhao, Sarit Szpiro, and Shiri Azenkot. Foresee: A customizable head-mounted vision enhancement system for people with low vision. In *Proceedings of the 17th International ACM SIGACCESS Conference on Computers & Accessibility*, pages 239–249, 2015.

[ZSKA16] Yuhang Zhao, Sarit Szpiro, Jonathan Knighten, and Shiri Azenkot. Cuesee: exploring visual cues for people with low vision to facilitate a visual search task. In *Proceedings of the 2016 ACM International Joint Conference on Pervasive and Ubiquitous Computing*, pages 73–84, 2016.

[ZTZ20] Nasif Zaman, Alireza Tavakkoli, and Stewart Zuckerbrod. A mixed reality system for modeling perceptual deficit to correct neural errors and recover functional vision. In *2020 IEEE Conference on Virtual Reality and 3D User Interfaces Abstracts and Workshops (VRW)*, pages 269–274. IEEE, 2020.